THE UNIVERSITY OF MICHIGAN

COLLEGE OF ENGINEERING
High Altitude Engineering Laboratory
Department of Aerospace Engineering
Department of Atmospheric and Oceanic Science

Technical Report

ACOUSTICS OF METEORS—EFFECTS OF THE ATMOSPHERIC TEMPERATURE AND WIND STRUCTURE ON THE SOUNDS PRODUCED BY METEORS

Part 3. Conclusion

Douglas O ReVelle

ORA Project 010816

supported by:

NATIONAL AERONAUTICS AND SPACE ADMINISTRATION
GRANT NO. NGR 23-005-540
WASHINGTON, D. C.

administered through:
OFFICE OF RESEARCH ADMINISTRATION ANN ARBOR
September 1973

TABLE OF CONTENTS

TABLE OF CONTENTS (Part III) (Continued)

TABLE OF CONTENTS (Part III) (Concluded)

ACKNOWLEDGMENTS

While as always the help of the Staff of the High Altitude Engineering Laboratory is gratefully acknowledged, Part 3 of this report has of necessity been greatly influenced by many sources outside the University of Michigan as well.

The airwave data supplied by the late Mr. Vernon H. Goerke (NOAA, Boulder Colorado) for the Revelstoke, Kincardine and Holbrook fireballs represents 60% of the existing unclassified information on this subject. In addition, the airwave data supplied by Dr. E. M. Shoemaker (California Institute of Technology) for the Holbrook fireball and that supplied by Dr. Charles R. Wilson (University of Alaska) for the Alaskan fireball of December 19, 1969 is also gratefully acknowledged.

Dr. R. E. Folinsbee (University of Alberta) has kindly provided detailed position estimates and maps with regard to the Revelstoke entry. This information is gratefully acknowledged.

Once again I must also thank Dr. R. E. McCrosky for his detailed information with regard to the Prairie Network fireballs. I also would like to thank him for making a copy of the sonic boom tape of the April 25, 1969 Bovedy fireball available to me.

The early efforts of Dr. R. W. Procunier (of Hewlett Packard) with regard to possible data on this subject in the frequency range 1-20 Hz is also gratefully acknowledged as was his encouragement and interest in this field of study.

Finally I thank my doctoral committee Co-Chairmen,

Professors F. L. Bartman and L. M. Jones for their efforts during the course of this investigation. I would especially like to thank Professor Jones for his early suggestion with regard to undertaking research in the field of Atmospheric Acoustics.

This research was supported by NASA grant NGR-23-005-540.

LIST OF FIGURES

LIST OF FIGURES (continued)

LIST OF FIGURES (concluded)

LIST OF TABLES

LIST OF SYMBOLS

A	weak shock or linear absorption effects on the variation of the fundamental wave period
C	adiabatic sound speed
C_g	adiabatic sound speed at the ground
C_o	adiabatic sound speed at the observer
C_z	adiabatic sound speed at the source altitude
$\overline{C}$	mean adiabatic sound speed between the source and the observer
"C"	Plooster's adjustable parameter which determines the region in which the transition from strong shock to weak shock behavior occurs
C. S. T.	central standard time
C. I.	color index ($M_{pan} - M_v$)
d_a	remaining propagation distance of the disturbance
$d_m(z)$	meteor diameter as a function of altitude
d_{mE}	meteor diameter at z'
d_s	distance to the "shocked" state
d'	10% distortion distance
D	direction of wave propagation with respect to variations in the fundamental wave period
D(R)	absorption decay parameter ($\Delta p / \Delta p_z$)
$D_L(R)_{z \to g}$	linear absorption evaluated between the source altitude and the ground
$D_L(R)_{t \to g}$	linear absorption evaluated from the transition altitude (where $d' > d_a$) to the ground
$D_{ws}(R)_{z \to t}$	weak shock wave absorption from the source altitude to the transition altitude (where $d' > d_a$)

E	kinetic energy of the meteor (preatmospheric value)
E_z	kinetic energy of the meteor at the source altitude
E_o	energy deposited per unit length of trajectory
E. D. T.	eastern daylight time
E. S. T.	eastern standard time
f_m	fundamental frequency of the disturbance
$f(x)$	as defined originally by equation (12a)
$f(\omega, x)$	as defined by equation (77)
G	initial wavefront geometry effects on variations in the fundamental wave period
G. M. T.	Greenwich mean time
H	scale height of the isothermal atmosphere
$k(z)$	characteristic velocity within the entry plane as a function of altitude
$k'(z)$	characteristic velocity outside the entry plane as a function of altitude
k_1	as defined by equation (85)
ℓ	line source length
L. T.	local time
m	meteor mass
M_z	meteor Mach number at the source altitude
M_E	meteor Mach number at z'
$M(z)$	meteor Mach number as a function of altitude
M_{pan}	panchromatic meteor magnitude
M_v	visual meteor magnitude

M. S. T.	mountain standard time
n	number of bodies considered in the physical theory of meteors
N	nonlinear effects on the variations in the fundamental wave period (or no. meteors/unit area unit time)
N_I	the mean meteor influx
N_{SP}	number of meteors which produce sound per unit area per unit time (for line source theory)
N_G	number of meteor induced ground sound arrivals per unit area per unit time
N_D	number of meteors per unit area per unit time for which photographic documentation is possible
NOAA	National Oceanographic Atmospheric Administration
p(z)	ambient hydrostatic pressure as a function of altitude
p_o	ambient hydrostatic pressure at an observer
p_g	ambient hydrostatic pressure at the ground
p_z	ambient hydrostatic pressure at the source altitude
p/p_o	pressure ratio at the shock front
Δp	overpressure of the disturbance (maximum value of the positive phase)
$\Delta p_{o \rightarrow p}$	the zero to peak value of the overpressure (of the positive phase)
$\Delta p_{p \rightarrow p}$	the peak to peak value of the overpressure (from the maximum positive value to the maximum negative value)
$\Delta p_{z \rightarrow g}$	predicted ground overpressure
$\Delta p_{z \rightarrow t}$	overpressure at the transition altitude (where $d' > d_a$)
$\Delta p/p_o$	overpressure ratio for a weak disturbance
p*	modified ballistic entry parameter

$\overline{p^*}$	geometric mean pressure between the source altitude and the observer
$\overline{p^*}_{z \to g}$	geometric mean pressure between the source altitude and the ground
$\overline{p^*}_{z \to t}$	geometric mean pressure between the source altitude and the transition altitude (where $d' > d_a$)
P. S. T.	pacific standard time
r_m	meteor radius (or at the source altitude)
$r_m(z)$	meteor radius as a function of altitude
r_{mE}	meteor radius at z'
R	radial distance from the observer to the meteor trajectory
R_g	ground reflection coefficient
R_h	horizontal range distance from the observer to the meteor trajectory
R_o	relaxation radius of the cylindrical blast wave
R_s	relaxation radius of the spherical blast wave
$R_{z \to g}$	total distance from the observer to the meteor trajectory
$R_{z \to t}$	distance from the source altitude to the transition altitude (where $d' > d_a$)
S	geometrical dispersion effects on the variations in the fundamental wave period as produced by gradients of atmospheric structure parameters
t_d	total duration of the meteor entry
t_D	total duration of a dispersive wave train
t_e	time of the meteor entry
t_o	observation time of airwaves induced by meteor entry
t_p	propagation time of the disturbance

T	effects on the variations in the fundamental wave period as caused by atmospheric turbulence
$T(z)$	atmospheric temperature as a function of altitude (absolute temperature)
U. T.	universal time
V	meteor velocity (or at the source altitude)
V_E	meteor velocity at z'
$V(z)$	meteor velocity as a function of altitude
V_T	trace velocity of a disturbance across a ground plane defined by the microphone array
$W(z)$	magnitude of the horizontal wind as a function of altitude
WKB	Wenzel-Kramers-Brillouin
x	R/R_o; scaled distance from the meteor trajectory
x_g	predicted value of x at the ground
$x_{z \rightarrow g}$	value of x at the ground
$x_{z \rightarrow t}$	value of x at the transition altitude
z	altitude (geometric), increasing upward from z = 0 at the surface of the earth, for the isothermal atmospheric model
z'	altitude at which the meteor deceleration is first zero
z''''	altitude at which the meteor deceleration is again zero
z_{ni}	altitude, increasing upward from z = 0 at the surface of the earth, for the nonisothermal atmospheric model
z_z	source altitude
α	Mach angle of the meteor shock cone
β'	elevation angle of the disturbance across the microphone array
γ	ratio of the specific heat of air at constant pressure to that at constant volume

" δ "	efficiency with which cylindrical line source strong shock waves are generated as compared with the results of the asymptotic strong shock solution due to Lin (1954)
$\bar{\epsilon}$	zenith angle of the ray
θ	entry elevation angle of the meteor
θ'	elevation angle of the acoustic ray
Λ	wavelength of the disturbance
ρ_m	meteor density
ρ_{mE}	meteor density at z'
σ	ablation parameter
τ_g	fundamental wave period at the ground
τ_m	fundamental wave period as a function of x
τ_{mo}	fundamental wave period at x = 10
$\overline{\tau_m}$	mean value of τ_m during the propagation
$\Delta \tau_m$	variations in τ_m as produced by geometric effects, etc.
τ_{fp}	free path time
τ_{vp}	characteristic time scale for variations in the induced pressure field
ϕ	azimuth angle of the meteor heading
$\Delta \phi$	absolute value of the azimuth interval of the initially downward heading rays outside the entry plane
χ	observed azimuth angle of the airwave arrival
$\psi(z)$	azimuthal direction the horizontal winds are coming from as a function of altitude measured as increasing clockwise from North as viewed from above
$\overline{\omega}$	assumed wave shape induced by the source

FOREWARD

This is the third and final section of the meteor acoustics report. Its primary objectives are to assess the probability of occurrence of meteor generated sound, analyze existing infrasound from meteors and finally to summarize the present research as well as to suggest topics for future research.

VI. PROBABILITY OF OCCURANCE OF SOUND PRODUCING METEORS

A. PHOTOGRAPHIC DATA

In Figures 118-120, the influx of meteors versus respectively pre-atmospheric mass (in grams), kinetic energy (in ergs) and panchromatic magnitude (M_{pan}-M_v = -2.0 which is the assumed constant color index; McCrosky, 1968, where M_v is the visual magnitude of the meteor) are shown. The panchromatic magnitude then is related to the brightness of a given event. For $M_v \lesssim -3$, the entering meteoroid is generally termed a fireball. Presumably the larger r_{mE} and M_E are, the more negative M_v will become (within limits). M_{pan} is not constant along the meteor trajectory. The values of M_{pan} shown in Figure 120 refer to the maximum value attained during the entry. The variability of M_{pan} thus implies that radiation losses are not uniform along the line trajectory between z' and z''''. Since in Section IV A (Part 2), radiation losses appeared to be generally quite small (with regard to predicting the overall attenuation of the pressure wave), no further mention of the luminous efficiency factor or of the variation of M_{pan} with altitude will be made.

The basis for the groupings a, b and c shown in Figures 117-120 is as follows:

Group a. r_{mE}=0.5 cm; $0.3 \leq \rho_m \leq 7.7 g/cm^3$

Group b. r_{mE}=5.0 cm; $0.3 \leq \rho_m \leq 7.7 g/cm^3$

Group c. r_{mE}=50.0 cm; $0.3 \leq \rho_m \leq 7.7 g/cm^3$

While other investigators have published information deduced by photographic methods for groups b and c, the PN (Prairie Network) data represents direct measurement for these large bodies. Generally,

other research groups have made linear extrapolations from influx data for much smaller bodies to determine the influx rate for groups b and c (Cosby and Lyle, 1965). Group a information as a function of pre-atmospheric mass is plotted in Figure 117. Here the estimates of two groups are compared. It should be noted that all of the mass-influx plots are for photometric mass, rather than dynamic mass. The dynamic mass is determined by observing meteor decceleration in the atmosphere which can be very difficult (McCrosky, 1971). For the single body model the concept of dynamic and photometric mass are equivalent. Thus the one symbol m has been used throughout this report to denote the meteor mass, since only single body theory has been considered.

In Figures 121 & 122 the percentage influx of meteors versus the horizontal entry angle θ is plotted. While entry can take place over almost the entire range of $0 < \theta < 90$ degrees, the maximum percent occurance is always for $\theta \leq 55^{o}$. Three different groups of astronomers who have published information on this subject have been considered in these figures. It is to be noted that each data grouping shown has a slightly different panchromatic magnitude range. In addition, there is a tendency within this data for a greater percent occurance of meteors with smaller values of maximum θ for increasing negative magnitude (i.e., increasing brightness). This effect is to be expected. Of the three groups of data, the results of Jacchia, Verniani and Briggs is closest to corresponding to the group designation a. The data from the Prairie Network (McCrosky et. al., 1968) corresponds best to groups b and c. It is reasonable to conclude from Figures 121 & 122 that, independent of attenuation effects, a sizeable fraction of the meteors observed have values of θ such that equations (34) and (35)

can be satisfied. It remains to be seen whether or not this fact is very significant. It should be recalled, however, that in order to apply (34) and (35), a given meteor must first penetrate to a region of the atmosphere such that the Knudsen number is small, but with $\dot{V}(z) >> C(z)$. Only for the Prairie Network fireballs are these above conditions likely to be satisfied.

In Figure 123 the number of meteors observed versus monthly intervals from June, 1966 to December 1969 for the PN are shown (McCrosky, 1972, Private Communication). This diagram was not corrected for percent cloudiness, etc., but was determined directly from raw night - time photographic data. The general conclusion that can be reached from this figure is that from June to December, even if the effects of shower meteors are removed, the sporadic meteor flux rate still tends to increase. Shower meteors generally have sizes in the range $0.05 \leq r_{mE} \leq 0.5$ cm, i.e. including meteors in group a, but with the majority of the flux rate occuring for $r_{mE} \leq 0.1$ cm. (Millman, 1970). Note that the PN seasonal dependence of the flux rate is about 180^{o} out of phase with the seasonal dependence determined by using the recent lunar seismograph stations (Dorman et. al., 1973). In addition, the total influx rate determined by seismographic methods on the Moon is much smaller (Wood, 1973) than the rate determined by McCrosky (1968). While this lunar data will not be discussed further in this analysis, it appears that at present the difference between these two predicted influx rates is unreasolvable. Since McCrosky's methods are much more direct, it is felt that his influx rates are probably more reliable. They are substantiated in fact to a large degree by the military airwave data which are discussed in Section VI B.

B. MILITARY AIRWAVE DATA

The influx of meteors versus mass, determined using sensitive military microbarographs, is shown in Figure 124 (Lowry and Shoemaker, 1967; Gault, 1970). In addition, the influx data of McCrosky is also shown in this Figure. Note the relatively good agreement between the airwave data and that determined photographically by McCrosky, over the range $10^4 \leq m \leq 10^8$ (in grams).

The actual observations which the meteor influx microbarograph data are based upon are classified. The usefullness of such data in the open literature is obvious. It is the hope of the author that current plans to correlate infrasonic pressure data with Prarie Network photographic data in the near future will make such information available to all who desire it.

Using the military airwave data, Figure 124 predicts that at 10^4 grams about $5.1 \cdot 10^5$ meteors/yr enter the earth's atmosphere. This corresponds to about 12 meteors per night (12 hrs) over an area equivalent to the continental U. S.. The Prairie Network records on the average about 1 event per night. See Figure 123. The majority of these meteors have masses of about 10^3 grams or less however (McCrosky, 1968). The predicted influx rate due to McCrosky over an area equivalent to that of the continental U. S. is about 1 meteor/night at 10^4 grams. In Section VI C, the integrated influx effect over all masses greater than 10^4 grams will be briefly considered.

It should be noted at this point that the determination of the meteor influx rate for $m \gtrsim 10^3$ grams has been accomplished only in relatively recent times. McCrosky's network began operation in 1964. Presumably the classified microbarograph data acquisition

system began in the early 1960's due to the nuclear test ban agreements which were signed. The lunar seismograph data began, on the other hand, in the late 1960's with the advent of the NASA Apollo program. Thus the influx rates are not necessarily final and "new" methods, including unclassified microbarograph systems have the potential for providing new information on this subject. In addition, the recent (January, 1971) 12 station automatic photographic fireball detection system set up in the Canadian Prairies by Dr. Ian Halliday (of the National Research Council of Canada) is also another potential source for further knowledge of the meteor influx rate.

C. PROBABILITY OF LINE SOURCE METEOR INDUCED AIRWAVES

Using an assumed influx rate it is then possible to estimate the number of sound arrivals at a given fixed ground array per unit time. Note that a distinction can be made here between sound producing meteors in general and meteors which may produce sound that can be recorded at the ground. Using the information in Section III (Part 1), sound producing meteors (using a line source theory) begin for $r_{mE} \geq 0.5$ cm. As has been previously discussed the minimum value depends on many parameters. Using a Mach number of 100, the relaxation radius, R_o, for the minimum r_{mE} case would be 1 meter. According to the attenuation models developed in Section V (Part 2), the minimum R_o of interest is about 10 meters. Thus, generally speaking, meteors with an associated relaxation radius such that $1 \lesssim R_o \lesssim 10$ meters will not produce recordable sound at the ground. It remains to be seen however whether or not high altitude balloon platforms, suitably instrumented with acoustic sensors, might be able to record this intermediate R_o range.

It is interesting also to note that the cases with R_o = 10 meters can be interpreted as d_{mE}= 20 cm, with ρ_m = 3g/cm^3 at M_E = 50, i.e. m ~ 10^4 grams. That this is the smallest mass shown for the military airwave influx data may or may not be purely coincidental. Note that only one straight line is drawn for the military airwave data, not the individual data points necessary to evaluate the significance of the slope of that one line. While McCrosky has forced a straight line fit to his data, he has also shown the data points necessary to interpret his results. Measurements throughout the entire meteor size spectrum (including the micrometeoroids) have shown that there is no a priori reason to expect a straight line fit over a widely varying mass range (See for instance, Millman, 1970).

Thus it is somewhat difficult at the present time to accurately estimate the probability of occurance at a given infrasonic airwave station of meteor induced line source pressure signals. This is due at least in part to the basic uncertainty in the flux rate. As has been discussed throughout this report, the meteor phenomena is most complex. The bolide nature of meteors has been avoided here for the most part . To reproduce this type of effect the present meteor models must be considerably improved. In addition depending on the altitude of the "point" type explosion, the coupling of the spherical blast wave energy to the ambient atmosphere must be understood in detail. Above certain altitudes Groves (1963) has shown that both atmospheric and "explosion" related quantities must be studied to determine their interplay. Fortunately most of the bolide effects will probably occur at relatively low altitudes where the above coupling process is more efficient than at great altitudes where the air density is small. The

analysis of Lowry and Shoemaker of the existing unclassified airwave data i. e. Figure 99 (Part 2) seems to imply that at least some of this data has been considered (or interpreted) in terms of a "point" source energy release using the wave guide mode theory. Note that for the present line source problem at distances exceeding the line source length spherical wave expansion was predicted. With our present instrumentation set up, the attenuation calculations in Section V (Part 2) indicate that detection may at times be difficult for line source airwaves at these relatively great distances. Also the decay of Δp for spherical waves is faster than cylindrical decay due to the difference in the divergence of the wavefronts for waves of spherical and cylindrical geometry (Few, 1969). In a uniform medium linear spherical waves decrease in overpressure as R^{-1}. For linear cylindrical waves an $R^{-1/2}$ dependence is eventually approached. (Officer, 1958). Thus beyond $R = \ell$ in the line source meteor sound case, i. e., $x \sim 10^4$, somewhat greater attenuation due to spreading decay of spherical wavefronts should occur. Such effects have not been formally calculated in this analysis however. The classified military microbarograph instrumentation may be more sensitive than present commercial microbarograph systems. Therefore some of their recorded meteor sound data may be of both initial varieties (line and point source type). Without further access to such data or more elaborate meteor models, it is difficult to make a more definitive judgment on these possibilities.

We will proceed then knowingly ignoring the bolide nature of some meteors. For the present we will also make the following assumptions:

1) Knowledge of the event is possible independent of the continuously recorded infrasonic pressure wave data.

This knowledge may originate in reports from the mass media or via photographic fireball networks in general. For this reason we are therefore most interested in meteors which enter the earth's atmosphere during the night-time hours. As will be seen in Section VII, without some knowledge with respect to the event very little useful information can be obtained using the present theory:

2) The event is equally likely to occur at any given time in any direction with respect to an observer at a given latitude and longitude. Since the primary passband of detectable line source airwaves appears at present to be in the range of from 1 to about 10 seconds (far from the source) the individual pressure sensors should be about 500 feet apart for adequate resolution of all the signals of interest. Thus a relatively small latitude and longitude ground area will be covered by the array ($\sim$ 0.02 mi^2).

3) The detection system is capable of recording overpressures as small as 0.1 dynes/cm^2, peak to peak, under conditions of low "wind noise.," etc.

If all of the above conditions are satisfied the other primary variables of interest are:

1) $d_m(z)$
2) $M(z)$
3) ρ_m
4) θ (considered constant between z' and z'''')
5) ϕ
6) R (from the sensor to the trajectory)
7) t_e - time of the meteor entry
8) T (z)
9) W (z)
10) ψ (z)

The first two quantities listed determine R_o. Using ρ_m and item four in conjunction with the first two items allows an estimate of the source altitude region to be made using the meteor models developed in Section III (Part 1). The next four items (4 - 7) determine the geometrical possibilities as well the time displacement between a fixed ground array and the possible arrival of the pressure waves. The last three items in conjunction with items four and five allow the refractive possibilities to be determined. Lastly, item six, is very useful when attenuation considerations are made (in conjunction with a knowledge of R_o as determined above). Note that if an extended source concept is considered, rather than the present instantaneous source assumption, t_d, the duration of the entry, is also of interest when attenuation calculations are made.

With knowledge of the above quantities and the present meteor models an estimate can be made of the probability of occurrence of line source airwaves. In what follows the smallest possible d_m (or R_o once M_E is specified) will be used since as Figures 117 & 118 show, the probability of occurrence of meteors increases tremendously as smaller masses are considered. Also in what follows the atmospheric quantities considered and their variations in season and altitude are values representative of mean middle latitude northern hemisphere conditions.

During entry refraction effects may be very important. If θ is about 50^o or less, the wind effects in the entry plane are not significant. Near the source outside the entry plane only certain directions are optimum for refraction to the ground. In general, the effectiveness of certain scales of atmospheric turbulence in breaking up the line source pressure signal will determine (along with the geometrical condition $R \sim \ell$) in what region a transition from cylindrical

to spherical wave expansion occurs. For this analysis we have assumed that the turbulent scattering effects are not very significant with regard to changing the cylindrical spreading decay before R = ℓ is reached. Thus, in the vicinity of the source, the direction of entry with respect to the observer is very important primarily because of the highly directional nature of the line source as a radiator of pressure waves. As has been seen, the wind effects on long distance ducting of the signal through the lower sound channel are also dependent on this entry direction.

Lyubarskiy (1952) has given some estimates of entry direction as a function of time, i.e., a seasonal dependence, however it is felt that this information is probably not very statistically significant. In this regard two facts readily appear. The first is a quote from Lyubarskiy himself: "Most of the observations were acquired from random eyewitness accounts. The observational material is irregular, and in each isolated instance very incomplete; there is little information on bolide trajectories, on the exact time of observation, on the time of flight, etc. These deficiencies, however, are masked to a considerable extent by the large number of observations involved." The second fact is the discrepancy between the percent occurance of gross fragmentation effects as reported by Lyubarskiy and more recent determinations as noted by Baldwin and Sheaffer (1971). These are respectively, 19% and "almost half". Thus it would appear that further observational work needs to be done with regard to obtaining reliable statistical information on many meteor parameters, including the variation of ϕ as a function of the number of meteors observed. From what little information Lyubarskiy does give, the assumption that all ϕ values are equally probable does not appear very unreasonable however.

From the present meteor theory developed in Section III (Part 1) it appears that the smaller d_m is at z', the higher is the altitude at which V⟶C. The larger V_E is at entry, the deeper is the penetration, except for the effects of ablation i. e. for $V_E \gtrsim 15$ km/sec with $0 < \sigma \leq 5 \cdot 10^{-12}$ sec^2/cm^2. Therefore by considering the smallest possible d_m (at large M_E with a small Knudsen number), higher altitudes must be considered than for larger d_m. Thus, attenuation becomes more significant since the present theory using a cylindrical blast wave model to study hypersonic flow around a blunt body predicts relatively higher fundamental frequencies the smaller the body size is. As has been mentioned previously due to the directional characteristics of the source only a certain portion of the sound generated by an instantaneous line source will reach a given ground area. This is especially true for small Θ. Thus, two different stations, widely spaced, may not record equivalent pressure pulses or wave periods even if atmospheric conditions were equivalent. This is true in general both because R_o is a function of altitude as well as because of varying atmospheric conditions along different paths (causing ray focusing, etc.). In Section VII the above statement will be given further substantiation using the airwave data from the Holbrook Arizona Fireball which was recorded at two widely spaced stations.

Thus, even with all the previous simplifications, the problem of predicting the probability of line source airwaves is still not straight forward. If the lower sound channel is the primary route of the signal for long distance ducting then its seasonal behavior is significant. In addition meteorological disturbances in the troposphere can at times produce saturation of the sensitive pressure sensors. These conditions

are generally unpredictable. If the meteor pressure wave amplitude is large enough it may be detected if wind noise can be reduced to tolerable levels. In addition to "wind noise" effects many other natural pressure signals occur in the period range of interest. Of all of the possible natural sources in this range, microbaroms are probably the most significant (Donn and Rind, 1972), at least in middle latitudes. These signals produce a nearly continuous background to the atmospheric pressure wave environment at infrasonic frequencies between 1 and 0.1Hz. Their amplitudes are typically a few dynes/cm^2 so that the signal to noise ratio for meteor generated infrasound will rarely exceed one in the presence of microbaroms, far from the meteor. Microbaroms show diurnal, semidiurnal and season effects as well. Thus in addition to "wind noise" filters, some type of microbarom "filter" may be necessary to improve the signal to noise ratio sufficiently to increase the probability of detection. The "wind noise" problem mentioned above results from wind gusts (turbulent eddies moving with the prevailing wind) periodically producing pressure variations at the sensor. With present technology, for winds in excess of about 10 mi/hr, most "wind filters" cease to be very functional. In general then wind noise records should be obtained for each potential observing site and ultimately an area of "known" low winds should be sought. Thus, predicting areas where signals as small as 0.1 dynes/cm^2, as assumed previously, can be frequently observed, is a complicated problem.

If it is assumed that 12 sound producing meteors enter per night over the continental U. S. an estimate can then be made of how many of these could be recorded at a given airwave detection station. Assume that half are to the the west of the observer and

half are to the east. If the season is the northern hemisphere winter then the lower sound duct is defined to the east, i.e., the stratospheric winds are Westerly. Thus unless six of these events were very close to the observer only six could generate signals which could possibly duct toward the observer, i.e., only those waves originating to the West of the observer (except for small θ values). These comments apply only to the mean climatological conditions in the stratosphere and mesosphere. Conversely in the northern hemisphere summer only six per night to the East of the observer could duct in the observer's general direction. As was stated earlier other mechanism may also effect the possible ray directions but these have not been considered. Of the previously mentioned mechanisms, the bending of the rays due to the weak shock wave effects is probably the most significant in addition to the temperature and wind gradient effects presently being considered (Berthet and Rocard, to be published).

Of these six per night perhaps one will have a measureable signal at great distances from the source (under ideal atmospheric conditions in the troposphere). This last statement is probably quite subjective however. In the above estimates note that the influx rate has only been estimated using one body size, i.e., $d_{mE} \sim 20\text{-}40$ cm. Integration of the total effect however, indicates only a small contribution beyond 12 meteors per night over the continental U.S. For instance, a meteor one meter in diameter (with a mass of $\sim 1.6 \cdot 10^6$ g) is estimated from the military airwave data to occur at the rate of 1000-2000 per year over the entire earth. Compare this with the airwave estimate of 510,000 per year over the entire earth which was assumed

for bodies with d_m = 20 cm and $\rho_m \sim 3$ gm/cm^3. For a sphere if $\rho_m = 0.3$ g/cm^3, d_m would then be about 40 cm. Both of these have masses on the order of 10^4g. Thus the total effect is nearly that of the smallest size considered. Note that if the influx rate of McCrosky is used at 10^4 grams, the sound arrival estimate corresponding to ~ 1 signal/night, as given above, would become 0.083 per night (or about one signal every twelve nights). This estimate of about 30 signals per year of nights becomes about 38 signals if all masses $\gtrsim 10^4$ grams are considered.

Using the data of McCrosky (See Figure 119) the probability of occurence of sound producing meteors can be estimated from another view point. A numerical integration of the total number of encounters per unit area per unit time over the preatmospheric kinetic energy range of 10^{15} - 10^{19}ergs yields a value of about $1.25 \cdot 10^{-21}$cm^{-2}sec^{-1}. Within a circle of radius 100 km, centered about a given ground array, the number of meteor entries per year is then predicted to be 12.4. This is equal to $3.4 \cdot 10^{-2}$ entries per day (over 24 hrs.). Had the flux rate been estimated using a 10^{15}erg meteor alone, these rates would have been respectively: 9.9/yr., $2.7 \cdot 10^{-2}$/day. All of these calculations assume that the flux rate at 10^{15}ergs is $1 \cdot 10^{-21}$cm^{-2}sec^{-1}. The 10^{15} - 10^{19}erg range and beyond, constitutes roughly the expected range of line source sound producing meteors (as determined in Section III (Part 1)). The excess of about 2 meteors/yr between these two values are made up primarily of meteors which undoubtedly could be recorded (assuming average noise conditions). The remaining 10 meteors may or not be recorded depending on the attenuation effects. In addition, except for small θ, refraction effects may prevent detection at one fixed

ground station. At present knowledge of a meteor entry on any given night (via the photographic networks) is essential however, since otherwise vast amounts of continuously recorded infrasonic pressure waves would have to be analyzed using cross correlation techniques.

Thus ultimately in order to fully understand the prediction problem, four different groups of information must be considered. These are:

N_I - 1) The number of meteors per unit area, per unit time encountering the earths atmosphere, i. e. the mean influx rate.

N_{SP} - 2) Of these, the number per unit area, per unit time which produce sound. This value is limited at present by the restrictions of the line source theory.

N_G - 3) Of these, the number per unit area, per unit time which can be detected at the ground. This value is limited in addition by the ability to predict conditions at the ground such that detection may be possible.

N_D - 4) The number per unit area for which we have identifying information on any given night. This number represents the instantaneous value necessary to yield item 1) above after long term averaging. On any given night it is limited by the observing area of the photographic networks however.

Thus ultimately it is item 4) which limits the present prediction problem. Since at present this information is limited by the coverage provided by the Prairie Network, item 4) rarely exceeds about 1 meteor/night (as photographed by two or more cameras so that trajectory information can be determined; McCrosky and Posen, 1968). Of this one per night, they investigate about one of every three in great enough detail to be of use to the present problem. In addition, with respect to item 3), the Prairie Network data indicates

that 10^4 gram masses (the minimum line source ground detectable threshold) are about a factor of four less probable than 10^3 gram masses. Thus again with respect to item 4), only one event about every twelve days will be of sufficient magnitude to be worth checking in detail. This figure corresponds to about ten meteors over the winter season (120 nights) for which sufficient knowledge of the event will be available. Note that in Winter the lower sound duct is defined (on a mean basis) for areas of the Prairie Network for propagation toward Michigan. Note also that if strictly line source theory is assumed, meteors with values of ϕ from 180 degrees to about 300 degrees will be of primary interest depending on the value of θ for the entry.

If our present instrumentation technology allowed us to distinguish meteor sound arrivals (perhaps on the basis of small amplitude N like wave shapes) independent of having knowledge of the source, perhaps as many as 20 such events might be recognized at a single station over the Winter season. This estimate is based on the number of meteor entries with $E \gtrsim 15$ ergs within a 200 km radius of a given airwave detection station (based on McCrosky's N(E) influx data as discussed earlier). See Figure 119. Using the data of Shoemaker this number would increase correspondingly because of the present uncertainty in the flux rate at $m=10^4$ grams. The attenuation calculations discussed earlier indicate that the above distance range about a ground station for detectable line source airwaves with $R_o \gtrsim 10$ meters is not unreasonable. This also assumes that background noise levels are (or can be reduced to) a level of about 0.1 dynes/cm^2 (peak to peak). To more accurately refine the above estimates, much more observational and theoretical work needs to be done.

VII. THEORETICAL ANALYSIS OF EXISTING METEOR SOUND OBSERVATIONS

In the literature there are many specific reports of bright meteors producing audible sounds during entry (Nininger, 1952; Folinsbee et al., 1964, 1967 and 1969; and McCrosky, 1970 among others). The arbibrary choice of selecting certain specific cases to analyze has been made relatively easy in recent years since actual recordings of these sounds have also been made (Goerke, 1966, Lowry and Shoemaker, 1967; Millman, 1970; Öpik, 1970, Goerke, 1971). This problem actually had its modern beginnings on June 30, 1908 at about 7 a.m. local time in a remote area of the U.S.S.R. near Podkammennyy, Tunguska. The Great Siberian Meteor of 1908 as it has come to be called was audible over 600 miles from the place of the devastation (Cook, 1969) and its airwaves were recorded at several microbarograph stations in both the U.S.S.R. and Great Britain (Whipple, 1930). The dominant period of its wavetrain was in the internal gravity wave range (several minutes). This subject has been treated extensively in the Russian literature (Tsikulin, 1970). In the present analysis the restriction $R_o << H$ has been made; in the case of Tunguska, this was not the case. Thus in the present analysis only the airwaves from the smaller more commonly occuring meteors will be treated. Of the seven cases which follow, five of the meteors produced airwaves which were recorded, one of which was recorded by two stations. The other two cases, Lost City and Allende were chosen for special reasons which will be discussed shortly. In what follows then Sections IV and V (Part 2) will be used wherever possible to analyze the meteor entry with regard to the meteor sound phenomena.

A. THE BRITISH FIREBALL OF APRIL 25, 1969 (BOVEDY AND SPRUCEFIELD METEORITES)

This case was chosen for one major reason. It is the only documented case where audible sounds were recorded during a meteor entry (Millman, 1970; Öpik, 1970).

In Figure 125 the ground projection of this fireball is shown, along with suitable comments with regard to the audible sound phenomena. The ground area where the tape recording was made was some 30 km away from an area where meteorites were subsequently recovered. In Figures 126 and 127 surface weather maps near the time of fall are shown. In Figure 128 a portion of the tape recording as given by Millman (1970) is shown. The recording was made on a conventional cassette recorder which had a lower frequency cut off of about 30 Hz. In the amplitude versus time plot of Millman, dominant frequencies of 200-400 Hz are present. In addition, secondary peaks at 30-50Hz are also present. The recording was made at a point some 40-45 km perpendicular distance from the trajectory. Unfortunately amplitude information could not be obtained for the recording. In addition, the dominant frequency of the disturbance was probably below the cut off frequency of 30 Hz referred to above.

Thus while no theoretical analysis could be performed using this recording, it is by itself an impressive reminder of the great magnitude of certain natural events. The tape is quite impressive and demonstrates the multiple boom aspect of ablating bodies in supersonic flight quite distinctly. It would have been interesting to theoretically obtain a single body interpretation of the source however. In addition to the above effects, the rumbling phenomenon, which according to Wylie

(1932) and many others is similar to distant rolling thunder, is also evident on the tape.

A refraction analysis was not performed on this case even though the meteor heading was well defined. This was because θ was so small that the present refraction analysis would have been of little value. Various groups have determined θ such that: $4 \leq \theta \leq 11$ degrees. As has been shown in Section IV C. (Part 2) and as will be shown later in this section, independent of attenuation, for such small values of θ, refractive paths to the ground are very likely in almost any chosen direction with respect to the line source. In addition, the vertical temperature and wind structure up to the 500 mb level was checked and there were no conditions extraordinary enough to change the above conclusions for such small θ.

The other problem for this case relating to θ regards the upper altitude beginning of audible sounds as heard from the ground. Reports of several groups conflict whether this beginning height of audible sounds was near 100km or near about 50 km (Meighan and Doughty, 1969; Andrews et al., 1969; Hindley and Miles, 1970). In Section V (Part 2) values of this upper altitude maximum were quoted in the range 50-60km. Thus if 100 km is an accurate estimate for this fireball, it is indeed a rare exception. In addition,as was seen in Part 2, weak shock damping from 100 km downward, for a 1.0 Hz signal for example, is quite severe. Thus if 100 km is a reliable estimate of this upper altitude, this event must have been very energetic.

Even though no detailed analysis has been performed for this event, it has been included, primarily for the uniqueness of its sound recording. Observations of both audible as well as infrasonic

waves from bright fireballs may be potentially very useful. Since it is somewhat improbable that such audible sounds will ever be recorded again, the potential of infrasonic waves to study bodies from space should be more fully explored.

B. THE LOST CITY METEORITE

In Figure 129, the ground projection of the entry of the Lost City Meteorite into the atmosphere is shown. In addition the area where sonic booms were reported are noted. While sound recordings were not made in the case of Lost City (either in the audible or infrasonically), this event is one of the two existing events for which a recovered meteorite has had accurate trajectory information available (McCrosky, 1971). The other event was the Pribram meteorite referred to earlier in Section V A (Part 2) . For astronomers such trajectory information allows the orbit of the recovered meteorite, prior to the atmospheric encounter, to be accurately determined. Thus recovered material of known density can be traced to a certain set of positions in the solar system. For this analysis the concern is not with such problems however.

In Figures 130 and 131 surface and 500 mb weather maps are shown for times relatively close to the time of the meteor entry. As can readily be seen, a broad high pressure region was very evident over the central U. S.

In an effort to better understand the refraction problem involved, meteorological information on temperature and horizontal wind was tabulated in 5 km thick layers. The input data consisted of two types. First the Meteorological Rocket Network soundings (High Altitude Meteorological Data) were used wherever possible at a

location and time near the time and location of the entry. In the altitude range where such information was needed but not available, the 10 year mean data assembled from the Rocket Grenade Experiments were utilized (Theon et al., 1972). As was discussed in Part 1 of this report the temperature data was converted to the adiabatic sound speed via the relation $C = (\gamma RT/M)^{1/2} \simeq 20.06 \cdot T^{1/2}$ with C in meters/sec and T in degrees Kelvin (Bartman, 1967).

In the case of Lost City the following information was used:

1) HIGH ALTITUDE METEOROLOGICAL DATA
   White Sands, New Mexico
   January 3, 1970; 1930 GMT
   a) Temperature Information
      Available up to 30 km
   b) Wind Information
      Available up to 60 km

2) 10 YEAR CLIMATOLOGICAL MEAN DATA
   Wallops Island, Virginia - Winter
   a) Temperature Information
      From 33 to 90 km
   b) Wind Information
      From 60-90 km

As can be seen in Figure 129, the Lost City Meteorite first became visible at about 86 km altitude. Below 86 km to about 30 km altitude it was traveling faster than Mach 10. (See McCrosky, 1971). Thus the cylindrical blast wave refraction analysis shown in Figures 132 and 133 (for $\alpha = 0^{\circ}$) is valid between 30 and 86 km (assuming the Knudsen number was also sufficiently small below 86km). In Figure 132, the refraction analysis is shown for azimuth directions to the right (or Eastward) of the ground projection shown in Figure 129. In Figure 133, azimuth directions to the left (or Westward) are

shown. It should be noted at this point that in general such refraction analyses are only valid for acoustic frequencies, i.e. generally in the vicinity of the entry. This is especially true for the cases of Revelstoke and Kincardine to be discussed later in this section.

Note the results in Figures 132 and 133. In Figure 132, above 60 km, for $\Delta\phi \gtrsim 60^{o}$ from the trajectory, refractive paths to the ground are improbable. Below 60 km for $\Delta\phi \gtrsim 50^{o}$, from 48-30 km, again refractive paths to the ground are unlikely. The present theory does not predict k'(z) for $\alpha \neq 0^{o}$, i.e. below 30 km,but as α increases for fixed θ (above z''''), k'(z) should generally increase with decreasing altitude. Below z'''' for variable θ, the refraction problem is very complicated (due to the curving trajectory) and will not be considered in this analysis.

In Figure 133, a somewhat similar pattern is seen. Above 60 km, for $\Delta\phi \gtrsim 60^{o}$ refractive paths to the ground are again unlikely. Below 60 km, for $\Delta\phi \gtrsim 50^{o}$, from 38-30 km, refractive paths are also unlikely. Note that in the refraction analyses shown in this section, $\Delta\phi = 0^{o}$ is not shown, i.e. values of k(z). In all cases however, k'(z) has values far to the right for $\Delta\phi = 10^{o}$ so that refractive paths are always possible to the ground in the entry plane for all the θ, T(z), W(z) and ψ(z) values considered.

Upon checking with the late Mr. Vernon Goerke of the NOAA Geoacoustics Laboratory in Boulder, Colorado the author was informed that airwave signals from Lost City were not recorded in Boulder. This is especially interesting since the present refraction analysis (see Figure 133) shows without much doubt that directions toward Boulder were refractively possible (in terms of generally both the

upper (ground - ~ 100 km) and lower (ground - ~ 60 km) sound channels). In addition, the presence of a broad high pressure region over the area indicates that the neglect of horizontal atmospheric variations in the present refraction analysis is probably not very unreasonable, at least, for the case of Lost City.

As has been seen in Section V (Part 2) however for $R_o \lesssim 10$ meters, measurable sound arrivals at great distances from the source are not very likely. For the case of Lost City the following parameters are known:

$m \sim 25 - 30$ kg (17 kg of material were actually recovered)

$$\rho_m = 3 g/cm^3$$

By assuming a spherical shape, the radius for $m = 30$ kg is $\simeq 13.4$ cm or $d_m \simeq 26.8$ cm. Since $V_E \simeq 14$ km/sec, then $M_E \sim 47$; thus the maximum possible value of R_o is:

$$R_o \simeq M \cdot d_m \simeq 13 \text{ meters}$$

Using the above information, the fundamental frequency at $x = 10$ is:

$$f_m \simeq \frac{3 \cdot 10^2}{2.81\,(13)} \simeq 8.2 \text{ Hz}$$

Considering the fact that Boulder is about 1000 km from Lost City, Oklahoma, and from the attenuation calculations made in Section V (Part 2), it appears that one possible reason why the disturbance was not recorded in Boulder was due to energy damping as a function of altitude. For more comments on this see Section VII C. In addition, the NOAA microbarograph system responds very nonlinearly for periods less than about 1 second (Goerke, 1971). According to the

above calculations, assuming a measurable signal reached Boulder (which is unlikely from the results of the calculations however) its period would be in the appropriate range where the Boulder airwave system responds in a nonlinear manner.

Thus it would appear that the survival of a meteorite does not necessarily imply that sufficient energy was present so that airwaves can be recorded at any distance from the entry. This is especially true of Lost City since, as the refraction analysis implies, paths toward Boulder were refractively possible. Note that in the case of Lost City, the value of the kinetic energy at entry was on the order of 10^{16} ergs.

C. THE REVELSTOKE METEORITE

In Figure 134, the ground projection of the entry of the Revelstoke Meteorite into the atmosphere is shown. Again the area of sound detonations is also shown (Folinsbee et al., 1967). This is the first case of three which will be considered where sounds were both heard near the source as well as recorded infrasonically at great distances from the source (Goerke, 1971). The region shown within which violent sounds were heard is $\sim 1.2 \cdot 10^5 km^2$ as compared to about $10^3 km^2$ or less for the Lost City Event (McCrosky , 1971). In addition, seismic disturbances associated with the air blast from the event were also recorded (Folinsbee et al., 1967). Considering the magnitude of the airwaves recorded, it is interesting that the Revelstoke event produced the smallest recovered meteorite on record (Folinsbee et al., 1967). Apparently a large portion of its mass was deposited as dust in the atmosphere. This phenomena will be discussed in Section VII F, with regard to the overall energy deposition-ablation process.

While this event was not documented by the standard Prairie Network photographic techniques, it was observed by many people. From the many eyewittness accounts Folinsbee et al. concluded that at about 30 km the body disrupted (or violently fragmented) as a "point" source, but it continued on visibly (but redder) to an altitude of about 12 km as two major bodies before they ceased being visible. From their composite description it would appear that much energy was released at about 30 km ("it appeared as a brillant flash of white light"). Thus, even though a spherical blast wave solution may be more suitable for this event, since the amount of energy released in such "explosions" is generally unknown, a cylindrical blast wave line source interpretation of this phenomena will be made using the airwave data. It is interesting also to note that the time of flight for Revelstoke was approximately 8 seconds while Lost City was observed for 9 seconds. Before treating the airwave data, the refractive analyses performed will be discussed.

In Figures 135, 136 and 137, two surface maps and one 500 mb chart near the time of the Revelstoke entry are shown. As can be seen a stationary front existed in the region of Colorado. This system was not traced in detail as to deduce its movements during the time of the entry. It was a relatively weak front however.

In Figures 138 and 139, refractive analyses are shown. The following information was used to construct these figures:

1) HIGH ALTITUDE METEOROLOGICAL DATA
   Fort Churchill, Manitoba, Canada
   March 31, 1965, 2300 GMT (1700 CST)
   a) Temperature Information
      Available up to 30 km

b) Wind Information
Available up to 47 km

2) 10 YEAR CLIMATOLOGICAL MEAN DATA
Fort Churchill, Manitoba, Canada - Spring/Fall
a) Temperature Information
From 34-90 km
b) Wind Information
From 50 - 90 km

In the refraction analysis shown in Figures 138 and 139, it was assumed that from 90 km downward that cylindrical blast wave line source theory with $\alpha = 0^{o}$ was applicable. As was also the case with Lost City, below some altitude before ground impact, presumably α became nonzero. In the case of Revelstoke, due to lack of any photographic documentation,this lower altitude is not known. With the apparent "point" source detonation near 30 km of a comparitively large amount of energy however, below 30 km the line source theory is probably no longer applicable. After the detonation, a moving point source modified sonic boom theory for at least two individual bodies may then be appropriate.

From both Figure 138 (Propagation to the North of the trajectory) and Figure 139 (Propagation to the South) similar conclusions can be drawn. For $\Delta \phi \lesssim 75^{o}$ from 30 to 90 km, refractive paths to the ground were possible to both sides of the trajectory. This is primarily because of the small value of θ . It appears however that Boulder is such that $\Delta \phi > 90^{o}$ (for initially downward heading rays). While the case for initially upward heading rays has not been calculated in this case, it would appear that if the line source theory is at all applicable to this event, then attenuation for these rays must have been

relatively small (if refractive paths were possible to the ground for these rays). Since the period at maximum amplitude at Boulder was in the range of 15-18 seconds (see below) such propagation with relatively small attenuation may have been possible.

The Boulder airwave observations of this event were as follows (Goerke, 1972):

$\Delta p_{p \rightarrow p}$ = 8.0 dynes / cm^2 (peak to peak value)

τ_g = 15 seconds

χ = 331^o

R_h = 1550 km

t_o = 0715:00UT

t_D 20 minutes

See also Figs. 134 & 140, Figure 99 (Part 2) and Table 8. In the above, χ is the azimuth angle of the arrival of the disturbance as measured at Boulder toward Revelstoke, R_h is the horizontal range toward Revelstoke from Boulder, t_o is the beginning of the sound arrival in Boulder and t_D is the total duration of the airwave signal.

In the analysis which follows Δp was set equal to 4.0 dynes/cm^2 (the zero to peak value). In addition, since Shoemaker determined τ_g to be 18 seconds for the same airwave data which Goerke had access to, τ_g was set equal to an intermediate value of 16.5 seconds. Further, R_h was modified to the quantity desired, R, the total distance from source to observer, by adding 10% of R_h to R_h. Goerke determined a total range distance of 1600 km by taking the total transit time from the time of the entry to the arrival of airwaves in Boulder and dividing by a mean effective sound velocity over that entire

path (0.303 km/sec). Since cross winds were presumably quite important during the propagation (for rays initially traveling toward a Southerly direction in the presence of 50 m/sec zonal winds near 50 km) Goerke's method probably only allows part of the total propagation distance to be determined. Note that $\chi = 331^{o}$ does not intercept the known trajectory. Thus the value of R finally determined seems quite justifiable for the 1 hr and 28 minute transit time between source and observer. Note that this value, R = 1705 km, used later in the calculations represents a mean speed of 0.324 km/sec over the 88 minute transit time.

Using equation (94) from Section V (Part 2), when solving for $\overline{p^*}$, the following results (recalling that this form also assumes $x \gtrsim 10^2$ as an approximation to equation (92)):

$$\overline{p^*} = \frac{R \Delta p}{0.185 C_z \tau_m} \tag{94a}$$

Assuming $C_z = \overline{C} = 0.316 \cdot 10^5$ cm/sec., the above becomes:

$$\overline{p^*} = \frac{R \Delta p}{5.84 \cdot 10^3 \tau_m} \tag{94b}$$

with R in cm, Δp in dynes/cm^2 and τ_m in seconds to get $\overline{p^*}$ in dynes/cm^2.

Note that R_g has cancelled out of this equation since the observed value of $\frac{\Delta p}{\tau_m} = \frac{\Delta p R_g}{\tau_m}$ and R_g is also present on the right hand side of equation (92). Solving the above with the values discussed earlier, the result is:

$$\overline{p^*} = \frac{(1.71 \cdot 10^8 \text{cm})\ (4.0\ \text{dynes/cm}^2)}{5.84 \cdot 10^3 \left(\frac{\text{cm}}{\text{sec}}\right)\ (1.65 \cdot 10^1 \text{sec})} = 7.08 \cdot 10^3 \text{dynes/cm}^2$$

At this point however two points should be noted. Equation (94a) assumes both that D(R) = 1 as well as that the propagation occurred as a weak shock wave of cylindrical symmetry over the entire path between the source and the observer. Calculations of d' (equation (57)) revealed that at the ground at Boulder, the wave was definitely linear. This calculation is made as follows:

$$d' = \frac{C_g\ \tau_g}{34.3\ \frac{\Delta p}{p_g}} = \frac{(0.316 \cdot 10^5 \text{cm/sec})\ (1.65 \cdot 10^1\ \text{sec})}{(3.43 \cdot 10^1)\ \left(\frac{4\ \text{dynes/cm}^2}{1.013 \cdot 10^6\ \text{dynes/cm}^2}\right)}$$

or $d' = 3.86 \cdot 10^4 \text{km}$

where $\frac{\Delta p}{p_g} = 3.95 \cdot 10^{-6}$

Thus somewhere between Revelstoke and Boulder the wave propagation became linear. As was seen in Section V D (Part 2) this transition distance depends in general both on the source altitude as well as upon f_m (through R_o).

For disturbances generated by an instantaneous release of energy, D(R) should be included in (94a). The results of weak shock damping in Part 2 indicate that below certain altitudes ($\sim$ 70 km) for $R_o \gtrsim$ 10 meters, D(R) as calculated for weak shock waves is only a slowly varying function of source altitude. Thus by assuming a value of D(R) to be used in (94a), a determination of $\overline{p^*}$ (or eventually z_z) is not greatly jeopardized. Assuming then for Revelstoke that over a

1705 km path, D(R) for weak shock waves for $\overline{\tau}_m \sim 10$ seconds (a mean value of τ_m) is ~ 0.08, equation (94a) becomes:

$$\overline{p^*} = \frac{R \Delta p}{0.185 \cdot \overline{C} \cdot \tau_m \cdot D(R)} \tag{94c}$$

Thus equation (94b) becomes:

$$\overline{p^*} = \frac{R \Delta p}{4.68 \cdot 10^2 \tau_m} \tag{94d}$$

The earlier calculated value of $\overline{p^*}$ then becomes:

$$\overline{p^*} = 8.83 \cdot 10^4 \text{ dynes/cm}^2$$

But $$\overline{p^*} = (p_g p_z)^{1/2}$$

Assuming $p_g = 1.01325 \cdot 10^6$ dynes/cm^2

$$p_z = \overline{p^*}^2 / p_g = \frac{(8.83 \cdot 10^4)^2}{(1.01325 \cdot 10^6)} = p_z = 7.70 \cdot 10^3 \text{ dynes/cm}^2$$

Using Table 5 (Part 2), the source altitude then becomes: (for the assumed isothermal atmospheric model)

$$z_z \simeq 37 \text{ km}$$

Notice the relatively good agreement between this value and the 30 km "burst" altitude discussed earlier. If a line source model is applicable for this case note that at Boulder R exceeds ℓ (ℓ is at most

a few hundred km). In all the cases considered here, except perhaps for Section VII G , note that R probably exceeds ℓ. Thus spherical decay may have been appropriate for a linear disturbance at least over part of the propagation. Such decay has not been calculated in this analysis. If the source was primarily spherical in nature and propagation took place in a two-dimensional duct (or waveguide) between the source and the observer, then cylindrical decay would be appropriate far from the "point" source. This is also true for disturbances generated by spherical nuclear explosions in the atmosphere. In the latter case however this results because of the long wavelengths generated in comparison to H.

Since d' calculations at the ground for all the airwave data used in this report reveal that the disturbances recorded were linear, the results using (94c) to determine $\overline{p^*}$ and thus z_z are not applicable here. Therefore another method was needed to determine $\overline{p^*}$. This approximate method will be discussed shortly. Even though Revelstoke and Kincardine were probably "point" energy releases, a line source theory interpretation will be made for later comparison with all the other results.

Note that had the elevation angle across the array been determined, ray tracing techniques could have been used through an assumed atmospheric model to determine z_z. Throughout this analysis ray tracing techniques have not been carried out, even if the elevation arrival angle across the array was known. Such techniques will be used in a later report for sound arrivals from meteor entries where more precise trajectory information is available.

In Section V (Part 2), a comment was made with regard to reinitialization of equation (93) after equation (92) if first used. A

general form of this reinitialization can be written as (if d' is initially small compared to d_a):

$$\Delta p_{z\rightarrow g} = \Delta p_{z\rightarrow t} \cdot D_L(R)_{t\rightarrow g} \cdot \left(\frac{\overline{p^*}_{z\rightarrow g}}{\overline{p^*}_{z\rightarrow t}}\right)\cdot\left(\frac{x_{z\rightarrow t}}{x_{z\rightarrow g}}\right)^{\frac{1}{2}} \quad (95)$$

where

$\Delta p_{z\rightarrow g}$ = ground observed overpressure

$\Delta p_{z\rightarrow t}$ = overpressure at transition altitide (transition from weak shock to linear propagation)

$D_L(R)_{t\rightarrow g}$ = linear absorption from transition altitude to the ground (as in equation (92b))

$\overline{p^*}_{z\rightarrow g} = (p_z p_g)^{1/2}$ = geometric mean pressure between source and observer

$\overline{p^*}_{z\rightarrow t} = (p_z p_t)^{1/2}$ = geometric mean pressure between source and the transition altitude

$x_{z\rightarrow t} = \frac{R_{z\rightarrow t}}{R_o}$ = scaled distance from source (x = 1) to the transition altitude

$x_{z\rightarrow g} = \frac{R_{z\rightarrow g}}{R_o}$ = scaled distance from source to observer

In addition, for $x \gtrsim 10^2$:

$$\Delta p_{z\rightarrow t} = \frac{0.2917\cdot \overline{p^*}_{z\rightarrow t} \cdot D_{ws}(R)_{z\rightarrow t}}{x_{z\rightarrow t}^{3/4}} \quad (95a)$$

where

$D_{ws}(R)_{z\rightarrow t}$ = weak shock absorption from source altitude to the transition altitude (as in equation (92a)).

Using the above two equations in conjunction with equation (91), two equations in three unknowns can eventually be written (see (103) and (104)). These equations are derived from:

$$\tau_g = 0.562\ \tau_{mo}\ (x_{z\to t})^{1/4} \tag{96}$$

$$\Delta p_{z\to g} = \left[\frac{0.2917 \cdot \overline{p^*}_{z\to t} \cdot D_{ws}(R)_{z\to t}}{x_{z\to t}^{1/4}}\right] D_L(R)_{t\to g} \cdot \frac{\overline{p^*}_{z\to g}}{\overline{p^*}_{z\to t}} \cdot \frac{1}{x_{z\to g}^{\frac{1}{2}}} \tag{97}$$

Rewriting the above in terms of R_o, R (or $R_{z\to g}$) and $R_{z\to t}$, yields:

$$\tau_g = 0.562\ \left(\frac{2.81}{C_z}\right)^{3/4} R_o^{1/4} R_{z\to t} \tag{98}$$

$$\Delta p_{z\to g} = \left[\frac{0.2917\ D_{ws}(R)_{z\to t}}{R_{z\to t}^{1/4}} \cdot R_o^{3/4}\right] \cdot D_L(R)_{t\to g} \cdot \overline{p^*}_{z\to g} \cdot \frac{1}{R_{z\to g}^{1/2}} \tag{99}$$

Solving (98) and (99) for $R_o^{3/4}$ yields:

$$R_o^{3/4} = \frac{\tau_g\ C_z}{(0.562)(2.81)\ R_{z\to t}^{1/4}} \tag{100}$$

$$R_o^{3/4} = \frac{\Delta p_{z\to g}\ R_{z\to g}^{\frac{1}{2}}\ R_{z\to t}^{\frac{1}{4}}}{0.2917 \cdot D_{ws}(R)_{z\to t} \cdot D_L(R)_{t\to g} \cdot \overline{p^*}_{z\to g}} \tag{101}$$

Equating (100) and (101) and solving the result for $R_{z \rightarrow t}$, the following equation is obtained:

$$R_{z \rightarrow t} = \frac{1}{R_{z \rightarrow g}} \left(\frac{\tau_g \; C_z \cdot 0.2917 \cdot D_{ws}(R)_{z \rightarrow t} \cdot D_L(R)_{t \rightarrow g} \cdot \overline{p^*}_{z \rightarrow g}}{0.562 \cdot 2.81 \cdot \Delta p_{z \rightarrow g}} \right)^2 \tag{102}$$

Assuming $C_z = \overline{C} = 3.16 \cdot 10^4$ cm/sec (isothermal atmosphere value) and evaluating the constants, the above becomes:

$$R_{z \rightarrow t} = \frac{3.41 \cdot 10^7}{R_{z \rightarrow g}} \left(\frac{\tau_g \cdot D_{ws}(R)_{z \rightarrow t} \cdot D_L(R)_{t \rightarrow g} \cdot \overline{p^*}_{z \rightarrow g}}{\Delta p_{z \rightarrow g}} \right)^2 \tag{103}$$

In equation (103), the following quantities are known:

1) $\tau_g \simeq 16.5$ seconds

2) $\Delta p_{z \rightarrow g} \simeq 4.0$ dynes/cm^2 (zero to peak value)

3) $R_{z \rightarrow g} \simeq 1.705 \cdot 10^8$ cm

Note that in (103) the remaining parameters, $D_{ws}(R)_{z \rightarrow t}$, $D_L(R)_{t \rightarrow g}$, and $\overline{p^*}_{z \rightarrow g}$ are not free parameters. This is true since the solution to (103) is valid only such that:

$$R_o < R_{z \rightarrow t} \leq R_{z \rightarrow g} \tag{104}$$

Note however that when (103) is solved R_o, has not yet been determined. Thus the lower bound of (104) is difficult to evaluate.

Of the above three remaining parameters, the two damping parameters are the easiest to approximate. Since τ_g is known and

as was mentioned earlier at altitudes below about 70 km for $R_o \gtrsim 10$ meters, the D(R) terms are primarily functions of f_m and not z_z, the D(R) terms can be estimated. The $\overline{p^*}_{z\to g}$ term can then be varied so that (104) is physically satisfied. Note that the procedure used in (95)-(104) above can also be used to produce an equation analogous to (94c). This can be written as:

$$\frac{\Delta p_{z\to g}}{\tau_g} = \frac{0.185 \cdot \bar{C} \cdot \overline{p^*}_{z\to g} \cdot D_{ws}(R)_{z\to t} \cdot D_L(R)_{t\to g}}{R_{z\to g}^{1/2} \cdot R_{z\to t}^{1/2}} \qquad (105)$$

Thus for the more general case where Δp is both reduced by absorption mechanisms and the observed signal has finally become linear, $R_{z\to g}$ is replaced in (94) by $R_{z\to g}^{1/2} \cdot R_{z\to t}^{1/2} / D_{ws}(R)_{z\to t} \cdot D_L(R)_{t\to g}$.

Recall that in Section V D, z_z and R_o were assumed known (as was $\bar{\epsilon}$) and all other quantities were calculated from a knowledge of these. The reverse problem is evidently not as straight forward. This is true in part because $R_{z\to g}$ must include z_z, i.e. it is the total slant distance between source and observer. For a nonducted straight line path, $R_{z\to g} = (R_h^2 + z_z^2)^{1/2}$. In (94) it has been assumed that $R_h >> z_z$ so that $R_{z\to g} \simeq R_h$. Thus the increasing of R_h by $0.1\, R_h$ was done to account somewhat for the generally longer ducted ray path between the source and the observer. Note then, within the limits imposed by (104), $\overline{p^*}_{z\to g}$ can be decreased (higher source altitude) and $R_{z\to t}$ will become smaller. For direct ray paths between z_z and the observer, (103) can be written in the form:

$$R_{z\to t} = \frac{3.41 \cdot 10^7 \cdot p_g \cdot p_z}{(R_h^2 + z_z^2)^{\frac{1}{2}}} \left(\frac{\tau_g \cdot D_{ws}(R)_{z\to t} \cdot D_L(R)_{t\to g}}{\Delta p_{z\to g}} \right)^2 \qquad (106)$$

where $p_g = 1.01325 \cdot 10^6 \text{dynes/cm}^2$ for the assumed isothermal atmospheric model

Note that with the above form (although it is less useful for present purposes) additional restraints are imposed on $R_{z \rightarrow t}$ since as p_z decreases, if $z_z \sim R_h$, the total distance between the source and the observer also increases. At present however use has been made of (103) with p_g having the value given above.

For $R_{z \rightarrow t} < R_{z \rightarrow g}$ (see below), with $\overline{\tau}_m = 10$ seconds, $D_{ws}(R)_{z \quad t}$ is approximately 0.1. In addition, $D_L(R)_{t \rightarrow g} \sim 0.5$. As was noted earlier, linear damping is also a slowlying varying function of altitude (below $\sim$ 60 km for $R_o \gtrsim 50$ meters). Thus the method being used here is not applicable for meteors with relaxation radii below some 50 meters and at high source altitudes. Thus, for Revelstoke (103) can now be written as: $R_{z \rightarrow t} = 8.63 \cdot 10^3 p_z$

Since the lower bound of (104) is yet unknown, an assumption will now be made with regard to the relationship between $R_{z \rightarrow t}$ and $R_{z \rightarrow g}$. From the d' calculations made in Section V(Part 2), $R_{z \rightarrow t} \sim \frac{2}{3} R_{z \rightarrow g}$. For long ducted ray paths, this value is probably an upper limit. For the present then it will be assumed that $R_{z \rightarrow t} = 0.5 \cdot R_{z \rightarrow g}$. From the above equation, p_z (and z_z) can then be determined as:

$$p_z = 9.88 \cdot 10^3 \text{ dynes/cm}^2$$

$$z_z = 34 \text{ km}$$

Using $R_{z \rightarrow t} = 852.5$ km, R_o can be determined from equation (100).

$$R_o = \frac{1}{R_{z \to t}^{1/3}} \left(\frac{\gamma_g \bar{C}}{1.579} \right)^{4/3} = 5.186 \cdot 10^2 \text{meters}$$

With knowledge of R_o, several quantities can be ascertained about the meteor which produced the airwaves. Since $R_o \simeq M \cdot d_m$, if M can be estimated, d_m can be determined. If a shape and meteor density are assumed, the mass can also be deduced. Knowing the mass and the velocity (from an isothermal atmospheric model using M from above) the kinetic energy can also be determined. In addition E_o can be deduced from R_o using the isothermal model from above. These quantities are determined as follows:

1) From the data of Folinsbee et al., $M \simeq 38$, i.e. $V \simeq 12$km/sec.

$$\therefore \quad d_m \simeq \frac{R_o}{M} = \frac{518.6}{38} = 13.7 \text{ meters}$$

2) $$m = \rho_m \frac{4}{3} \pi \left(\frac{d_m}{2} \right)^3$$

Using $\rho_m = 3 \text{g/cm}^3$; Revelstoke was a Type I carbonaceous chrondite (Folinsbee et al., 1967), yields $4.0 \cdot 10^9$ grams.

3) $E_z = \frac{1}{2} m V^2 = 2.9 \cdot 10^{21}$ ergs (not the preatmospheric value, but that available at the time of the explosion). As was noted in Section V B (Part 2), Shoemaker estimated E_z as $10^{19} - 10^{20}$ ergs (Carr, 1970). Note however that an order of magnitude uncertainty in d_m produces at least two orders of magnitude uncertainty in E_z even if V is known accurately. Considering all the approximations

made up to this point, these estimates of uncertainty are probably not unreasonable in d_m and E_z.

4) $E_o = R_o^2 \pi p_z = (5.186 \cdot 10^4 \text{cm})^2 \pi \ (9.88 \cdot 10^3 \text{dynes/cm}^2)$

$E_o = 8.4 \cdot 10^{13}$ ergs/cm

This concludes the discussion for the Revelstoke Meteorite. In Section VII D, E and G , similar analyses are possible. Rather than repeating the above method, the results will be summarized in Table 8. Airwave data will be listed in each part as before however. In Section VII F, no airwave data is available (at least in the unclassified literature), but a refraction analysis and a discussion of the Allende event will be presented.

D. THE HOLBROOK ARIZONA FIREBALL

In Figure 141, the ground projection of the entry of the Holbrook Arizona Fireball into the atmosphere is shown (Goerke, 1972). The general area where sounds were reported is also shown (Shoemaker, 1972). This is the second case where sounds were both heard near the source and recorded infrasonically far from the source. In addition, the Holbrook event was recorded infrasonically both near Flagstaff (Shoemaker, 1972) as well as in Boulder (Goerke, 1972).

Again, to the authors knowledge, this event was not photographed. Reports of this bright fireball appeared in at least two newspapers in Arizona however (in the "Flagstaff Sun" and Phoenix newspapers). This event was also entered into the Smithsonian Institution, Center For Short-Lived Phenomena as event notification reports no. 293 and 300. Unfortunately a description comparable to that of

Revelstoke (in terms of changes with altitude) for this fireball has not appeared to the authors knowledge in the open literature.

In Figures 142 and 143, surface and 500mb charts for the time of Holbrook are shown. As was the case with Lost City, a broad high was centered in the Southwestern U. S.. Since θ was unknown for this case, two values were chosen for the refraction analysis, namely 20 and 40^{o}. For angles much greater than 40^{o}, the event would probably not have been as widely seen (or as bright). In addition for θ much greater than 40^{o}, the refraction analysis in Section IV C. (Part 2) indicates that in general ground arrivals out of the entry plane are unlikely. Thus if the line source theory is reasonable to apply to this case, θ in the range 20 to 40^{o} is also reasonable. In Figures 144-147, two refraction analyses are shown for these two different θ values. The first group is for $\theta = 20^{o}$; the second is for $\theta = 40^{o}$. In Figure 144 azimuth directions to the North of the trajectory are shown (as is also the case in Figure 146). In Figures 145 and 147 azimuth directions to the South of the trajectory are shown.

The data necessary to construct these figures came from the following sources.

1) HIGH ALTITUDE METEOROLOGICAL DATA
   White Sands, New Mexico
   December 13, 1968, 1900 GMT
   a) Temperature Information
      Available up to 59 km
   b) Wind Information
      Available up to 64 km

2) 10 YEAR CLIMATOLOGICAL MEAN DATA

Wallops Island, Virginia - Winter

a) Temperature Information

From 60 - 90 km

b) Wind Information

From 65 - 90 km

Again it was assumed that below 90 km the line source refraction analysis was valid. As before, the lower altitude limit where α became nonzero is also unknown. In both Figures 144 and 145, for $\Delta\phi \gtrsim 70^{\circ}$, refractive paths to the ground were unlikely. As can be seen in Figure 141, for the $\Delta\phi$ values for which allowed paths to the ground exist, refractive paths toward Boulder also exist. In the case of the Flagstaff observations, either the fireball detonated as a "point" source or again the upward heading rays (from the line source theory) may account for the presence of sound arrivals (as may have also been the case with Revelstoke). Note also that an exact determination of the endpoint for Holbrook was not made. Had the flight continued slightly further than shown in Figure 141, downward rays from a line source could also have produced the arrivals.

In Figures 146 and 147 similar conclusions can be drawn also. In these cases however due to the larger θ value chosen, the values of $\Delta\phi$ for which refractive paths to the ground exist are generally such that $\Delta\phi \lesssim 55^{\circ}$. It is unfortunate in this case that θ was not determined since the airwave recordings were available from two widely spaced stations. Had θ been determined a fair test of the applicability of the line source theory could have been made. In what follows, the two airwave observations of this event will be referred to respectively as Holbrook - F (Flagstaff) and Holbrook - B (Boulder).

In Figures 148 and 149 the Holbrook - F and Holbrook - B airwave recordings are shown (Shoemaker, 1972; Goerke, 1972). The airwave data is listed below for these two observations for convenience.

Holbrook - F

$\Delta p_{p \to p} = 0.5$ dynes/cm^2

τ_g = 4 seconds

χ - This was apparently not determined but $\sim 115^o$ would appear reasonable

$R_h \simeq$ 134 km

$t_o \simeq$ 1:39 a. m. M. S. T.

$t_D \simeq$ 12 seconds

Holbrook - B

$\Delta p_{p \to p} = 2.2$ dynes/cm^2

τ_g = 2 - 3 seconds (2.5 sec. was used in the calculations)

$\chi = 216 \pm 2^o$

$R_h \simeq$ 720 km (This also was not determined but is being estimated by the present author).

t_o = 2:22:25 a. m. M. S. T.

$t_D \simeq$ 10 seconds

In addition to the above data, Goerke (1972) reported the trace velocity of the disturbance, V_T, across the array as 410 m/sec. This implies that the elevation angle, β', across the array was on the order of 43^o, assuming C = 300m/sec and no wind. This fact will be discussed further shortly (where $\cos \beta' = C/V_T$).

As before the Δp values used were assumed to be one half of the peak to peak values quoted. Also again $R_{z \to g}$ was determined

using $R_{z \rightarrow g} = R_h + .1\, R_h$. The propagation travel times were respectively $\sim$ 7 minutes and $\sim$ 43 minutes for Holbrook - F and Holbrook - B. Note in the case of Holbrook-B that although ℓ is unknown R certainly exceeds ℓ.

Knowledge of $\overline{p^*}_{z \rightarrow g}$ in this case might be inferred by reverse ray tracing techniques from the Boulder data since both χ and β' were determined. In other words an assumed atmospheric model allowing for cross winds might be used to trace the ray back to the altitude region where it would intersect the trajectory. Unfortunately since ϑ is unknown in this case as is the exact trajectory endpoint, such ray tracing would prove to be relatively useless.

According to Goerke (1972), $\beta' = 43^o$ implies that the signal may have traveled in a sound channel via the ground and the 100 km region. In the Holbrook - F observation, since χ and β' were apparently not determined, little can be said regarding z_z. It is interesting however to note that the value of Δp in the case of Holbrook - F is about a factor of four less than the Holbrook - B observation. This may imply either that the value of z_z for Holbrook-F exceeded that of Holbrook-B, i.e. different damping occurred as a result, or R_o may have varied significantly along ℓ, so that the two stations did not receive signals from an equivalent source. Note that the first implication is opposite ot the observational facts, i.e. the meteor was decreasing in altitude going toward Holbrook. Note however that a decrease in energy of the source is reasonable as the meteor headed deeper into the atmosphere toward Holbrook. In addition, as was discussed before, a "point" explosion may also have occurred.

Throughout this analysis it has been assumed that the

recorded airwaves were initiated by a cylindrical blast wave source model. In the lower Mach number limit ($\lesssim$ Mach 10) as total breakup possibilities increase for deeper penetration into the atmosphere the above source model assumption becomes far less realistic. Thus application of the present theory, independent of line or point source geometry may not always be appropriate. The apparent discrepancy between the amplitudes of the Holbrook-F and Holbrook-B data amply illustrate the above point. In addition to difficulties in specifying source characteristics as a function of altitude, atmospheric refraction and subsequent ray focusing effects (especially near z'''' as the trajectory rapidly approaches $\theta = 90^{o}$) may also be of great significance.

As was the case with Revelstoke, d' calculations reveal that both Holbrook - F and Holbrook - B were recorded as linear waves. See Table 8 for a summary of the results obtained using the Holbrook-F and Holbrook - B airwave data (assuming V = 11.2 km/sec). In the calculations as before it was assumed that $R_{z \rightarrow t} = 0.5\, R_{z \rightarrow g}$. Had $R_{z \rightarrow t}$ been assumed equal to $R_{z \rightarrow g}$, a 30% decrease in R_o would result. Allowing $R_{z \rightarrow t}$ to be a smaller fraction of $R_{z \rightarrow g}$, still larger values of R_o would result. Note that for Holbrook -F a source altitude 30 km above that of Holbrook - B was finally determined. In addition, rather large damping ($D_L(R)_{t \rightarrow g} = 0.1$) was also assumed.It appears that the Holbrook-F and the Holbrook - B observation are not consistent, at least using the present theoretical analysis. Temperature and wind gradient effects have not been included in the present theory however. In addition, as was noted in Section V(Part 2), it is difficult to interpret airwave data with regard to energy or size predictions over long ducted ray paths due to the atmospheric dispersion of the wave

energy. In the case of Holbrook - F, Shoemaker (1972) estimated that the airwave data suggested a "point" source of energy equivalent to 100-200 tons of TNT ($\sim 2.5 \cdot 10^{18}$ ergs). The present line source interpretation of the Holbrook-B airwave data agree quite well with this estimate. The Holbrook-F data interpreted using line source theory tends to overestimate this value however.

In the analysis shown in Section VII C, it was assumed that $R_{z \rightarrow t} = 0.5\, R_{z \rightarrow g}$. It is possible however to calculate d' along the path of the airwaves assuming a mean value for τ_m. The expression determined for d' is as follows:

$$d' = \frac{\bar{C}\ \bar{\tau}_m \cdot R^{1/2}}{34.3 \cdot k_1 \left(\frac{p_z}{p_o}\right)^{1/2} \cdot D_L(R)_{z \rightarrow g} \cdot \left(\frac{C_z\ \tau_{mo}}{2.81}\right)^{1/2}} \qquad (107)$$

where

$R_o^{1/2} = \left(\frac{\tau_{mo} C_z}{2.81}\right)^{1/2}$ from equation (78) defining R_o

$D_L(R)_{z \rightarrow g}$ = linear damping (absorption) term as given by (92b)

Note however that $\tau_m \neq \bar{\tau}_{mo}$. Thus it is difficult to use (106) to calculate $R_{z \rightarrow t}$ very accurately. At the present, considering all the other uncertainties, it is adequate to assume $R_{z \rightarrow t} = 0.5\, R_{z \rightarrow g}$ in the calculations.

As can be seen in Table 8, the Holbrook Arizona Fireball, although quite large and energetic, was at least an order of magnitude less massive than the case of Revelstoke. Present theoretical results (and interpretations) do not allow a more accurate assessment of this uncertainty to be made.

E. THE KINCARDINE FIREBALL

In Figure 150 two ground projections of the possible entry of the Kincardine fireball are shown (Chamberlin, 1968; Goerke, 1972). This case is the third example of a fireball entry where sounds were both heard in the vicinity of the entry and recorded infrasonically at great distances from the source. Again, the ground area near the source where detonating sounds were heard is also indicated.

In the case of Kincardine, at least two photographs were taken (Chamberlin, 1968). These photographs indicate that a substantial amount of energy was released (as in a "point" source), possibly below 20 km. The trajectory above the burst altitude appears relatively uniform in comparison with the intenseness of the light near the end of the trajectory (Goerke, 1966). Thus again, the amount of energy released near the end of the flight probably exceeded the line source energy deposition. For consistency however this event will also be interpreted using a cylindrical blast wave line source model of the airwaves which subsequently arrived in Boulder. Estimates of the flight time of this fireball range from five to ten seconds or more (Chamberlin, 1968).

Unfortunately in the case of Kincardine, the meteorites, if any reached the surface, probably fell into Lake Huron. Thus as was also assumed for Holbrook, the density range 0.3 - 3g/cm^3 was later used in order to calculate meteor parameters from the airwave data. Before considering these calculations, the refractive analyses performed will first be discussed.

In Figures 151, 152 and 153, two surface maps and one 500mb chart near the time of the Kincardine entry are shown. As was also the case with Holbrook, a broad high existed (over a major third of the Eastern U. S.) during the general period of the airwave detection.

In Figures 154 and 155, refractive analyses were again performed. The data from the following sources were used to construct these figures.

1) HIGH ALTITUDE METEOROLOGICAL DATA
   Wallops Island, Virginia
   September 17, 1966 0402 GMT
   a) Temperature Information
      Available up to 52 km
   b) Wind Information
      Available up to 51 km

2) 10 YEAR CLIMATOLOGICAL MEAN DATA
   Wallops Island, Virginia - Spring/Fall
   a) Temperature Information
      From 53 - 90 km
   b) Wind Information
      From 55 - 90 km

In the analyses shown in Figures 154 and 155, it was assumed that below 90 km $\alpha = 0^{o}$ was applicable for the fireball entry. Below about 20 km, the "point" source burst invalidates the above assumption however.

In Figure 154, Propagation to the South of the trajectory is considered. In Figure 155, Propagation to the North is considered. From both figures similar conclusions can be drawn. In Figure 154, for $\Delta\phi \lesssim 60^{o}$, refractive paths toward the ground are probable for all source altitudes. This is also true in Figure 155. Note that the case $\Delta\phi = 70^{o}$ is not symmetric about the trajectory with respect to allowing ground arrivals. In Figure 154, the wavefronts originating in the region from 33 to 60 km for $\Delta\phi = 70^{o}$ can reach the ground via refraction. In Figure 155, this altitude region extends from 35-85 km. In general, it is the small θ value which produces the optimistic refraction picture for most directions.

Note again that directions toward Boulder via a line source theory (with initially downward heading rays) are not refractively possible. As before however, refractive interpretations could also be made using initially upward heading rays (for a line source), or using the source geometry appropriate for a "point" energy release. Due to the large amount of energy released near the end of the flight in the case of Kincardine, the latter interpretation would probably be more correct however.

The airwaves from this fireball were recorded in Boulder, Colorado by Goerke (1966) after about a two hour transit time. The airwave data on this fireball are as follows:

$\Delta p_{p \to p} = 2.5$ dynes/cm^2

$\tau_g = 54$ seconds

$\chi = 75 \pm 2^o$

$R_h = 2270$ km (as measured from Boulder to a mean distance along the trajectory as determined by Chamberlin)

$t_o = 02{:}49$ UT

$t_D = 34$ minutes

In Figure 156, the airwaves from this fireball are shown (Goerke, 1966).

According to Goerke the value of χ indicates that the airwaves came from an altitude in the vicinity of 50 km (assuming Chamberlin's derived trajectory is correct). The photographs indicate that a substantial amount of energy was released near 20km however. In the calculations shown in Table 8, a source altitude of 64 km was eventually determined assuming that $D_{ws}(R)_{z \to t} = 0.1$, $D_L(R)_{t \to g} =$

0.5 and $R_{z \rightarrow t} / R_{z \rightarrow g} = 0.5$. The present weak shock and linear absorption theories used assume however that $\gamma H >> \Lambda$, i.e. the ordinary irrotational longitudinal acoustic wave approximation. Since at 54 seconds period the above inequality is not satisfied, the earlier absorption decay is not strictly applicable to this large a period. Thus the results determined in the case of Kincardine, independent of point or line source theory are probably not very dependable. Further work using an acoustic-gravity wave guide mode theory interpretation in the case of Kincardine appears warranted.

In addition, the observed signal in Boulder probably followed a combination of ducted paths. This would account for the long dispersive wave train that was recorded. Apparently light Easterly winds (assuming "point" source theory) above 50 kilometers may have prevented the signal from arriving at the former NOAA microbarograph station in the vicinity of Rockville, Maryland (Woodward and Goerke, 1967). Note also that d' calculations reveal that the disturbance recorded in Boulder was linear. This was true of all the airwave recordings treated in this report. Thus again $R_{z \rightarrow t}$ must be determined. This was done as before using the method as first discussed in Section VII C.

Before ending this case two interesting points should be noted. The first is that Kincardine was apparently more energetic than the case of Revelstoke. The long period, 54 seconds, implies a large energy release; however since R_s is inversely related to $p_z^{1/3}$, the large value of τ_g may be partly due to a higher altitude energy release than that of Revelstoke. In addition, multipath dispersion effects can also influence τ_g (and thus energy estimates). Thus the nearly

50 meter diameter estimate of Kincardine is not to be interpreted as very realistic.

The second point is a description made available by an observer of Kincardine of the sound phenomena produced by an entering fireball. From Chamberlin (1968), the following quote stands out with regard to this event: "We would put the time from sixty to ninety seconds after the brightness when we heard the first 'explosion.'.... The noise was unlike anything we had heard before. It was not a steady rumble or roar, and it was not one distinct crash. It was not like thunder. It could be compared to systematic cannon fire, or distant drum beats on very large drums. It was very audible and very grotesque, and there were definite pauses between noises." (Mrs. John E. Guza, Bad Axe, Michigan, September 22, 1967).

This concludes the treatment of the Kincardine Fireball. The excellent description above provided via Chamberlin (1968), amply points out just how complex the meteor sound phenomena is. Note that in the case of Holbrook, Kincardine and in VII G (The Alaskan Fireball of December 19, 1969), V = 11.2 km/sec was assumed during the calculations for d_m, E_z, etc. If V was actually larger than this value, d_m, E_z, etc. would be correspondingly reduced and visa versa.

F. THE ALLENDE METEORITES

In Figure 157, the ground projection of the entry of the Allende fireball is shown (Fireman, 1969; Carr, 1970). Observations of both explosions as well as strong seismic disturbances in the vicinity of the fall (within $\sim$ 125 miles from where the many meteorites were found) were also reported. The seismic effects may have included both

direct P and S waves from earth impact as well as air-coupled Rayleigh waves as was discussed briefly in Part 1 of this report. According to Carr (1970), this event was not observed infrasonically by Shoemaker in Flagstaff, Arizona at the U. S. Geological Survey microbarograph station. Apparently the Boulder NOAA microbarographs also didn't record the airwaves from Allende (Goerke, 1972).

In the case of Allende, observers reported the color of the fireball as bluish white. It broke up eventually into two large pieces (each of which exploded), but the altitude of the "explosion" was apparently not determined. From the values on estimated preatmospheric mass and energy (as computed by McCrosky and his associates at the Smithsonian Astrophysical Observatory in Cambridge, Mass.), the size of the Allende event can be estimated as (assuming a spherical shape):

$$d_m = 2 \cdot \left(m / \rho_m \frac{4}{3} \pi \right)^{1/3} = 1.08 \text{ meters}$$

where

$m \simeq 2 \cdot 10^6$ grams ($5 \cdot 10^5$ grams were actually recovered)

$\rho_m = 3 \text{g/cm}^3$ (a Type III Carbonaceous chrondite)

Using the energy estimate from Carr (due to McCrosky and his associates) the velocity of Allende can be estimated as:

$$V = \left(2E/m \right)^{1/2} = 31.6 \text{ km/sec}$$

where

$E \simeq 1\text{-}4 \cdot 10^{19}$ ergs ($2 \cdot 10^{19}$ ergs was used in the above calculation) This is an estimate of the preatmospheric kinetic energy.

Assuming as before, C = 0.316km/sec. (M = 100), then a calculation of R_o reveals that:

$$R_o = 108 \text{ meters}$$

$$\therefore \quad \tau_{m_o} (\text{at } x = 10) = \frac{2.81 \cdot 108}{316} = 0.960 \text{ seconds}$$

At $x = 10^4$ (assuming nonlinear spreading of τ persists to that scaled distance),

$$\tau_m = 0.562 \quad \tau_{m_o} (10^4)^{1/4} = 5.4 \text{ seconds}$$

Note that with R_o = 108 meters, $x = 10^4$ corresponds to R = 1080 km from Allende. Flagstaff is about 1100 km from the ground impact area of Allende (The Boulder microbarograph station is about 1450 km from the impact area of Allende). Thus on the basis of attenuation as a function of distance at least, propagation toward either station and eventual detection seems possible.

There are three additional aspects of Allende that should be considered however. The first is a refraction analysis using line source theory. The second is a consideration of the area weather pattern at the time of the event and the third relates to the altitude of the "explosions." The refraction analysis will be presented first.

In Figures 158-161, two surface maps and two 500 mb charts near the time of the Allende entry are shown. These will be discussed shortly.

The data used to perform the refraction analyses shown in Figures 162 and 163 came from the following sources:

1) HIGH ALTITUDE METEOROLOGICAL DATA
White Sands, New Mexico
February 7, 1969 2315 GMT
a) Temperature Information
Available up to 62 km
b) Wind Information
Available up to 62 km

2) 10 YEAR CLIMATOLOGICAL MEAN DATA
Wallops Island, Virginia - Winter
a) Temperature Information
From 63 - 90 km
b) Wind Information
From 65 - 90 km

In Figures 162 and 163 the refraction analyses are presented. Figure 162 shows azimuth intervals to the West of the trajectory. Figure 163 shows azimuth intervals to the East of the trajectory. In both figures, the small θ value allows refractive paths to the ground from all altitudes for $\Delta\phi \lesssim 75^{\circ}$. Again it is assumed that $\alpha = 0^{\circ}$ is appropriate from 90 km downward. Since the altitude of the "explosion" was apparently not determined, the lower altitude limit of $\alpha = 0^{\circ}$ is again unknown. Since the Allende event survived to earth impact, a modified sonic boom theory for the lower part of the trajectory (with $\alpha \neq 0^{\circ}$) may be needed to adequately model the low altitude sound producing region (depending on what velocity it had at impact).

From the above results it does not appear that refraction during entry was very significant for most directions in preventing sounds from arriving at the ground. Note however that toward Flagstaff $\Delta\phi$ is $\sim 70^{\circ}$ from a point 1000km from Flagstaff along ℓ whereas for Boulder from the same position the $\Delta\phi$ value of $\sim 30^{\circ}$ is within the range for line source refraction to the ground. For closer distances

from Allende to Flagstaff, R=950 km and $\Delta \phi \simeq 82^{o}$ for example, the present analysis predicts that ground arrivals are unlikely however. Since the "explosion" altitude is also unknown, it is difficult to refine the value of $\Delta \phi$ necessary so that line source airwaves wouldn't be recorded at Flagstaff. Thus the refraction may or may not be significant in terms at least of detection of the Allende airwaves at Flagstaff.

The next consideration is that of the local weather at the time of the Allende entry. Allende entered the atmosphere at about 1:09 a.m. C.S.T. on February 8, 1969. In Figures 158 and 159 the surface and 500mb charts are shown respectively for Friday, February 7, 1969 at 7 a.m. E.S.T (6 a.m. C.T). Note the strong cold front running along a line from NE to SW. It was attached to a stationary front running nearly West to East beginning in central Wyoming and ending in the Atlantic somewhere off the surface map. The 500 mb chart indicates a deep trough above the surface front in the Utah, New Mexico, Arizona area. In Figures 160 and 161, surface and 500 mb charts are shown for February 8, 1969 at 7 a.m. E.S.T. (6 a.m. C.S.T.) just some 4 hours and 51 minutes after Allende entered the atmosphere. In the upper air the trough has moved Eastward and deepened. It would appear then that the front was West of the impact point during the time of the entry. Although the stationary front present on the February 7, 1969 surface map is primarily absent on the February 8 surface map, it would appear that between Allende and both Flagstaff and Boulder a somewhat strong front was evident. While the effects of scattering of the wave energy have not been studied it is difficult to know whether the presence of such a front can effectively scatter (and reduce the amplitude) of the Allende induced airwaves. In addition, winds behind the front may have been large enough to mask

a signal on the order of a few dynes/cm^2 peak to peak at either Boulder or Flagstaff. Without studying the scattering problem more carefully as well as tracing the frontal patterns in greater detail, it is very hard to be more precise on this matter.

The last item is related to the source altitude of the "explosion". Presumably this was below 50km since substantial seismic and airwave activity was noticed in the vicinity of the source. At higher altitudes $\sim$ 100 km and above Groves (1964) has shown that for E_t in the range 10^{11} - 10^{15} ergs coupling of the released energy directly to the neutral gas may be reduced. For correspondingly smaller energy releases lower altitudes would be indicated by the theory presented by Groves. Presumably E_t exceeded 10^{11} ergs in the case of Allende. This is probably true since Carr quotes a value of some 10^{19} ergs available prior to the entry.

Thus generally speaking both atmosphere and "explosion" related quantities must be studied to ultimately determine their interplay. Apparently in the case of Allende, the energy release was large enough and the detonation altitude low enough so that this coupling problem was not of great importance.

The last topic to be discussed relates to the comments by Carr (1970) comparing and contrasting the Revelstoke and Allende events. Carr concludes that Allende did not generate a sizeable airwave even though both events had similar total energy estimates, since Revelstoke was recorded and Allende wasn't. In this analysis there has been some evidence put forth to answer why airwaves were not recorded. This consisted of refractive considerations, local weather conditions and atmosphere - explosion interaction processes.

But even with the uncertainty in the above, Allende must have generated a sizeable airwave. The description provided by observers near the entry supports this fact (Fireman, 1969). Further, Carr contends that Revelstoke (which dispersed largely as dust in the atmosphere) could generate a sizeable airwave while Allende which violently fragmented into many large pieces could not. As was discussed in Part 2, ablation is the mechanism which in general removes energy available to the shock wave at progressively lower altitudes. Thus the less ablation there is, generally the more energy there is to couple to the atmosphere in the form of an "explosive" process. To reduce Revelstoke to dust may have taken less energy than to cause Allende to explode as many fragments, but in any case both events probably coupled much energy to the atmosphere. Further research work on the ablation problem using an n body physical theory of meteors in needed to better understand this energy transfer process in detail.

This concludes the discussion of the Allende event. It remains in this section to discuss the Alaskan Fireball of December 19, 1969 and the airwaves it subsequently produced.

G. THE ALASKAN FIREBALL OF DECEMBER 19, 1969

In Figure 164 a map of the general area of the entry of the Alaskan Fireball of December 19, 1969 is shown. As is noted in the figure neither ϕ nor θ are known in this case. As a result no refraction analysis was carried out. While the author is not aware of actual audible sound reports in this case, an infrasonic airwave observation from this event was made by Johnson and Wilson (Wilson, 1972). The airwaves are shown in Figure 165 as recorded by the College,

Alaska microbarograph array (the pressure signals of three of the four sensors are superimposed in this figure). The passband of the College array is about 7 - 70 seconds. A summary of the known facts regarding this event and the calculations made are shown in Table 8. The actual airwave data are reproduced here for convenience:

$\Delta p_{p \rightarrow p} = 4.6$ dynes/cm^2

$\tau_g = 12$ seconds

$\chi = 353^o$

$R_h = 327$ km

$t_o = 19{:}12$ L. T.

$t_D =$ Not Determined

In the above it should be noted that Johnson and Wilson (Wilson, 1972) computed a distance of 305 km from the meteor using an 18 minute delay time observed between the time of the airwave arrival and the time as recorded on a 35 mm photograph taken of the fireball on an all sky camera. In addition the event was also recorded independently on two auroral photometers operating at 4578 and 4858 $\mathring{A}$ which were pointed at the magnetic zenith (Wilson, 1972). In order to compute R, Johnson and Wilson used a value of 282 m/sec for a mean speed between source and observer. Using a mean speed of 300 m/sec a distance R of 360 km is determined. Thus in this case R_h was determined in reverse order (although it wasn't used however) to what it was in the previous parts of this section. That is R determined above (assuming a mean speed of 300 m/sec) divided by 1.1 yields R_h. In any case R is not very different from the value which Johnson and Wilson determined (it is larger by less than 12%). Johnson

and Wilson in an unpublished one page summary of these observations (Wilson, 1972) report that the 18^{o} difference in azimuth direction as determined by using the 35 mm photograph and the actual airwave data "is probably due to the mach cone effect from the meteor shock cone." In addition, cross winds may have also contributed to the observed azimuth difference.

The calculations shown in Table 8 using the above data were made as noted earlier. The final value of z_z determined here seems somewhat high considering that β' was about 34^{o} (V_T was about 363 m/sec according to Johnson and Wilson). If 61 km is a reasonable estimate for the source of these airwaves, then this fireball is comparable to that of Revelstoke in size. As was the case of all the other airwave observations other than Revelstoke, V = 11.2 km/sec was assumed for the meteor velocity.

It would appear that central Alaska is a relatively good place to record meteor generated infrasound. Low mean surface winds allow weaker signals to be recorded more regularly (assuming meteor influx rates at about 60^{o} North are similar to the middle latitude flux rates discussed in Section VI).

Wilson (1972) has noted that several pulses similar to the one shown in Figure 165 have been recorded on the College infrasonic microbarograph array. He also noted that many of these are probably associated with entering fireballs. What is needed however in addition to the pressure sensor equipment is an adequate ground photographic network similar to the ones previously discussed in both the U. S and

and Canadian Prairies. As was noted in Section VI what is needed at this point is not just knowledge of the influx rate, but instead photographic documentation of a given meteor event. This is necessary to better delineate the magnitude of difficulty of regularly recording meteor induced pressure waves at a given microbarograph array.

This concludes a theoretical analysis of existing meteor sound observations and their possible association with a given meteor entry. In the next section a summary of the work completed, the conclusions reached, as well as suggestions for future research will be discussed.

VIII. CONCLUSIONS AND SUGGESTIONS FOR FUTURE RESEARCH

A. SUMMARY AND CONCLUSIONS

This subsection will be divided into six brief areas. Further, within each area a listing of the major assumptions and the major conclusions reached will be made. Immediately following this subsection, in subsection VIII B., suggestions for future research will be made.

1. Effective Meteor Line Source Model

   a. Major Assumptions

      (1) Hydrostatic isothermal plane parallel atmosphere

      (2) Ballistic entry (no lifting forces present)

      (3) Spherical shaped single body meteor model

      (4) Isotropic ablation which ceases at V(z) = 3 km/sec

      (5) Small Knudsen number and large Mach number define the continuum flow regime with regard to meteor bow shock generation. Izakov (1971) has shown that in order to pass from the Boltzmann equation to the hydrodynamic equations generally both the Knudsen number must be small as well as the ratio of the free path time to a characteristic time scale for the variation of a macroscale parameter of interest. In the case of hypersonic meteor entry, the free path time is a function then of the translational relaxation time as well as that of the rotational, vibrational and electronic relaxation times. All of the above relaxation times are not well known, especially for the extreme nonequilibrium conditions that exist initially during the entry.

It was implicitly assumed then that this latter condition discussed by Izakov was also satisfied during the meteor entry. The blast wave description of the pressure waves (induced by the hypersonic meteor entry) is not valid at very small x ($\lesssim 0.05$) at least in part because of the failure of the ratio τ_{fp}/τ_{vp} to be small compared to one. Here τ_{fp} is the free path time and τ_{vp} is a characteristic time scale for the variation of the induced pressure field. Thus, at very small x the integration of the Boltzmann equation cannot validly be performed since the macroscopic parameters do not change slowly over the free path length or during the free path time.

(6) The horizontal entry angle of the meteor is not a function of the meteor velocity (skip phenomena as the meteor approaches atmospheric entry are not considered).

(7) Between z' and '''', the acceleration due to gravity can be neglected for purposes of calculating the velocity altitude profiles. Thus, between z' and z'''' the trajectory is a straight line.

(8) Significant mass loss only occurs below z'.

(9) The drag coefficient can be given by the continuum flow value, even though the flow regime is not constant.

(10) Bolide effects or gross fragmentation effects are not present during the entry.

b. Major Conclusions

(1) Only certain combinations of meteor parameters are

allowed such that bow shock wave generation is possible.

(2) In addition to entry kinetic energy, both θ and ρ_{mE} need to be specified before the previous statement can be expressed quantitatively.

(3) Ablation reduces the energy available for the bow shock wave at progressively lower altitudes.

(4) The p^*= constant solution does not necessarily emply that r_m = constant.

(5) As was shown in Section VI., most meteors do not enter vertically ($\theta = 90^o$). Thus, the earlier conclusions of Riddell and Winkler (1962) are incorrect. For this reason under the limitations of the plane parallel atmosphere assumption θ has been allowed values between 10 and 90^o.

(6) The assertion by Wegener (1917) that meteors are producing sound only while they are luminous cannot be generally correct. The latter statement can be found on p. 95 of Whipple (1928). In addition to the dark flight trajectory (below a velocity $\sim$ 3 km/sec) sound producing, as was mentioned in Section III., the shock wave can begin (for $d_m \gtrsim 1$ cm) long before the body first becomes luminous (assuming this occurs at and below z'). As the calculations in Section V. have shown, attenuation for propagation downward from great altitudes may prevent an observer (or recorder) from "hearing" the sound. The latter conclusion is also consistent with the conclusion of Whipple (1928).

2. Source Characteristics

a. Major Assumptions

(1) Similarity assumption, i.e., under certain conditions of flight the pressure field induced near a hypersonic body can be modeled using the cylindrical blast wave theory (for $x \gtrsim 0.05$) with $\gamma = 1.4$. Note that the nonlinear blast wave theory does not include the gravity term in the hydrodynamic equations.

(2) Bolide and gross fragmentation effects do not occur during entry.

(3) The ambient density is essentially constant out to a distance R_o from the trajectory if $R_o << H$. The strong shock wave effects ($p/p_o > 10$) are confined within this distance from the trajectory. The atmosphere into which the blast wave expands is at rest.

(4) The variations in ambient density along ℓ do not invalidate the results as long as p/p_o remains very large.

(5) The cylindrical geometry of the shock wave is maintained until distances $R \sim \ell$ are reached. Beyond this distance range, spherical geometry is appropriate. The above conclusion results by first assuming that the atmosphere is nonturbulent. The line source must also be free of finite boundaries for this geometry to be strictly maintained.

(6) Beyond R_o, the limit equation of the overpressure developed by Jones et al. (1968) i.e., with "C"="δ"=1, can be used to predict the decay of the overpressure

into the weak shock region. See further discussion on this below.

(7) For nonlifting hypersonic entry the drag force can be equated to the energy deposited per unit of length by the meteor atmosphere interaction.

(8) In the strong shock region, radiation and heat conduction energy losses are not significant. In addition viscous effects can also be assumed negligible.

(9) R_o can be equated to the product of the meteor Mach number and the meteor diameter. This was done following the experimental work of Tsikulin (1970).

(10) The wavelength of the disturbance spreads as $x^{1/4}$ beyond x=10 as long as weak shock wave effects persist.

b. Major Conclusions

(1) Only for very large and very fast bodies can the energy release be considered as instantaneous over the entire entry. For such bodies $R_o \sim H$ or larger.

(2) Following the work of Tsikulin (1970) and Pan and Sotomayer (1972), the blast wave analogy to hypersonic flight is valid as long as the meteor velocity is constant and yet much greater than the adiabatic sound speed.

(3) At present it is not theoretically possible to analytically model the pressure field induced by a reentering body on a ballistic trajectory over the entire velocity range encountered. A gap in the treatment exists between the high Mach number limit where the cylindrical blast wave analogy to hypersonic flight can be made and the Mach

one limit where the sonic boom theory is applicable.

(4) Below the altitude region where the blast wave analogy fails, several interesting effects can occur. Of these, the thermal explosion effect and gross fragmentation are very difficult to theoretically model.

(5) For low altitude meteors which survive to dark flight (below $\sim$ 3 km/sec), a modified sonic boom theory for possibly multiple bodies may be needed to fully describe the induced flow field.

(6) From the numerical solutions of Plooster (1968), for the following initial conditions, the following values of "C" and " δ " can be used in the overpressure decay equation (13) to fit the numerically generated results (according to Plooster).

(a) Line source, ideal gas: "C" = 0.7, " δ " = 1, for $x < 7$ within 5% of the numerical results.

(b) Isothermal cylinder constant density, ideal gas, "C" = 0.7, " δ" = 1, for $0.05 < x < 7$ within about 5% of the numerical results.

(c) Isothermal cylinder, constant density, real gas equation of state, "C" = 0.7, " δ " = 0.66, for $0.05 < x < 5$ within about 5% of the numerical results.

(d) Isothermal cylinder, low density gas, ideal gas; for this case Plooster did not determine "C" and " δ ". Beyond $x \simeq 0.2$ however, the decay is nearly identical to that of groups (a) and (b) above.

(e) Isothermal cylinder, high density, ideal gas, "C" = 0.95, "δ" = 1.61, for $x > 0.2$ within 2% of the numerical results.

The form of the function f(x) as expressed in (12a) including "C" and "δ" can be written as:

$$f(x) = \left(\frac{3}{8}\right)^{-3/5} (\text{"C"})^{-8/5} \left\{ \left[1 + \left(\frac{8}{3}\right)^{8/5} (\text{"C"})^{-8/5} (\text{"}\delta\text{"})^{-1} x^2 \right]^{3/8} - 1 \right\}^{-1}$$

In addition, Plooster determined "C" and "δ" to be used in f(x) in order to fit the experimental results he obtained using Primacord. For his experiments when the values "C" = 0.95, "δ" = 2.62 for $x \gtrsim 0.3$ are substituted into f(x), the resulting overpressure decay curve fits the data points quite well.

It is interesting to note that the overpressure decay curves generated by using "C" = "δ" = 1 generally exhibit faster overpressure decay than that of the numerical solution using the initial conditions in (e) given above. This is also true with regard to the Primacord experimental data (which the conditions set in (e) were used to simulate numerically). Thus, it would appear that until "C" and "δ" (or a range of acceptable values) are better determined in the case of a "typical" meteor energy release (or a range of "typical" cases), the results obtained using meteor sound observations to

determine R_0 (and other properties such as d_m etc.) should not be considered as anything but preliminary. This is because both "C" and "δ" (interpreted via some set of initial conditions) act in determining the behavior of the overpressure decay. The effects of generalized ablation processes and how they influence "C" and "δ" for a typical meteor entry are not presently known.

(7) It is well known that cylindrical waves decay more slowly than spherical waves (Few, 1969). In his experimental investigations, Tsikulin (1970) obtained expressions to relate both ideal "point" and "line" source theory to laboratory TNT explosions of spherical and cylindrical geometry. The "TNT equivalence" concept was necessary then to compare theory with experiment. In the case of cylindrical "line" explosions the energy release per unit path length, i.e. the drag, had to be doubled in order to obtain agreement with the TNT overpressure data. This accounts for the factor of two included in (17b). Presumably, Primacord data would give similar results. Thus, bodies in hypersonic flight are more efficient as shock wave producers than chemical high explosives. For meteors undergoing intense ablation this result probably needs further substantiation however.

(8) When interpreting meteor sound observations, the following items should be also be considered with respect to the airwave source.

(a) Wavefront geometry near the source-spherical, cylindrical or some combination of the two.

(b) A comparison of the magnitude of R_o (or R_s) with H. This may also influence the wavefront geometry if the energy release per unit pressure (in the spherical case) is large enough. In Section V. a discussion related this consideration to the dominant frequency of the wave.

(c) Ablation effects on geometry and on the induced wavelengths of the disturbance. See the discussion on attenuation which follows shortly.

(d) Independent of "line" or "point" source geometry effects (or some combination of these) a blast wave source description may not always be appropriate. Meteor sounds as described earlier in this analysis can be considered via several mechanisms including as limits blast wave theory and a modified sonic boom theory.

3. Atmospheric Refraction

a. Major Assumptions

(1) Horizontally stratified steady state atmosphere.

(2) Temperature and wind gradients are small in the distance of one wavelength of the wave, i.e., the WKB slowly varying medium concept is satisfied. This allows the reflection of the wave energy at each layer boundary to be neglected.

(3) Beyond R_o from the trajectory the original non-steady blast wave flow is steady and the wavefront

is approximately plane.

(4) At and beyond R_o, the characteristic velocity of the flow can be determined, i.e., the geometrical acoustics ray treatment is valid.

(5) The model atmosphere layer thickness is large enough compared to the wavelength of the disturbance so that diffraction effects can be neglected.

(6) Beyond R_o, the shock front velocity can be approximated by the phase velocity of sound.

(7) Nonlinear effects do not significantly alter the conventional small amplitude Snell's law approach beyond R_o from the trajectory.

(8) The refraction involved in an inhomogeneous moving medium is given correctly by the theory as derived by Groves (1955) and many other authors. See the recent work of Thompson (1972) for more details on this.

(9) Only rays with initially downward directions need to be considered in terms of ground arrivals.

b. Major Conclusions

(1) For $\Theta \leq 35$ to 40^o, for the mean atmospheric structure considered (without meridional winds) for most altitudes below 90 km, refractive paths to the ground exist for most azimuth directions, $\Delta\phi$, on either side of the trajectory (as well as within the entry plane).

(2) The line source is a highly directional sound source as compared to the originally isotropic point source case. Thus, in expression (26a), in the point source problem θ' is a free parameter. In the line source problem however, θ' is fixed once θ is determined (between z' and z'''').

(3) From the considerations in Section III. (the range of allowed meteor parameters), R_o rarely exceeds 200 meters from the trajectory. For this reason the refractive possibilities can be studied essentially from the source altitude outward.

(4) As was seen in Section VI. the maximum percent occurrence of θ is the range of 30^o to 40^o. Thus, refractive possibilities, in as realistic a model atmosphere as can be deduced, should be determined, especially when θ exceeds the above range.

(5) In the absence of wind with $V >> C$, the characteristic velocity can be represented as an ellipse symmetric along the meteor trajectory as viewed in the horizontal plane, As θ approaches 90^o, this ellipse approaches a circle. As θ approaches O^o, this ellipse greatly ellongates along the trajectory axis.

(6) In the presence of steady wind the above ellipse becomes skewed due to the anisotropic nature of the vector wind field.

(7) Half of the ellipse mentioned in (5) above can be used to study initially downward heading rays with directions away from that of the meteor entry. The other half of the ellipse can be used to study initially upward heading rays with general directions toward the meteor heading, ϕ.

(8) As $\alpha \rightarrow \theta$ during the entry k(z) becomes very large.

4. Attenuation Predictions

a. Major Assumptions

(1) Hydrostatic isothermal plane parallel atmosphere - since the atmosphere is assumed to be nonturbulent the line source cylindrical geometry is maintained out to distances where $R \sim \ell$. Thus, scattering of the wave energy need not be considered.

(2) Shock fronts can be treated as strictly discontinuities in the pressure wave pattern.

(3) The relaxation radius is small compared to the scale height. This assures excitation of primarily acoustic frequencies in the disturbance. This is also the primary frequency range of most of the existing meteor sound observations.

(4) The meteor energy release can be assumed to be instantaneous. In Section IV A., this assumption was shown to be valid only for the more energetic meteors.

(5) Among the possible absorption loss mechanisms,

shear viscosity and heat conduction are predominant in this frequency range.

(6) The initial wave shape and period are known via the results of the classical cylindrical blast wave theory. After a short travel distance beyond x=10, the waveform assumes an N wave shape. This resultant N wave is balanced so that Δp in the compression phase equals Δp in the rarefaction phase.

(7) A comparison of the value of d' with the distance the disturbance will propagate before it is observed gives a valid indication of the transition between weak shock and linear wave propagation.

(8) The weak shock theory of Morse and Ingard (1968) for absorption of continuous saw toothed "shocked" acoustic plane waves remote from their source is applicable beyond R_o to an N wave shaped pulse induced by an instantaneous meteor entry (in a continuous flow regime).

(9) After the wave has become linear, the damping predicted by the plane wave theory for continuous small amplitude sine waves is then applicable. Thus, after d' exceeds d_a a transition in wave shape is assumed from a balanced continuous N wave to a continuous small amplitude sine wave.

(10) Since theoretical viscosity and heat conduction damping calculations generally underpredict the amount of damping which is actually observed in

the atmosphere, the theoretically predicted value of $\overline{\alpha}$ can be increased slightly so that the theoretical calculations are in better agreement with observations.

(11) The wave frequency can be held constant at its x=10 value for purposes of calculating the absorption of the wave energy.

(12) Ablation does not significantly alter the wave characteristics as predicted by blast wave theory.

(13) The weak shock wave predictions in a uniform atmosphere are applicable to a nonuniform atmosphere (where density and pressure are functions of altitude) as modified by the $\overline{p^*}$ parameter (following the work of Friedman et al., 1963; Kane, 1966 and Pierce and Thomas, 1969 among others).

(14) For purposes of predicting the wave period, the $x^{1/4}$ nonlinear spreading dependence as derived for a weak shock wave in a uniform (constant density) atmosphere is applicable to the nonuniform atmosphere case as long as $d' < d_a$.

(15) The wave period is defined throughout the propagation as it is for small amplitude sine waves.

b. Major Conclusions

(1) For $R_o \lesssim 10$ meters, ground detection of line source airwaves from meteors are very unlikely. The horizontal detection distance about an entry with $R_o = 10$ meters is about 200 km. This distance

depends in general, however, on source altitude, ground winds, refractive possibilities, etc.

(2) Weak shock propagation effects may be present throughout all or part of the propagation. How far beyond R_o these effects persist depends on such quantities as wave period and the overpressure ratio. In addition, the absorption of wave energy as a function of the initial source altitude as well as of the fundamental wave frequency may also greatly influence the results.

(3) For real meteors since the instantaneous energy release assumption is generally not valid, an extended source concept can be utilized to improve the absorption modeling of the damping phenomena. In going from the assumption of an instantaneous energy release to an extended source concept, if the meteor velocity indefinitely remained constant (hence, deceleration didn't occur) a steady state theory with D(R)=1 must in the limit be realized. When the energy release is not strictly instantaneous d' calculations indicate that the disturbance will remain a weak shock wave out to relatively larger scaled distances. Note that these d' calculations were made assuming τ_m remained constant during the propagation.

(4) From the available experimental and theoretical data on $f(\bar{\omega}, x)$, an overall uncertainty of about a

factor of two exists (Dawson et al., 1968; Plooster, 1968; Few, 1969; Tsikulin, 1970; Hilton et al., 1972; and Pan and Sotomayer, 1972). This uncertainty estimate is made independent of the possible ablation influences. In addition, part of the uncertainty estimate is dependent upon how R_o is defined. This was discussed previously in IV A. (Part 2).

Also, in the present analysis τ_m has been defined using the conventional small amplitude wave definition of period. Using the "duration" definition of Hilton et al., (1972) and other authors, the present value of τ_m would be reduced by a factor of about 2.8 at x=1 and by a factor of about 1.7 at x=10 assuming Plooster's numerical calculations are correct. Still other authors, Pan and Sotomayer (1972) attempt only to predict the duration of the positive (compressional) phase of the disturbance. Further, comparisons using (91) and the observational data of Hilton et al. (1972) at Mach 16 agree within a factor of about two. If the data of Hilton et al. (1972) are interpreted using the definition of τ_m as used in this analysis, agreement within a few percent is obtained. Note that in this analysis the body shape has been assumed as spherical. Since Tsikulin has shown that for other body shapes (and drag coefficients) the simple expression $R_o = M \cdot d_m$ does not result, ultimately f_m will have a

slightly different value if the value of $f(\bar{\omega}, \mathbf{x})$ subsequently remained unchanged. Care must be taken then to see that the same definition for τ_m is being utilized when such comparisons are made.

(5) Many authors have presented results for the variations in τ_m for the propagation of either weakly nonlinear or linear disturbances of either spherical or cylindrical geometry in a uniform or nonuniform medium (Otterman, 1959; Meyer, 1962; Groves, 1964; Tsikulin, 1970; Hayes, 1971 and Pan and Sotomayer, 1972, among others). Various apparently contradictory results have been obtained. These appear to result from the order of the various approximations utilized to obtain solutions. In this analysis, other than in the absorption calculations, an $x^{1/4}$ nonlinear spreading effect in τ_m has been assumed. Recent results from Seebass and George (1973) have shown that for steady hypersonic source motion, τ_m will eventually decrease ($\tau_m/2$ for a balanced N wave) for waves propagating downward into an isothermal atmosphere (the calculations were actually carried out to study the changes in Δp and in the positive phase impulse of the wave). The distortion results from at least two factors in the steady hypersonic source case. The first is that since D(R)=1, the amplitude of the disturbance is not reduced by the action of viscosity and heat

conduction. As was shown by Lighthill (1956) under these conditions the shock thickness is only widened slightly (smeared out) by the action of these mechanisms. The second factor involves the effect of the increasing more dense atmosphere in a downward direction. For such propagation it appears physically very reasonable that such distortion should result since the wave energy, depleted only through spreading into a larger volume, is continually being merged into a greater mass of gas (depending on $\Delta p/p_o$ and τ_m). For upward propagation into a less dense medium, spreading of τ_m should occur. The latter statement is consistent with the results of Kahalas and Murphy (1971) where $D(R) \approx 1$ due to the low f_m value induced by a large "point" source energy release.

In the present situation since $D(R) \neq 1$, except under certain circumstances, the reduction of Δp by absorption mechanisms would tend to disperse the distorting wave as it propagates into a medium of increasing density. The net effect is unknown in this case, at least during the part of the propagation for which the disturbance can be considered as weakly nonlinear. Thus, the dependence of Δp on scaled distance is directly dependent upon the variation of τ_m with scaled distance. In this analysis for an $x^{-3/4}$ overpressure decay an $x^{1/4}$ spreading of τ_m

was assumed. If such decay corrected by $\overline{p^*}$ in a nonuniform medium is appropriate, then the present D(R) calculations (assuming τ_m=constant) represent the worst damping which can occur.

From a more general standpoint in a realistic atmosphere, the variations in τ_m caused by the competing processes of distortion and dispersion can be functionally summarized as:

$$\Delta\tau_m = f(G, A, N, S, T, D) \text{ with } \gamma H >> \Lambda$$

where

$\Delta\tau_m$ = variations in the period of the disturbance

G = initial wavefront geometry (this depends also on linearity or nonlinearity of the disturbance)

A = weak shock or linear absorption (for the cases with D(R) unequal to or equal to one)

N = nonlinear versus linear wave effects

S = atmospheric structural parameters such as temperature and wind gradients producing geometrical dispersion effects

T = atmospheric turbulence effects on the return of the underpressure phase of the disturbance to "ambient" conditons

D = direction of propagation (into a medium of increasing or decreasing density)

(6) For the spherical blast wave problem, if E_t is released at altitudes where p_z is small, relatively

large values of R_s (or large values of τ_m) can result. For the energy range of $E_t = 10^{16}$ to 10^{20} ergs (assuming all the energy was deposited instantaneously at a "point"), for altitudes between 10 and 70 km, values of τ_m at x=10 predicted using (78) are on the order of 1-50 seconds. The 50 second value is a factor of about 10 longer than the value obtained in the line source problem at x=10, for R_o=300 meters. The concentration of a relatively large amount of energy in the "point" source problem, when coupled into a relatively low density gas, produces this relatively lower fundamental wave period.

(7) The transition between weak shock and linear waves as calculated here is only approximate. Independent of whether d' or d_s is used to determine this transition, τ_m has been held constant during the distortion distance calculations. The precise variation of τ_m with x however, in the actual disturbance depends on whether weak shock or linear propagation is evident (among other factors as were briefly listed in item (5)).

(8) Since in the cases of Revelstoke, Kincardine and Holbrook sounds were heard near the source and yet recorded infrasonically far from the source, ultimately geometrical dispersion effects must be significant with regard to the lowering of f_m. In the case of Kincardine material dispersion effects

may also have been of some significance.

5. Probability of Meteor Generated Ground Sound Arrivals

a. Major Assumptions

(1) The photographic influx results of McCrosky (1968) and the airwave influx data due to Lowry and Shoemaker (1967) and Gault (1970) are essentially correct.

(2) Bolide effects occur statistically for less than 50% of entering bright fireballs (Lyubarskiy, 1952; Baldwin and Sheaffer, 1971). Thus, it is sufficient to consider primarily the attenuation of line source airwaves.

(3) Knowledge of the source is available during the night-time hours.

(4) Amplitudes as small as 0.1 dynes/cm^2 peak to peak can be resolved during optimum ground conditions, i.e., very small surface winds.

(5) The overall yearly statistical distribution of the meteor heading is isotropic and independent of the observers latitude and longitude.

(6) The linear band pass region of the pressure sensor used to detect these airwaves is in the range predicted in Section V. (Part 2), namely 1-10 seconds.

b. Major Conclusions

(1) At present, knowledge of the source is essential to better define the observational searching techniques.

(2) Of the four parameters, N_I, N_{SP}, N_G and N_D, the following relation can be written:

$$N_I > N_{SP} > N_G > N_D$$

Since present photographic coverage is quite small in comparison to the total surface area of the earth, it was shown earlier that, based on the present theory, N_G should exceed N_D.

(3) Perhaps as many as 50 arrivals might be eventually recognizable during a six month period, if a mean wave shape, period range and amplitude could be determined on a statistical basis (simultaneously using photographic and infrasonic detection techniques). This number is based on a mean flux rate whose value is intermediate to that of McCrosky and Shoemaker.

(4) Based on present source knowledge availability, perhaps as many as 10 arrivals might occur in six months for a ground station within the PN. For a ground station in Michigan the above number would be reduced to about 1.5. These numbers assume that McCrosky's flux rate is correct.

6. Analysis of Existing Data

a. Major Assumptions

(1) All of the airwave observations treated are correct, i.e., the signals were induced by a meteor-atmosphere energy deposition process.

(2) The energy deposition process can be adequately

modeled using the present cylindrical blast wave line source theory (for a spherically shaped single body with a constant drag coefficient and with $\gamma = 1.40$).

(3) The observations were a distance R_h from the meteor such that $R_h^2 >> z_z^2$.

(4) Source altitudes were low enough so that the D(R) terms could be estimated based only on a mean period $\overline{\tau}_m$ and were subsequently independent of the source altitude.

(5) Setting $R_{z \rightarrow t} = 0.5\ R_{z \longrightarrow g}$ is a reasonable approximation during the analysis. The results in Section V. indicate that the value of $R_{z \longrightarrow t}$ calculated using d' is a variable depending on both source altitude and the magnitude of R_o (or on the energy released per unit length), but that for long ducted paths, the above approximation is not unreasonable.

b. Major Conclusions

(1) Had accurate amplitude and period information been determined for the airwaves from the British fireball of April 25, 1969, valuable information regarding the body (or bodies) which produced the airwaves could have been deduced.

(2) The airwaves from the Lost City Meteorite (if $R_o \simeq$ 13 meters) were probably extensively absorbed (as well as attenuated) before reaching the Boulder NOAA microbarograph stations. Refraction

calculations indicate that directions toward Boulder were definitely possible from Lost City.

(3) The Revelstoke Meteorite probably released a large amount of energy to the atmosphere near an altitude of 30 km (as a point source).

(4) The two Holbrook Fireball observations may or may not be consistent with each other. Photographic documentation of this entry would have greatly aided in interpreting the present results.

(5) The Kincardine Fireball probably released a large amount of energy to the atmosphere (as a point source). Atmospheric temperature and wind gradient dispersion over long multiple paths may greatly influence observed amplitudes and periods such that inaccurate estimates of the actual source energy from a single station might be made.

(6) The nonobservation of the Allende Fireball may be due to refractive factors, the local weather at the time of the entry, or to a coupling problem of the source energy to the atmosphere. Of the latter items, the strong frontal activity at the time of the entry may have played a significant role with regard to scattering of the wave energy.

(7) The energy release of the Alaskan Fireball of December 19, 1969 may be comparable to that of Revelstoke Meteorite entry.

(8) Well documented meteor entry (both photographically

and infrasonically when possible) have the potential for yielding valuable information with regard to meteor parameters (and thus, to a better understanding of their role within the solar system) as well with regard to a better understanding of the decay of nonlinear disturbances in the atmosphere.

B. FUTURE RESEARCH

Many possible theoretical refinements might now be made. In all cases, however, the actual meteor source characteristics need to be known better so that a valid comparison between theory and observation can be made. Thus, at present, what is needed most is not refinement of the present theory, but rather many well documented photographic and infrasonic recordings of the entry of bright fireballs into the atmosphere. These observations may greatly aid in determining the directions toward which future theoretical refinements should be headed. A brief listing of the many possible items which might be investigated in the future are as follows:

1. Skip phenomena during entry (as a function of V and θ).
2. Lift phenomena (nonballistic entry with changing θ and changing irregular body shape along with rotational effects).
3. An n-body physical theory of meteors (including a better ablation theory).
4. Point explosion energy releases (when the stagnation pressure exceeds the compressive strength of the meteor).
5. Effects of atmospheric turbulence.
6. Extension of the present theory to predict pressure wave amplitudes from entry velocities all the way through Mach 1

(including deceleration, intense ablation and/or the "thermal explosion" effect).

7. Numerical calculations in a realistic model atmosphere including both nonlinear source effects as well as geometrical and material dispersive effects (but of a more detailed nature than is presently provided by the acoustic-gravity wave guide mode theory since absorption effects are not considered).

Future progress in all of the above areas (theoretical and observational, as well as, experimental hypersonic Mach number data) have the potential for yielding much useful information. It is hoped that the observational attempts, which are just now beginning, will help direct future research efforts in order to adequately model this complex phenomenon.

BIBLIOGRAPHY (Part 3)

1. Abramowitz, M. and I. A. Stegun, Handbook of Mathematical Functions, National Bureau of Standards, Applied Mathematical Series 55, U. S. Department of Commerce, 1964.

2. Allen, H. J. and N. A. James, Prospects for Obtaining Aerodynamic Heating Results from Analysis of Meteor Flight Data, NASA TN D 2069, 1964.

3. Andrews, A. D. et al., The Meteorite of April 25, 1969, Nature, Vol. 222, p. 727, May 24, 1969.

4. Astapovich, I. S., Sound Phenomena Simultaneous with the Flight of Bolides, Meteoritika, Vol. 9, pp. 71-101, 1951.

5. Astapovich, I. S., Meteoric Pheonmena in the Earth's Atmosphere, State Publishing House of Physical and Mathematical Literature, Moscow, 640 pp. (in Russian), 1958.

6. Balachandran, N. K., Acoustic-Gravity Wave Propagation in Temperature and Wind-Stratified Atmosphere, J. Atmos. Sci., Vol. 25, No. 5, pp. 818-826, 1968.

7. Balachandran, N. K. and W. L. Donn, Dispersion of Acoustic Gravity Waves in the Atmosphere, T. M. Georges, Editor, ESSA-ARPA Symposium: Acoustic Gravity Waves in the Atmosphere, Boulder, Colorado, 11. 179-193, 1968.

8. Balachandran, N. K., W. L. Donn and G. Kaschak, On the Propagation of Infrasould from Rockets: Effects of Winds, J. Acous. Soc. Amer., Vol. 50, No. 2 (Part I), pp. 397-404, 1971.

9. Baldwin, B. and Y. Sheaffer, Ablation and Breakup of Large Meteoroids During Atmospheric Entry, J. Geophy. Res., Vol. 76, No. 19, 11. 4653-4668, 1971.

10. Barringer, B. and H. Hart, The Mechanism of the Sounds from Meteors, Cont. of the Meteor. Soc., pp. 507-518, 1949.

11. Bartman, F. L., The Rocket-Grenade Experiment for Upper-Air Temperature and Wind, Atmospheric Physics, The University of Michigan Engineering Summer Conferences, Chapter 4, June 5-9, 36 pp., 1967.

12. Bass, H. E., et al., Atmospheric Absorption of Sound: Analytical Expressions, J. Acous. Soc. Amer., Vol. 52, No. 3 (Part II), pp. 821-825, 1972.

13. Batten E. S., Wind Systems in the Mesosphere and Lower Thermosphere, J. Meteor., Vol. 18, pp. 283-291, 1961.

BIBLIOGRAPHY (Part 3) (Continued)

14. Berthet, C. and Y. Rocard, A New Mechanism for the Propagation of Infrasonic Waves at Long Distances in the Atmosphere, J. Acous. Soc. Amer., (to be published).

15. Blackstock, D. T., Finite-Amplitude Infrasonic Waves in the Atmosphere, J. Acous. Soc. Amer., (to be published).

16. Blackstock, D. T., A Comparison Between Weak Shock Theory and Burgers' Equation in Nonlinear Acoustics, Symposium on Aerodynamic Noise, Loughbourough, Leics, England, 21 pp., available from Technical Information Service as A71-17156, 1970.

17. Blokhintzev, D., Acoustics of an Inhomogeneous Moving Medium I, J. Acous. Soc. Amer., Vol. 18, No. 2, pp. 322-328, 1946.

18. Brode, H. L., Numerical Solutions of Spherical Blast Waves, J. Appl. Phys., Vol. 26, p. 766, 1955.

19. Brode, H. L., Blast Wave from a Spherical Charge, The Physics of Fluids, Vol. 2, No. 2, pp. 217-229, 1959.

20. Carr, M. H., Atmospheric Collection of Debris from the Revelstoke and Allende Fireballs, Geochimica et Cosmochimica Acta, Vol. 34, pp. 689-700, 1970.

21. Chamberlin, V. D. and D. E. Krause, The Fireball of December 9, 1965, J. Roy. Astron. Soc. Canada, Vol. 61, No. 4, pp. 184-190, 1967.

22. Chamberlin, V. D., Meteorites of Michigan, Bulletin No. 5 of the Geological Survey of Michigan, Lansing, Michigan, 1968.

23. Cook, R. K., Atmospheric Sound Propagation, Atmospheric Exploration by Remote Probes, Proc. of the Scientific Meetings of the Panel on Remote Atmos. Probing to the Comm. on Atmos. Science, National Academy of Sciences, and the National Research Council, Vol. 2, 11. 633-669, 1969.

24. Cosby, W. A. and R. G. Lyle, The Meteoroid Environment and its Effects on Materials and Equipment, NASA SP-78, 1965.

25. Cospar International Reverence Atmosphere 1965, North-Holland Publishing Company, Amsterdam, 1965.

26. Cotten, D. E., W. L. Donn, and A. Oppenheim, On the Generation and Propagationof Shock Waves from Apollo Rockets at Orbital Altitudes, Geophys. J. Roy. Astron. Soc., Vol. 26, pp. 149-159, 1971.

27. Cox, E. F., Sound Propagation in Air, Handbuch der Physik, Springer Verlag, Vol. 48, Chapter 22, pp. 455-478, 1958.

28. Craig, R. A., The Upper Atmosphere-Meteorology and Physics, Academic Press, New York, 1965.

29. Daily Aerological Record and Daily Weather Report of the British Meteorological Service, Bracknell, Berkshire, Great Britian, 1969.

30. Dawson, G. A., et al., Acoustic Output of a Long Spark, J. Geophys. Res., Vol. 73, No. 2, pp. 815-815, 1968.

31. Diamond M., Sound Channels in the Atmosphere, J. Geophys. Res., Vol. 68, No. 11, pp. 3459-3464, 1963.

32. Diamond M.. Cross Wind Effect on Sound Propagation, J. Appl. Meteor., Vol. 3, No. 2, pp. 208-210, 1964.

33. Donn, W. L. and D. Rind, Microbaroms and the Temperature and Wind of the Upper Atmosphere, J. Atmos. Sci., Vol 29, pp. 156-172, 1972.

34. Dorman, J., et al., Meteoroid Impacts on the Moon (Abstract), Trans. Amer. Geophys. Union, Vol. 54, No. 4, p. 343, 1973.

35. DuMond, J. W. M. et al., A Determination of the Wave Forms and Laws of Propagation and Dissipation of Ballistic Shock Waves, J. Acous. Soc. Amer., Vol. 18, No. 1, pp. 97-118, 1946.

36. Erdelyi, A., Editor, Higher Transcendental Functions, H. Bateman Manuscript Project, McGraw-Hill, Vol. II., pp. 396, 1953.

37. Evans, L. B. et al., Absorption of Sound in Air, Wylie Labs, Inc., Huntsville, Alabama, AD 710291, 1970.

38. Evans, L. B. et al., Atmospheric Absorption of Sound: Theoretical Predictions, J. Acous. Soc. Amer., Vol. 51, No. 5, (Part 2), pp. 1565-1576, 1972.

39. Few, A. A., Jr., et al., A Dominant 200-Hertz Peak in the Acoustic Spectrum of Thunder, J. Geophys. Res., Vol. 72, No. 24, 11. 6149-6154, 1967.

40. Few, A. A., Jr., Power Spectrum of Thunder, J. Geophys. Res., Vol. 74, No. 28, 11. 6926-6934, 1969.

41. Fireman, E. L., Freshly Fallen Meteorites from Portugal and Mexico, Sky and Telescope, Vol. 37, No. 5, 11. 272-275, 1969.

42. Folinsbee, R. E. et al., The Peace River Meteorite: Fall and Recovery, J. Roy. Astron. Soc. Canada, Vol. 58, pp. 109-124, 1964.

43. Folinsbee, R. E. et al., Revelstoke, a New Type I Carbonaceous Chrondite, Geochimica et Cosmochimica Acta, Vol. 31, pp. 1625-1635, 1967.

44. Folinsbee, R. E. et al., Vilna Meteorite - Camera, Visual, Seismic and Analytic Records, J. Roy. Astron. Soc. Canada, Vol. 63, pp. 61-86, 1969.

45. Francis, S. H., Propagation of Internal Acoustic-Gravity Waves Around a Spherical Earth, J. Geophys. Res., Vol. 77, No. 22, pp. 4221-4226, 1972.

46. Friedman, M. P. et al., Effects of Atmosphere and Aircraft Motion on the Location and Intensity of a Sonic Boom, AIAA Journal, Vol. 1, No. 6, 11. 1327-1335, 1963.

47. Gault, D., Saturation and Equilibrium Conditions for Impact Cratering on the Lunar Surface: Criteria and Implications, Radio Sci., Vol. 5, No. 2, pp. 273-291, 1970.

48. George, A. R. and K. J. Plotkin, Propagation of Sonic Booms and Other Weak Nonlinear Waves Through Turbulence, Phys. Fluids, Vol. 14, pp. 548-554, 1971.

49. Gille, J. C., Acoustic - Gravity Waves in the Earth's Atmosphere, Florida State University, Department of Meteorology, Technical Note No. 66-7, pp. 1-21, 1966.

50. Goerke, V. H., Infrasonic Observations of a Fireball, Sky and Telescope, p. 313, November 1966.

51. Goerke, V. H., Private Communication: July 1971, November 1971, March 1972, June 1972, July 1972, and October 1972.

52. Golitsyn, G. S., On Absorption of Sound in the Atmosphere and Ionosphere, Bull. Acad. Sci., USSR, Izv., Geophys. Ser., No. 6, pp. 618-621, 1961.

53. Grad, H., Equations of Flow in a Rarefied Atmosphere, Rand Corp. Report R-339, 11-1, 1959.

54. Greene, J. S. and W. A. Whitaker, Theoretical Calculations of Traveling Ionospheric Disturbances Generated by Low Altitude Nuclear Explosions, Acoutic Gravity Waves in the Atmosphere, T. M. Georges, Editor, U. S. Government Printing Office, Washington, D. C., pp. 45-64, 1968.

55. Groves, G. V., Geometrical Theory of Sound Propagation in the Atmosphere, J. Atmos. Terr. Phys., Vol. 7, pp. 113 127, 1955.

56. Groves, G. V., Velocity of a Body Falling Through the Atmosphere and the Propagation of its Shock Wave to Earth, J. Atmos. Terr. Phys., Vol. 10, pp. 73-83, 1957.

57. Groves, G. V., Initial Expansion to Ambient Pressure of Chemical Explosive Releases in the Upper Atmosphere, J. Geophys. Res., Vol. 68, No. 10, pp. 3033-3047, 1963.

58. Groves, G. V., Acoustic Pulse Characteristics of Explosive Releases in the Upper Atmosphere, Project Firefly (1962-3), AFCRL Report 364, p. 351, 1964.

59. Groves, G. V., Atmospheric Structure and Its Variations in the Region from 25 to 120 km, AFCRL-71-0410, Environ. Res. Paper, No. 368, 1971.

60. Halliday, I., The Meteorite Observation and Recovery Project, Bull. Radio and Electrical Engin. Div., Nat'l Res. Council of Canada, Vol. 20, No. 3, pp. 1-4, 1970.

61. Hawkins, G. S. and R. B. Southworth, The Statistics of Meteors in the Earth's Atmosphere, Smithsonian Contrib. to Astrophys., Vol. 2, No. 11, Washington, D. C., 1958.

62. Hayes, W. D. et al., Sonic Boom Propagation in a Stratified Atmosphere With Computer Program, NASA CR-1299, 1969.

63. Hayes, W. D., Sonic Boom, Annual Review of Fluid Mechanics, M. Van Dyke, W. G. Vincenti and T. V. Wehausen (Editors), Vol. 3, Annual Review, Inc., Palo Alto, CA., pp. 269-90, 1971.

64. High Altitude Meteorological Data, World Data Center A, U. S. Dept. of Commerce, NOAA, Asheville, N. C., Vol. III, No. 9, 1966; Vol. V, No. 12, 1968; Vol. VI, No. 2, 1969; and Vol. VII, No. 1, 1970.

65. Hilton, D. A. et al., Sonic-Boom Ground-Pressure Measurements from Apollo 15, NASA TN D-6950, 35 pp., 1972.

66. Hindley, B. and H. Miles, The Fireball and Meteorite of 1969, J. Brit. Astro. Assn., Vol. 80, No. 4, pp. 313-322, 1970.

67. Holmes, C. R., M. Brook, P. Krehbiel, and R. McCrory, On the Power Spectrum and Mechanism of Thunder, J. Geophys. Res., Vol. 76, No. 9, pp. 2106-2115, 1971.

68. Izakov, M. N., On Theoretical Models of the Structure and Dynamics of the Earth's Thermosphere, Space Sci. Rev., Vol. 12, No. 3, pp. 261-298, 1971.

69. Jacchia, L. G. et al., An Analysis of the Atmospheric Trajectories of 413 Precisely Reduced Photographic Meteors, Smithsonian Contrib. to Astrophy., Vol. 10, No. 1, 1967.

70. Jones, D. L., et al., Shock Wave from a Lightning Discharge, J. Geophys. Res., Vol. 73, No. 10, pp. 3121-3127, 1968.

71. Jones, D. L., Comments on Paper by A. A. Few, A. J. Dessler, Don J. Latham, and M. Brook, 'A Dominant 200-Hertz Peak in the Acoustic Spectrum of Thunder, J. Geophys. Res., Vol. 73, No. 14, pp. 4776-4777, 1968.

72. Kahalas, S. L. and B. L. Murphy, Second-Order Correction to the Reed-Otterman Theory, Geophys. J. Roy. Astron. Soc., Vol. 26, pp. 379-389, 1971.

73. Kane, E. J., Some Effects of the Nonuniform Atmosphere on the Propagation of Sonic Booms, J. Acou. Soc. Amer., Vol. 39, S26, 1966.

74. Korobeinikov, V. P., Gas Dynamics of Explosions, Annual Review of Fluid Mechanics, M. Van Dyke, W. G. Vincenti and T. V. Wehausen (Editors), Vol. 3, Annual Review, Inc., Palo Alto, CA, pp. 317-346, 1971.

75. Korobeinikov, V. P., P. I. Chushkin and L. V. Shurshalov, Gas Dynamics of the Flight and Explosion of Meteorite Bodies in the Earth's Atmosphere, UCRL-TRANS-10572, Available from NTIS, Springfield, Va., 33 pp., 1971.

76. Krinov, E. L., Principles of Meteoritics, Pergamon Press, New York, pp. 63-83, 1960.

77. Kushner, S. S. and J. W. Wescott, Propagation of Sound in Air, (A Bibliography with Abstracts), The University of Michigan, College of Engineering, 1965.

78. LaPaz, L., Effects of Meteorites Upon the Earth, Adv. in Geophys., Vol. 4, pp. 219-350, 1958.

79. Lighthill, M. J., Viscosity Effects in Sound Waves of Finite Amplitude, in Surveys in Mechanics, G. K. Batchelor and H. Bondi (Editors), Cambridge University Press, pp. 251-350, 1956.

80. Lin, S. C., Cylindrical Shock Waves Produced by Instantaneous Energy Release, J. Appl. Phys., Vol. 25, No. 1, pp. 54-57, 1954.

81. Liszka, L. and S. Olsson, On the Generation and Detection of Artificial Atmospheric Waves, J. Atmos. Terr. Phys., Vol. 33, pp. 1933-1939, 1971.

82. Lowery, C. J. and E. M. Shoemaker, Airwaves Associated with Large Fireballs and the Frequency Distribution of Energy of Large Meteoroids, J. Meteor. Soc., Vol. 3, No. 3, pp. 123-124, 1967.

83. Lyubarskiy, K. A., A Statistical Study of Bolides, Meteoritika, Vol. 11, pp. 153-164, 1952.

84. McCarty, V. M. and I. Dalins, Frequency Shift in Air-Coupled Surface Waves Originated by Rocket Launches, J. Geophys. Res., Vol. 76, No. 29, pp. 7027-7034, 1971.

85. McCrosky, R. E. and A. Posen, Prarie Network Meteor Data, Smithsonian Astrophysical Observatory, Special Report 273, 1968.

86. McCrosky, R. E., Distribution of Large Meteoritic Bodies, SAO Special Report 280, 1968.

87. McCrosky, R. E., The Lost City Meteorite Fall, Sky and Telescope, pp. 154-158, March 1970.

88. McCrosky, R. E. and Z. Ceplecha, Fireballs and the Physical Theroy of Meteors, Bull. Astron. Inst. Czechoslovakia, Vol. 21, No. 5, pp. 271-296, 1970.

89. McCrosky, R. E. et al., Lost City Meteorite--Its Recovery and a Comparison with other Fireballs, J. Geophys. Res., Vol. 76, No. 17, pp. 4090-4108, 1971.

90. McCrosky, R. E., Private Communication: June 1971, July 1971, August 1971, December 1971, April 1972, June 1972, and December 1972.

91. Meighan, I. and P. Doughty, Recent Fall of the Bovedy Meteorite, Northern Ireland, Nature, Vol. 223, pp. 24-29, July 5, 1969.

92. Meteorological Rocket Network Firings - Data Report, Vol. XLIII, IRIG Document 109-62, U. S. Army Electronics Research and Development Activity, White Sands Missile Range, N. M., 1965.

93. Meyer, R. E., On the Far Field of a Body Rising Through the Atmosphere, J. Geophys. Res., Vol. 67, No. 6, pp. 2361-2366, 1962.

94. Millman, P. M., A Tape Recording of the Belfast Meteorite, J. Roy. Astron. Soc. of Canada, Vol. 64, No. 1, pp. 57-59 1970.

95. Millman, P. M., Meteor Showers and Interplanetary Dust, Space Res. X, N. Holland Publishing Co., Amsterdam, 1970.

96. Morse, P. M. and K. U. Ingard, Theoretical Acoustics, McGraw-Hill, 927 pp., 1968.

97. Nininger, H. H., Out of the Sky - An Introduction to Meteoritics, Dover Publications Inc., New York, 1952.

98. Officer, C. B., Introduction to the Theory of Sound Transmission-Application to the Ocean, McGraw-Hill, New York, 1958.

99. Öpik, E., Physics of Meteor Flight in the Atmosphere, Interscience Publishers, Inc., New York, 1958.

100. Öpik, E., The Sonic Boom of the Boveedy Meteorite, Irish Astron. Journal, Vol. 9, No. 8, pp. 308-310, 1970.

101. Otterman, J., Finite Amplitude Propagation Effect on Shock-Wave Travel Times from Explosions at High Altitudes, J. Acous. Soc. Amer., Vol. 31, No. 4, pp. 470-474, 1959.

102. Pan, Y. S. and W. A. Sotomayer, Sonic Boom of Hypersonic Vehicles, AIAA Journal, Vol. 10, No. 4, pp. 550-551, 1972.

103. Pan, Y. S. and M. O. Varner, Studies on Sonic Boom at High Mach Numbers, 5th AIAA Fluid and Plasma Dynamics Conference, Boston, MA, Available from Tech. Inform. Serv. as A 72-34082, 11 pp., 1972.

104. Parker, L. W. et al., Godunov Method and Computer Program to Determine the Pressure and Flow Field Associated with a Sonic Boom Focus, NASA CR 2127, 109 pp., 1973.

105. Pierce, A. D. and C. Thomas, Atmospheric Correction Factor for Sonic-Boom Pressure Amplitudes, J. Acous. Soc. Amer., Vol. 46, p. 1366, 1969.

106. Pierce, A. D., J. W. Posey and E. F. Iliff, Variation of Nuclear Explosion Generated Acoustic - Gravity Wave Forms with Burst Height and with Energy Yield, J. Geophys. Res., Vol. 76, No. 21, pp. 5025-5042, 1971.

107. Plooster, M. N., Shock Waves from Line Sources, NCAR TN 37, 84 pp., National Center for Atmospheric Research, Boulder, Colorado, 1968.

108. Plooster, M. N., The Propagation and Decay of Acoustic Waves from Lightning Strokes, unpublished manuscript received in private communication, 13 pp., 1970.

109. Plooster, M. N., Numerical Simulation of Spark Discharges in Air, Phys. of Fluids, Vol. 14, No. 10, pp. 2111-2123, 1971.

110. Procunier, R. W., Private Communication, July 1971.

111. Procunier, R. W. and G. W. Sharp, Optimum Frequency for Detection of Acoustic Sources in the Upper Atmosphere, J. Acous. Soc. Amer., Vol. 49, No. 3, (Part 1), pp. 622-626, 1971.

112. Rajchl, J. et al., On the Fireball of March 22, 1968 and Two Groups of Fireballs, Bull. Astron. Inst. Czechoslovakia, Vol. 20, No. 3, pp. 111-117, 1969.

113. Reed, J. W., Attenuation of Blast Waves by the Atmosphere, J. Geophys. Res., Vol. 77, No. 9, pp. 1616-1622, 1972.

114. Reed, J. W., Airblast Overpressure Decay at Long Ranges, J. Geophys. Res., Vol. 77, No. 9, pp. 1623-1629, 1972.

115. Reed, S. G., Note on Finite Amplitude Propagation Effects on Shock Wave Travel Times from Explosions at High Altitude, J. Acous. Soc. Amer., Vol. 31, p. 1265, 1959.

116. Riddell, F. R. and H. B. Winkler, Meteroites and Re-Entry of Space Vehicles at Meteor Velocities, ARS Journal, pp. 1523-1530, 1962.

117. Romig, M. F. and D. L. Lamar, Anomalous Sounds and Electromagnetic Effects Associated with Fireball Entry, Rand Corporation Memorandum RM-3724-ARPA, 1963.

118. Romig, M. F. and D. L. Lamar, Electromagnetic Effects Associated with the San Francisco Fireball of November 7, 1963, Meteoritics, Vol. 2, No. 4, pp. 301-310, 1965.

119. Sakurai, A., Blast Wave Theory, Basic Developments in Fluid Dymanics, M. Holt Editor, Vol. 1, pp. 309-375, Academic Press, New York, 1965.

120. Seebass, A. R. and A. R. George, Sonic Boom Reduction Through Aircraft Design and Operation, AIAA Paper No. 73-241, Presented at AIAA 11th Aerospace Sci. Meeting, Washington, D. C., pp. 1-21, 1973.

121. Shoemaker, E. M., Private Communication, June, 1972.

122. Smith, F. L. and C. Smith, Numerical Evaluation of Chapman's Grazing Incidence Integral ch(X, x), J. Geophys. Res., Vol. 77, No. 19, pp. 3592-3597, 1972.

123. Strelitz, R. A., Meteorite Impact in the Ocean (Abstract), Trans. Amer. Geophys. Union, Vol. 54, No. 4, p. 352, 1973.

124. Taylor, G. I., The Formation of a Blast Wave by a Very Intense Explosion I. Theoretical Discussion, Proc. Roy. Soc. London A., Vol. 201, pp. 159-186, 1950.

125. Theon, J. S. et al., The Mean Observed Meteorological Structure and Circulation of the Stratosphere and Mesosphere, NASA TR R-375, 1972.

126. Thompson, R. J., Ray Theory for an Inhomogeneous Moving Medium, J. Acous. Soc. Amer., Vol. 51, No. 5 (Part 2), pp. 1675-1682, 1972.

127. Towne, D. H., Wave Phenomena, Addison-Wesley, Mass., 1967.

128. Troutman, W. W., Numerical Calculation of the Pressure Pulse from a Lightning Stroke, J. Geophys. Res., Vol. 74, No. 18, pp. 4595-4596, 1969.

129. Tsikulin, M. A., Shock Waves During the Movement of Large Meteorites in the Atmosphere, Trans. Div. U. S. Naval Intelligence Command, Alexandria, Va., available from the Nat'l Tech. Inform. Serv., Springfield, Va. as AD 715-537, 1970.

130. U. S. Department of Commerce, NOAA, Daily and Weekly Weather Map Series, U. S. Government Printing Office, Washington, D. C., 1965, 1966, 1968, 1969, and 1970.

131. U. S. Standard Atmosphere Supplements, 1966, U. S. Government Printing Office, Washington, D. C., 1966.

132. Varley, E. and E. Cumberbatch, Large Amplitude Waves in Stratified Media: Acoustic-Pulses in a Stratified Atmosphere, Center for the Application of Mathematics, Lehigh University, Technical Report No. CAM-110-8, 45 pp., 1969.

133. Vincenti, W. G. and S. C. Traugott, The Coupling of Radiative Transfer and Gas Motion, Annual Review of Fluid Mechanics, M. Van Dyke, W. G. Vincenti and T. V. Wehausen (Editors), Vol. 3, Annual Review Inc., Palo Alto, CA., pp. 89-116, 1971.

134. Warfield. J. T., Acoustic Ray Propagation in Channels With a Horizontal Sound Speed Gradient, Ph. D. Thesis (Applied Mathematics), Rensselaer Polytechnic Institute, 198 pp., 1971.

135. Wegener, A., Das detonierende Meteor vom 3 April 1916, 3-1/2 uhr nachmittags in Kurhessen, Schriften der Gesellshaft zur Beforderung der gesamten Naturwissenschaften zu Marburg, Band 14, Erstes Heft, 11. 1-83, 1917.

136. Whipple, F. J. W., The Detonating Meteor of September 6, 1926. An Instance of an Outer Zone of Audibility, Proc. Roy. Soc. London, Series A, Vol. 2.2, pp. 89-96, 1928.

137. Whipple, F. J. W., The Great Siberian Meteor and the Waves, Seismic and Aerial, which it Produced, Quart. J. Roy. Meteor. Soc., Vol. 56, pp. 287-304, 1930.

BIBLIOGRAPHY (Part 3) (Conclusion)

138. Whitham, G. B., Linearized Flow of a Supersonic Projectile, Comm. Pure and Applied Math, Vol. 5, pp. 301-348, 1952.

139. Whitham, G. B., On the Propagation of Weak Shock Waves, J. Fluid Mech., Vol. 1, Part 3, pp. 290-318, 1956.

140. Wilson, C. R., Private Communication, June, 1972.

141. Wood, J. A., Stony Meteorite Orbits, Month. Not. Roy. Astron. Soc., Vol. 122, No. 1, pp. 79-88, 1961.

142. Wood, J., Fourth Lunar Science Conference, Science, Vol. 181, No. 4100, pp. 615-622, August 17, 1973.

143. Woodward, M. W. and V. H. Goerke, Infrasound from the September 18, 1966, Meteorite (Abstract), Trans. Amer. Geophys. Union, Vol. 48, No. 1, pp. 81-82, 1967.

144. Wylie, C. C., Sounds From Meteors, Popular Astronomy, Vol. 40, No. 5, Whole No. 395, pp. 289-294, 1932.

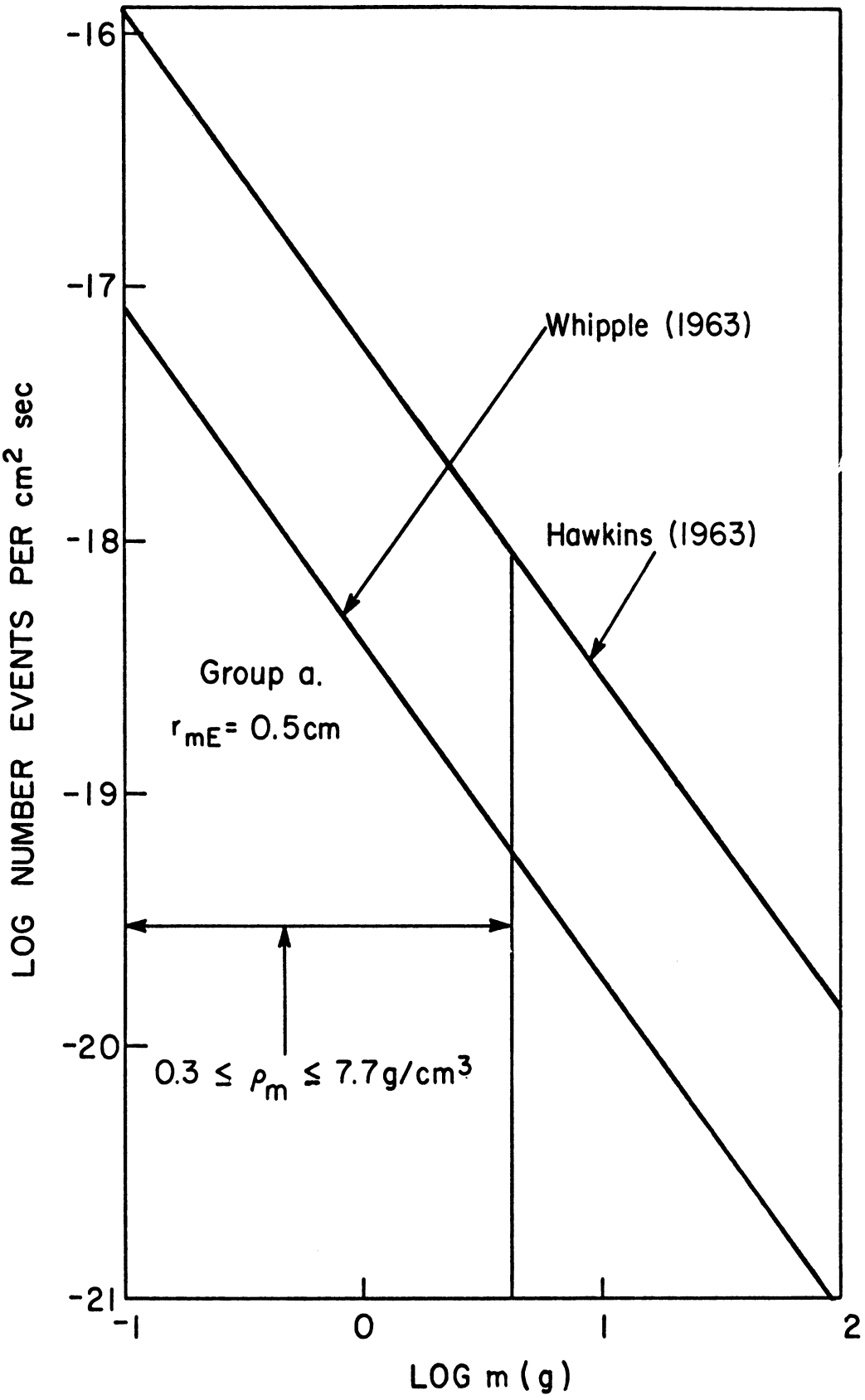

Figure 117. Meteor mass as a function of the number of events per cm^2 sec, after Cosby and Lyle, 1965 (Group a)

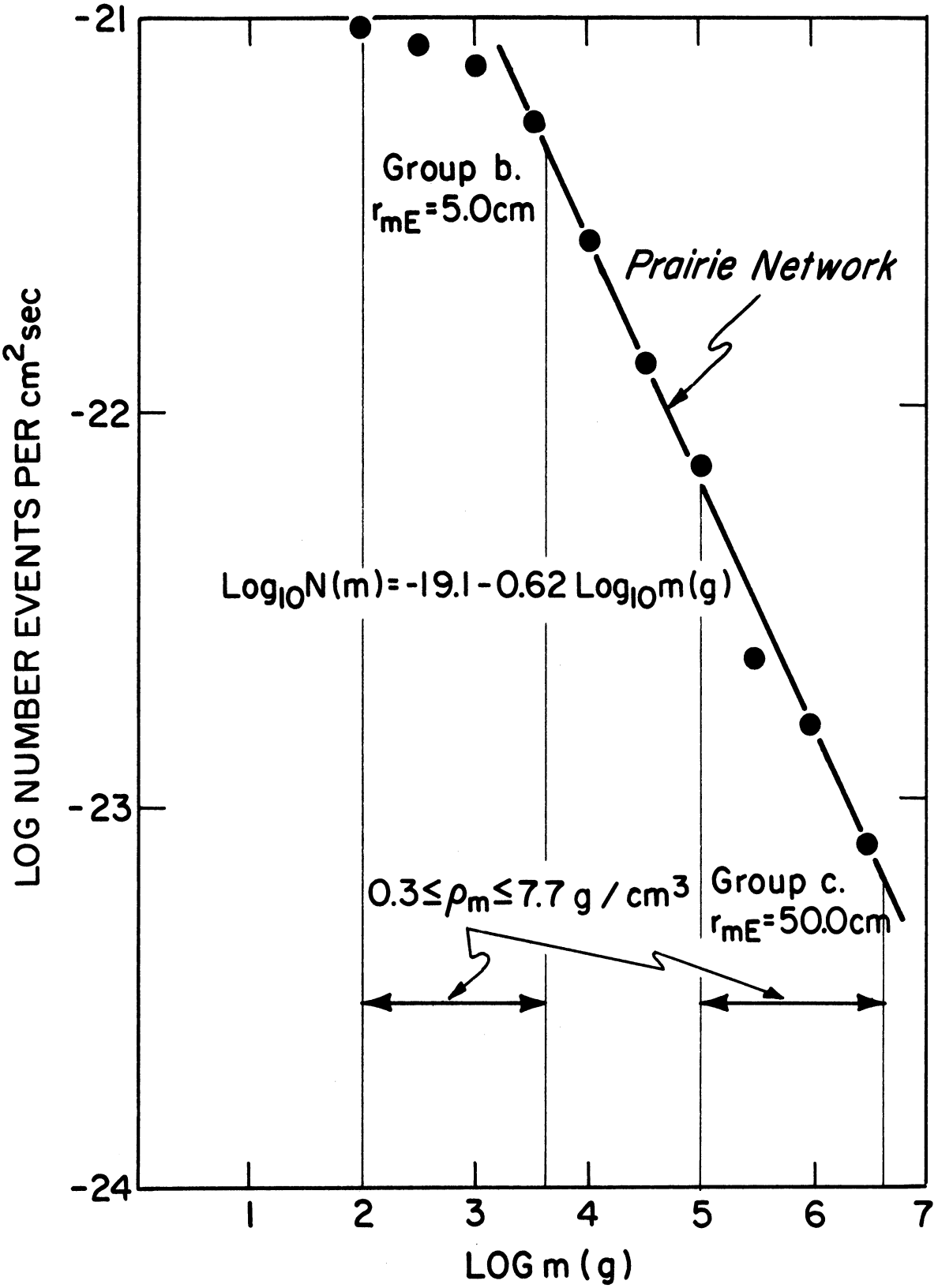

Figure 118. Meteor mass as a function of the number of events per cm^2 sec, after McCrosky, 1968 (Groups b and c)

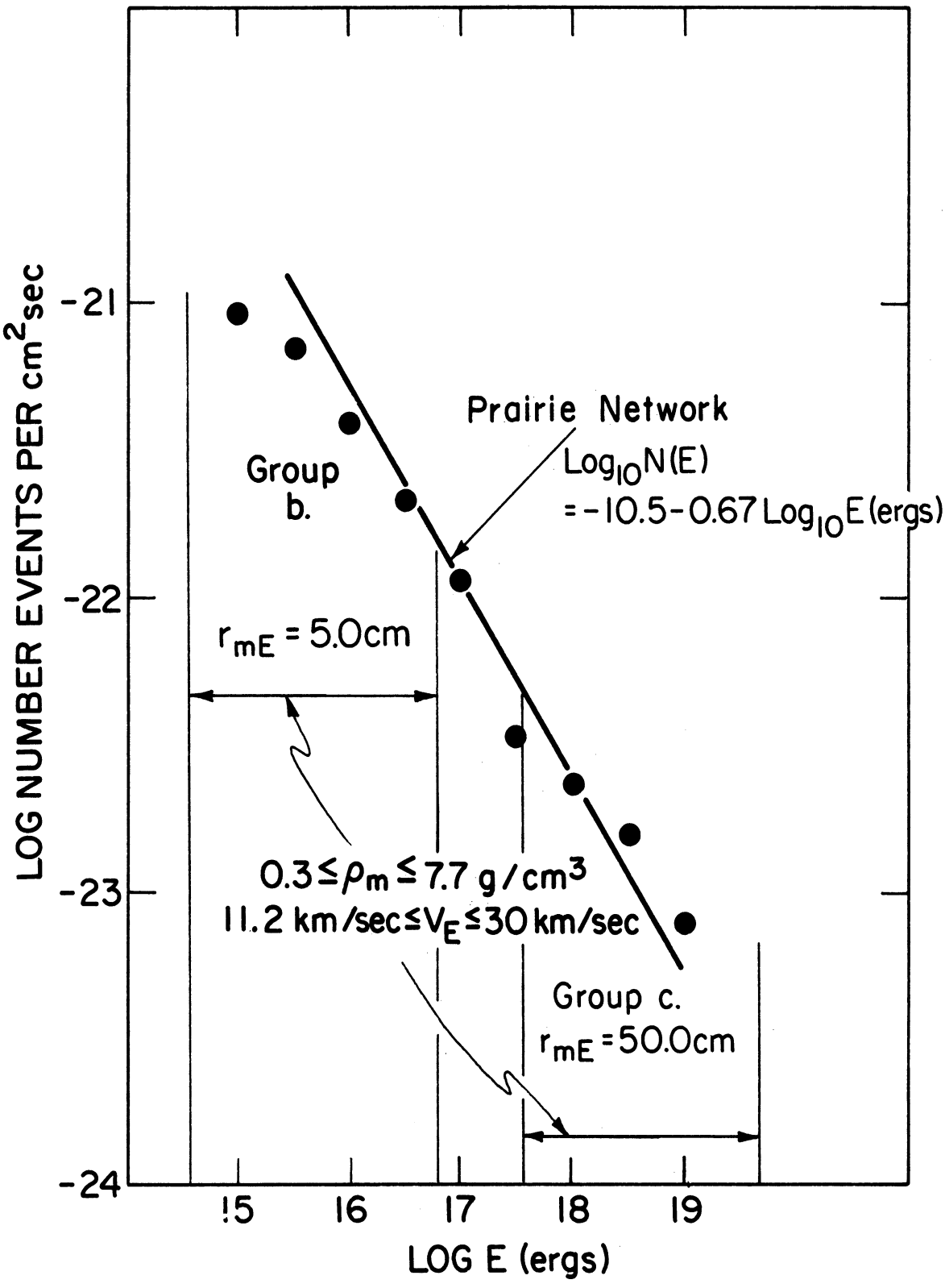

Figure 119. Preatmospheric value of meteor kinetic energy as a function of the number of events per cm^2 sec, after McCrosky, 1968 (Groups b and c)

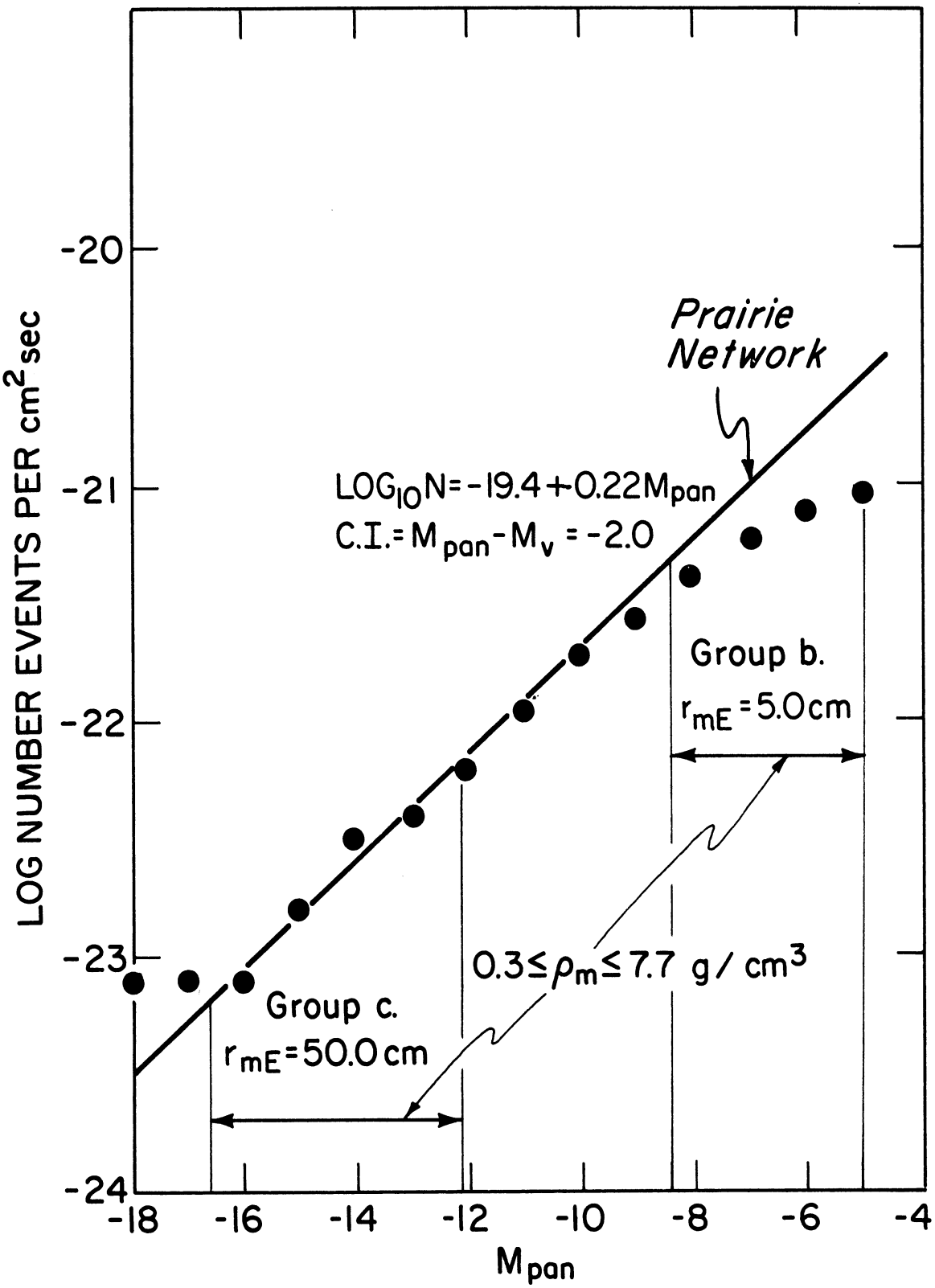

Figure 120. Maximum value of the panchromatic magnitude as a function of the number of events per cm^2 sec, after McCrosky, 1968 (Groups b and c)

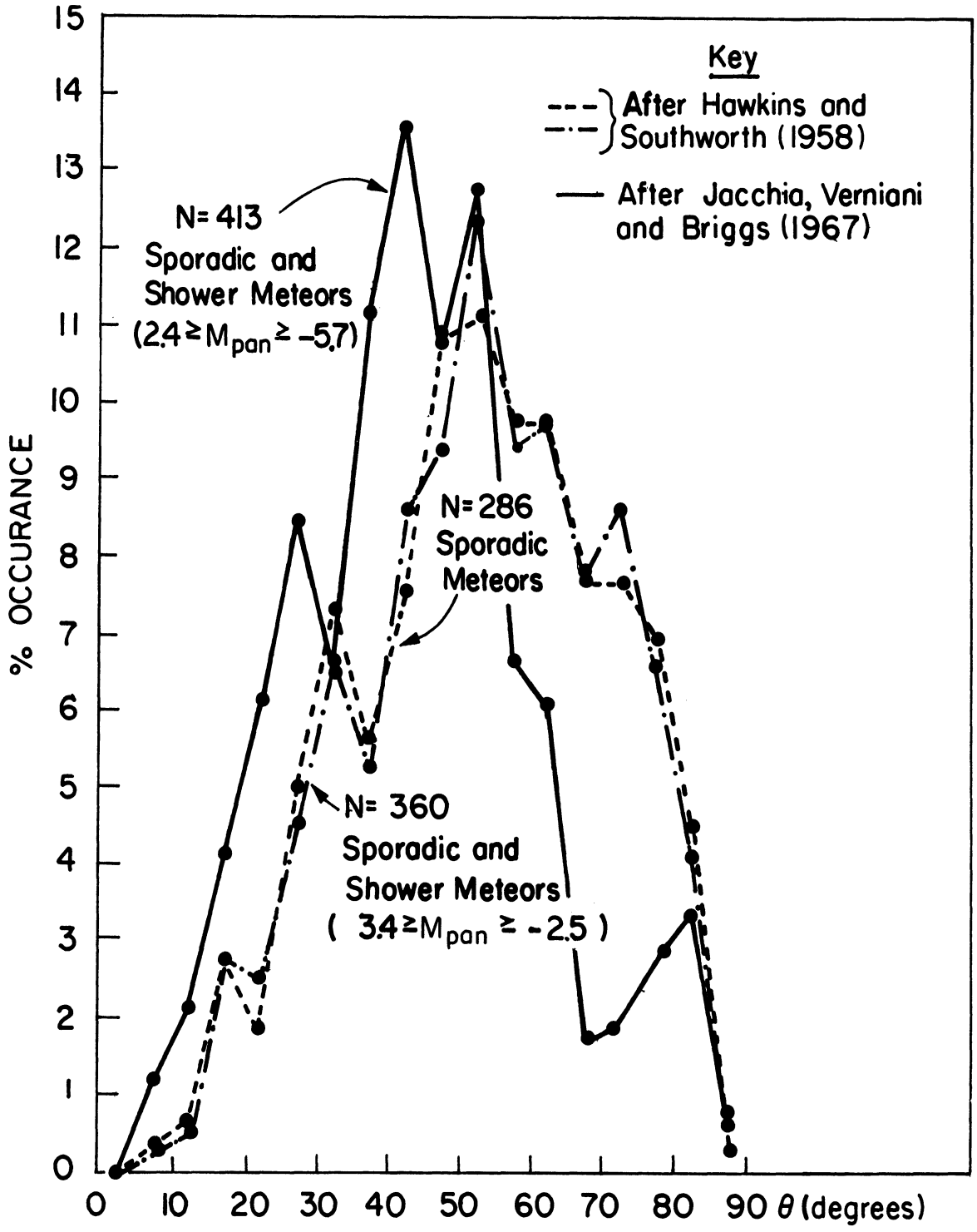

Figure 121. Meteor entry elevation angle as a function of the percent occurrence for meteors such that $3.4 \geq M_{pan} \geq -5.7$, after Hawkins and Southworth, 1958 and Jacchia, Verniani and Briggs, 1967 (Points are plotted in five degree intervals at the center of each interval)

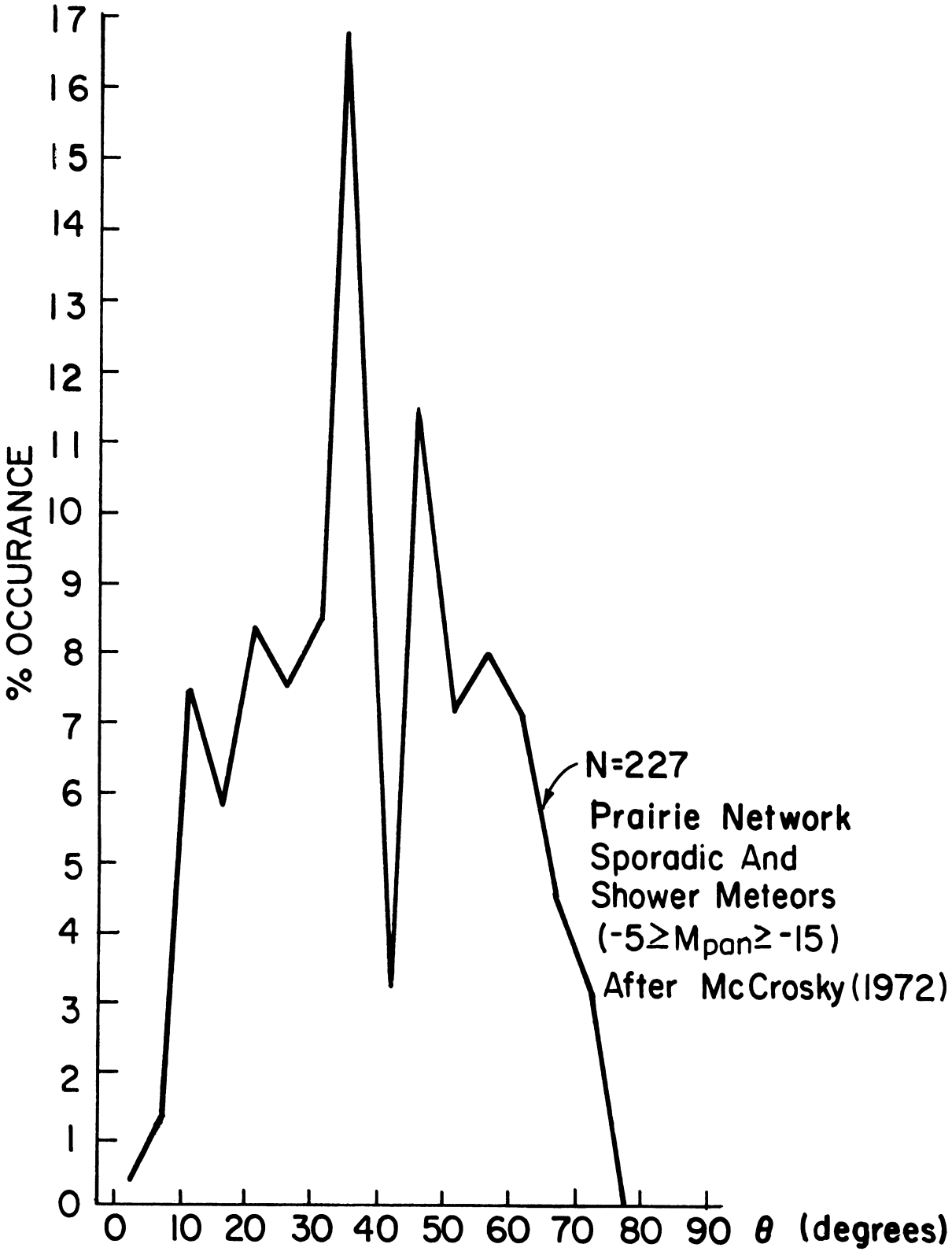

Figure 122. Meteor entry elevation angle as a function of the percent occurrence for meters such that $-5 \geq M_{pan} \geq -15$, after McCrosky, 1972 (Points are plotted in five degree intervals at the center of each interval)

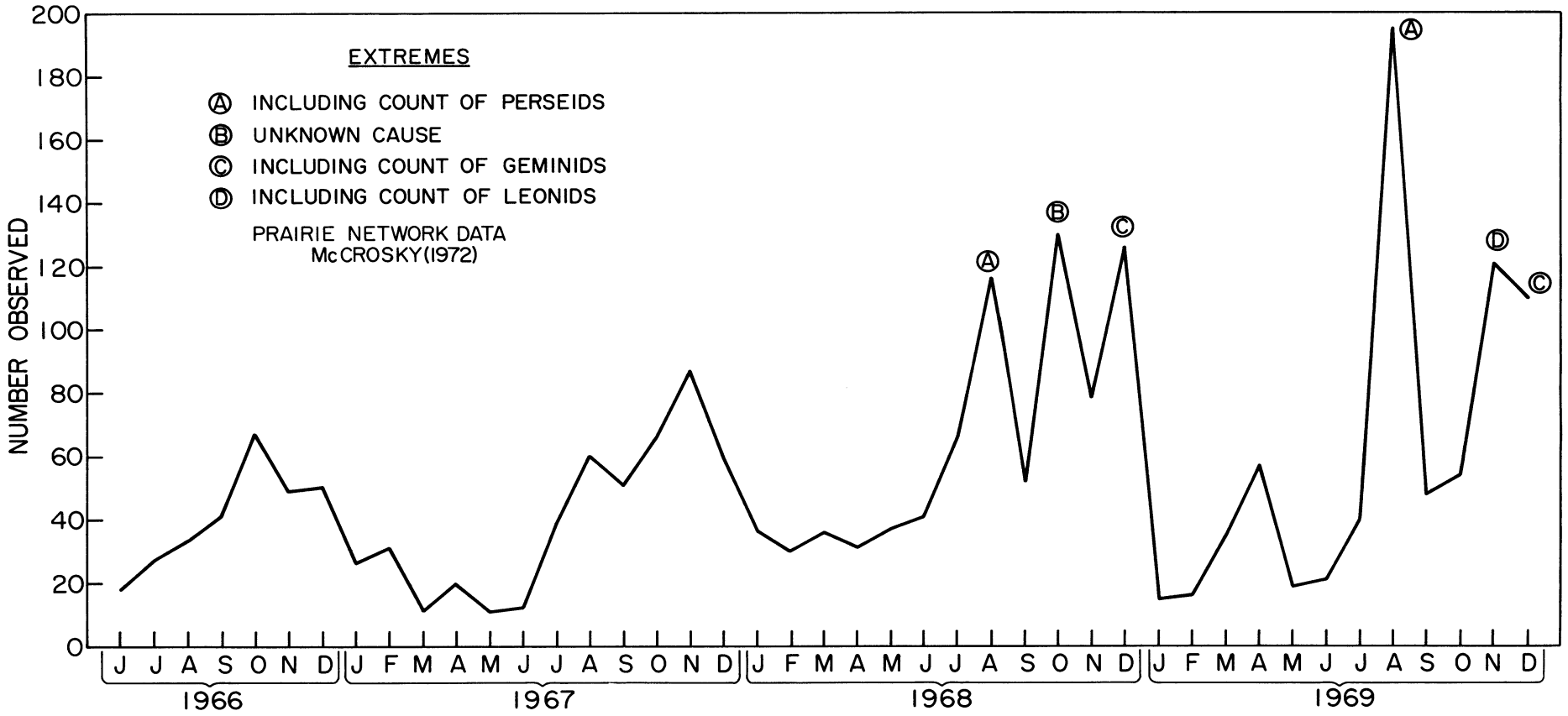

Figure 123. Number of meteors observed as a function of the month of the year from June 1966 to December, 1969, after McCrosky, 1972.

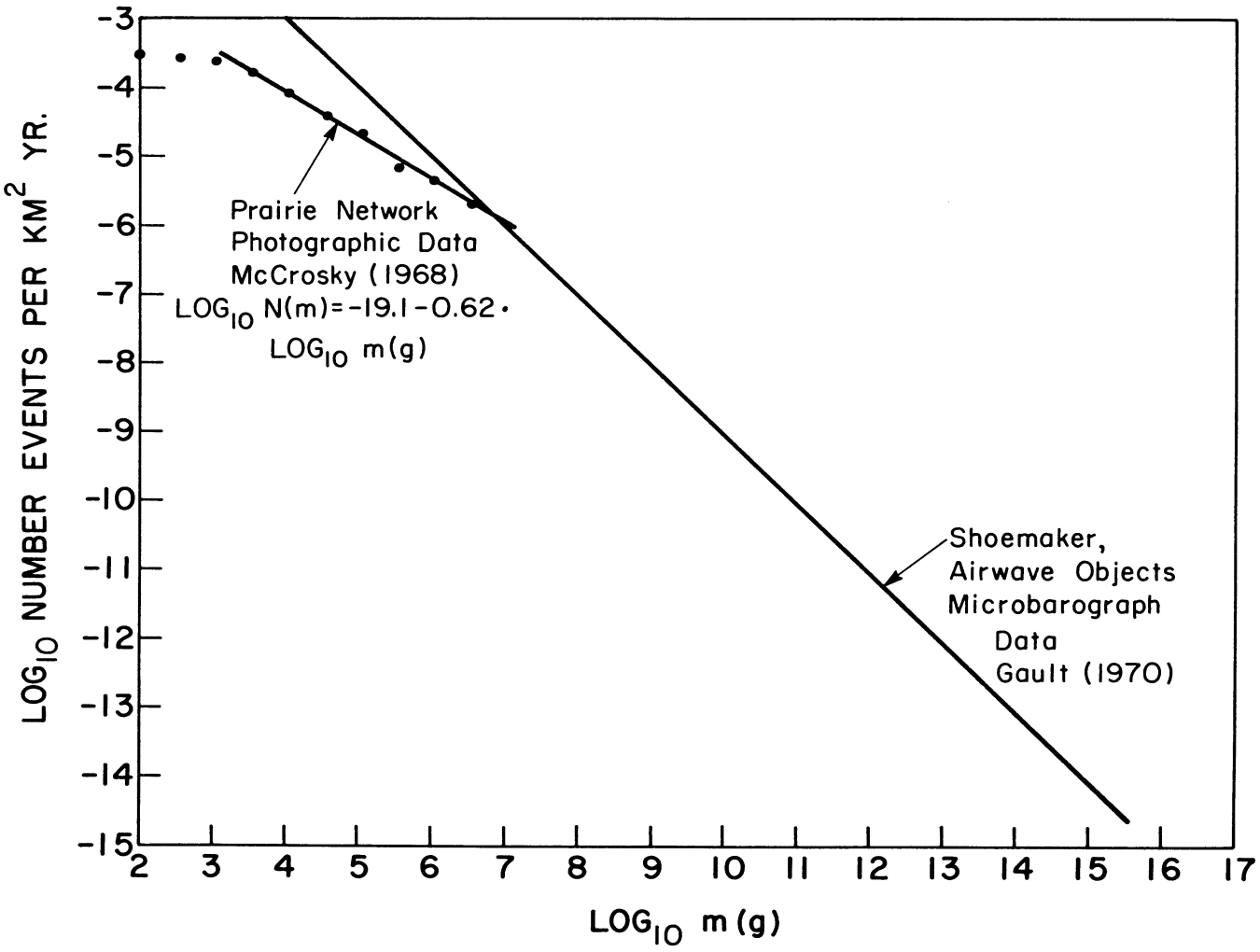

Figure 124. Meteor mass as a function of the number of events per km^2 yr, after McCrosky, 1968 and Gault, 1970.

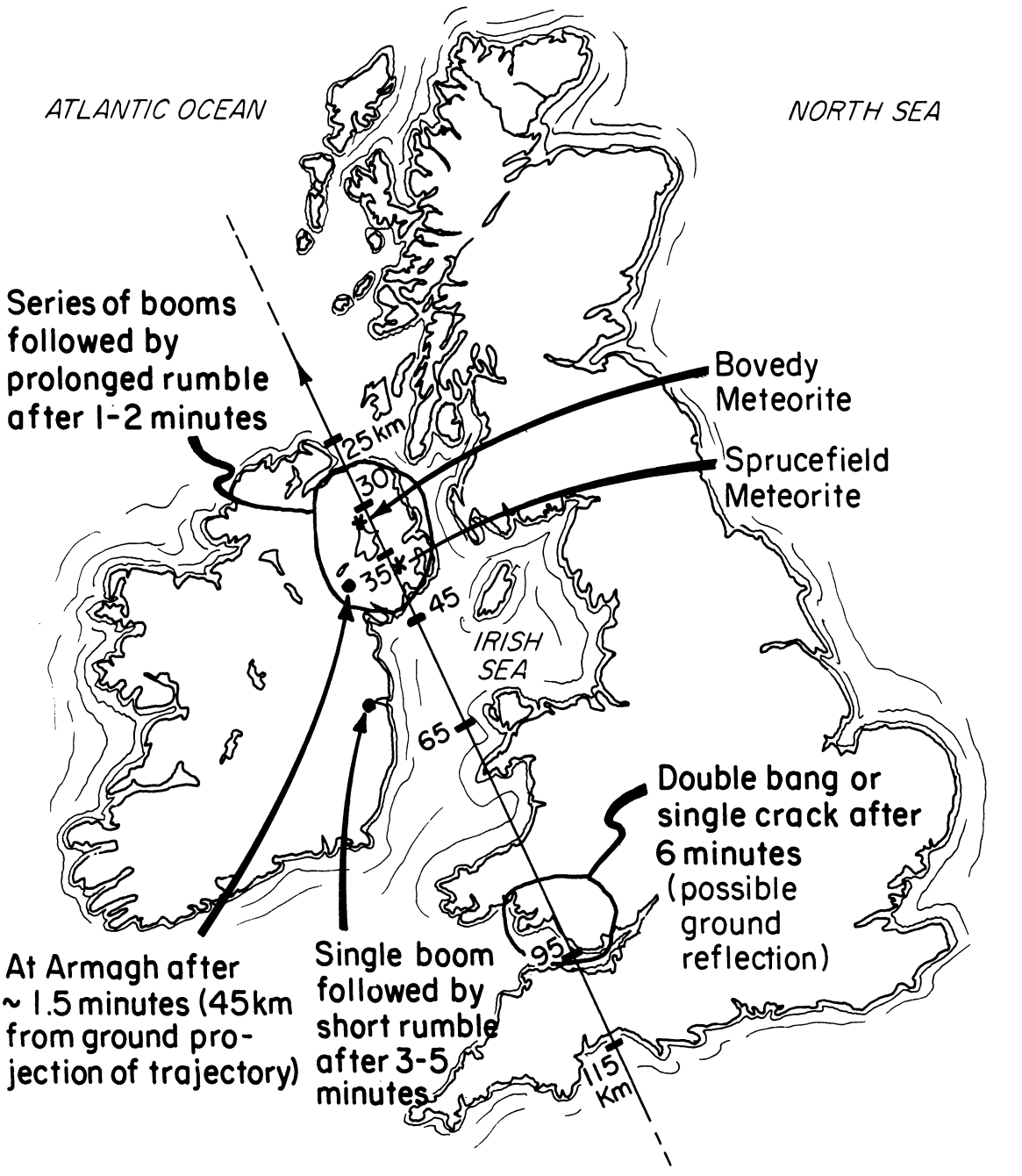

Figure 125. Ground projection of the entry of the British Fireball of April 25, 1969, after Hindley and Miles, 1970.

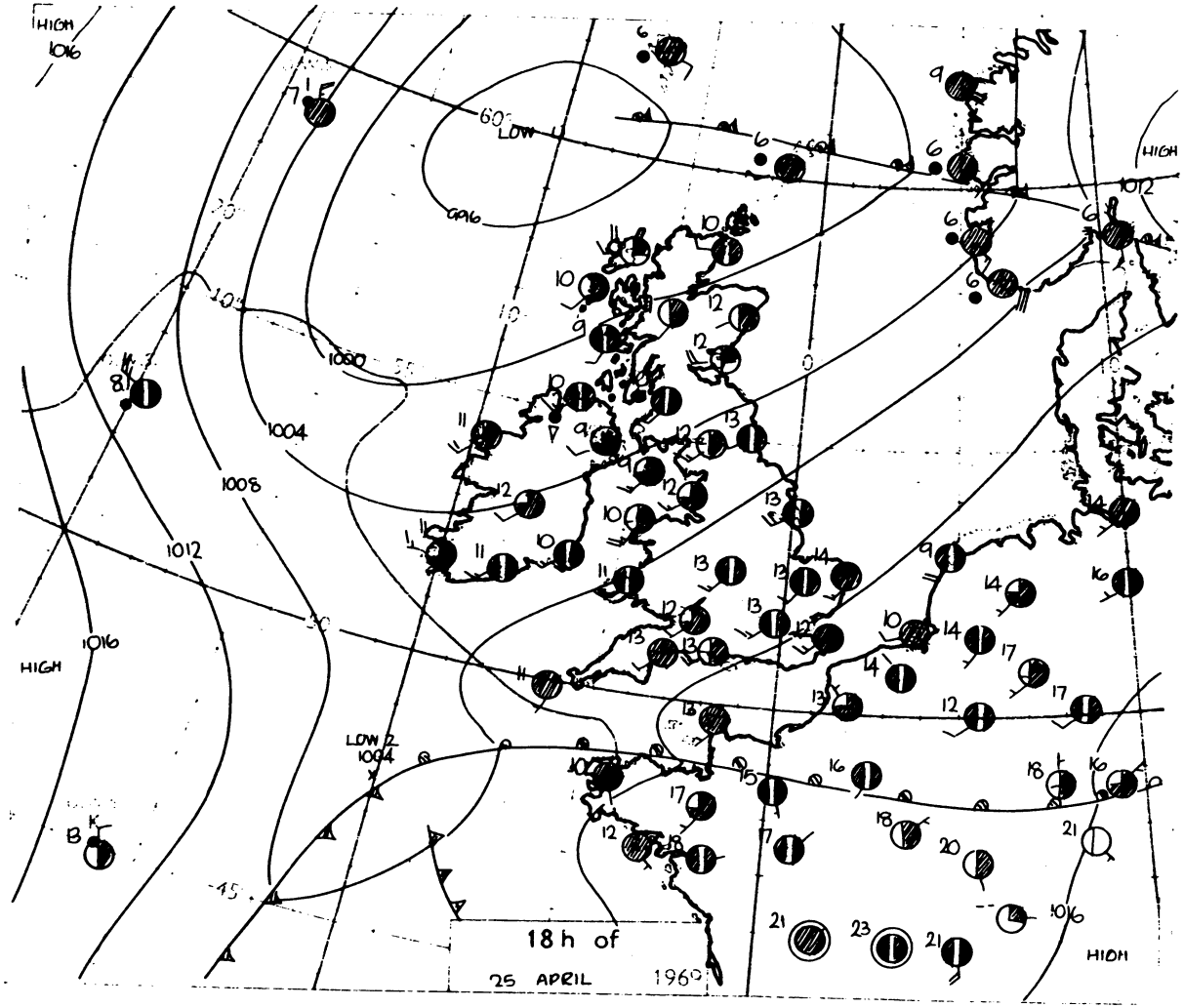

Figure 126. Surface weather map of the British Isles, 18 h of April 25, 1969 (British Meteorological Service)

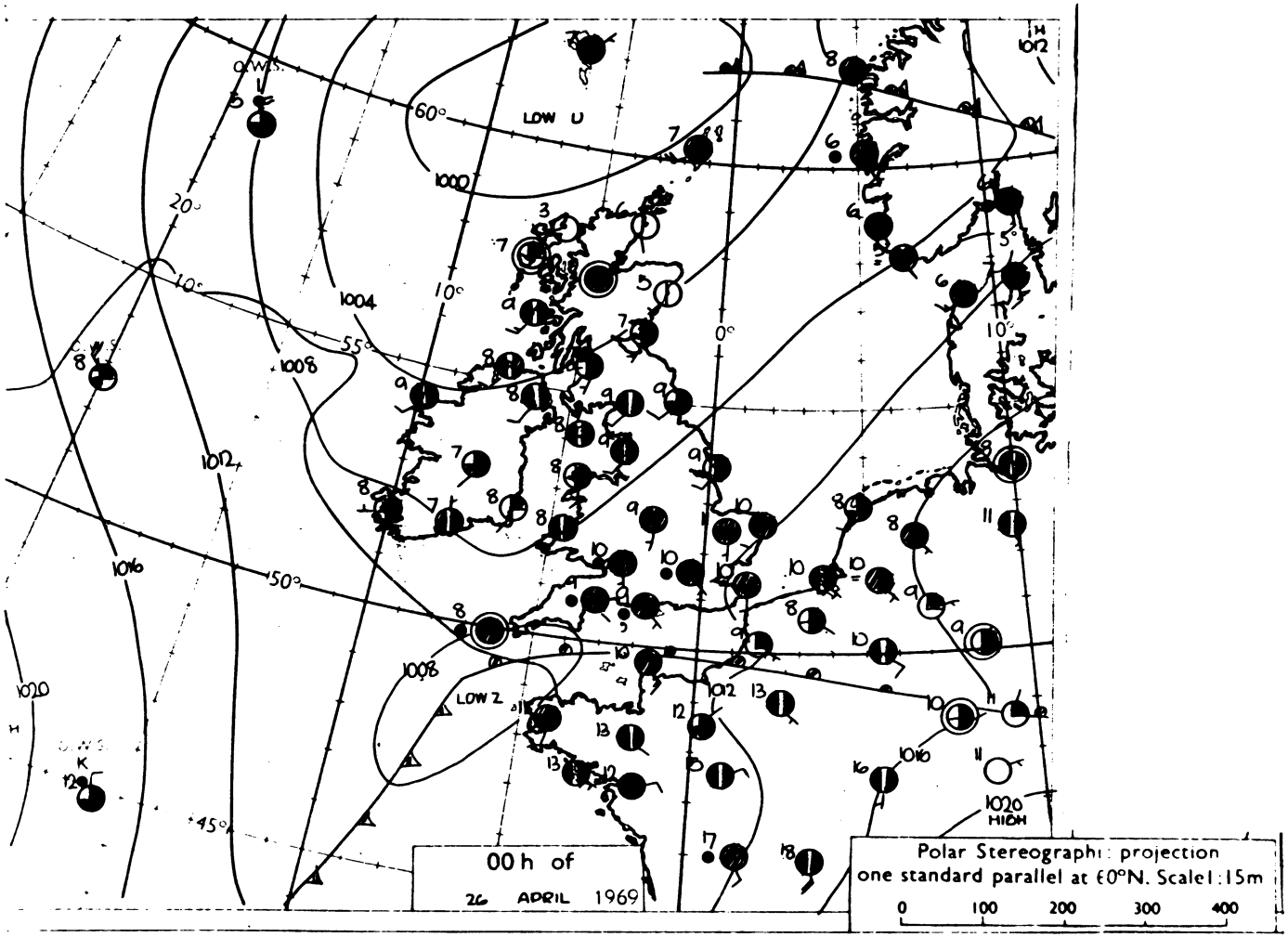

Figure 127. Surface weather map of the British Isles 00h of April 26, 1969 (British Meteorological Service)

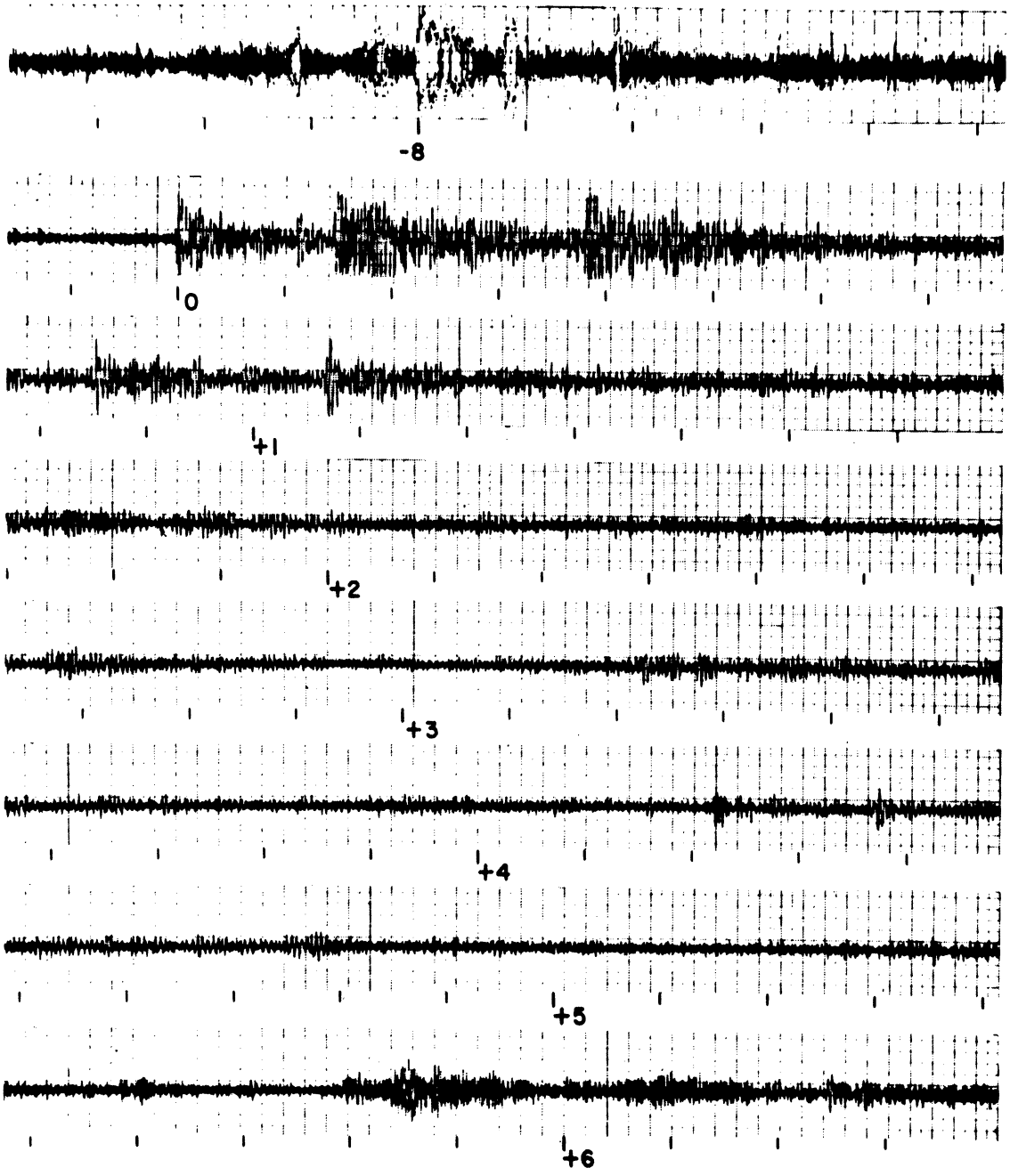

Figure 128. The sonic boom recording of the British Fireball of April 25, 1969, after Millman, 1970 ("There is a large gap in time between lines 1 and 2 and a small gap between lines 7 and 8, the remainder of the recording being continuous. Amplitude for the paper recording was cut to quarter strength after line 1.")

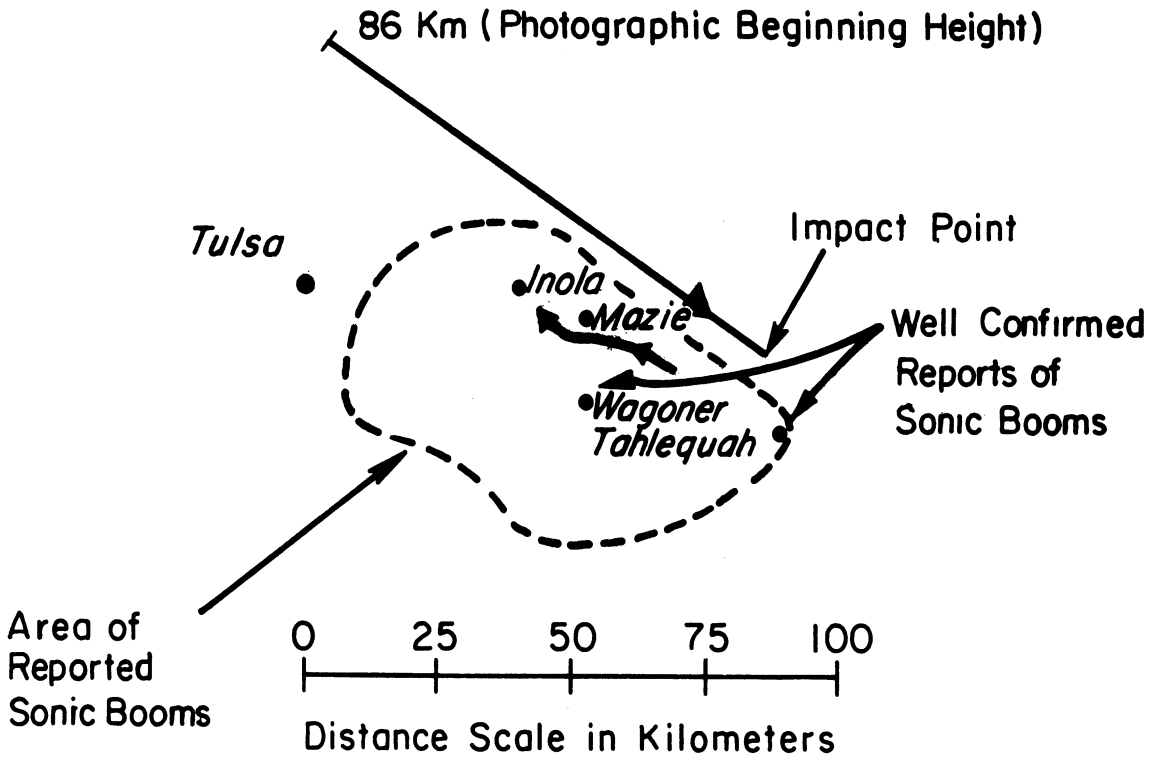

Figure 129. Ground projection of the entry of the Lost City Meteorite of January 3, 1970, after McCrosky, 1971.

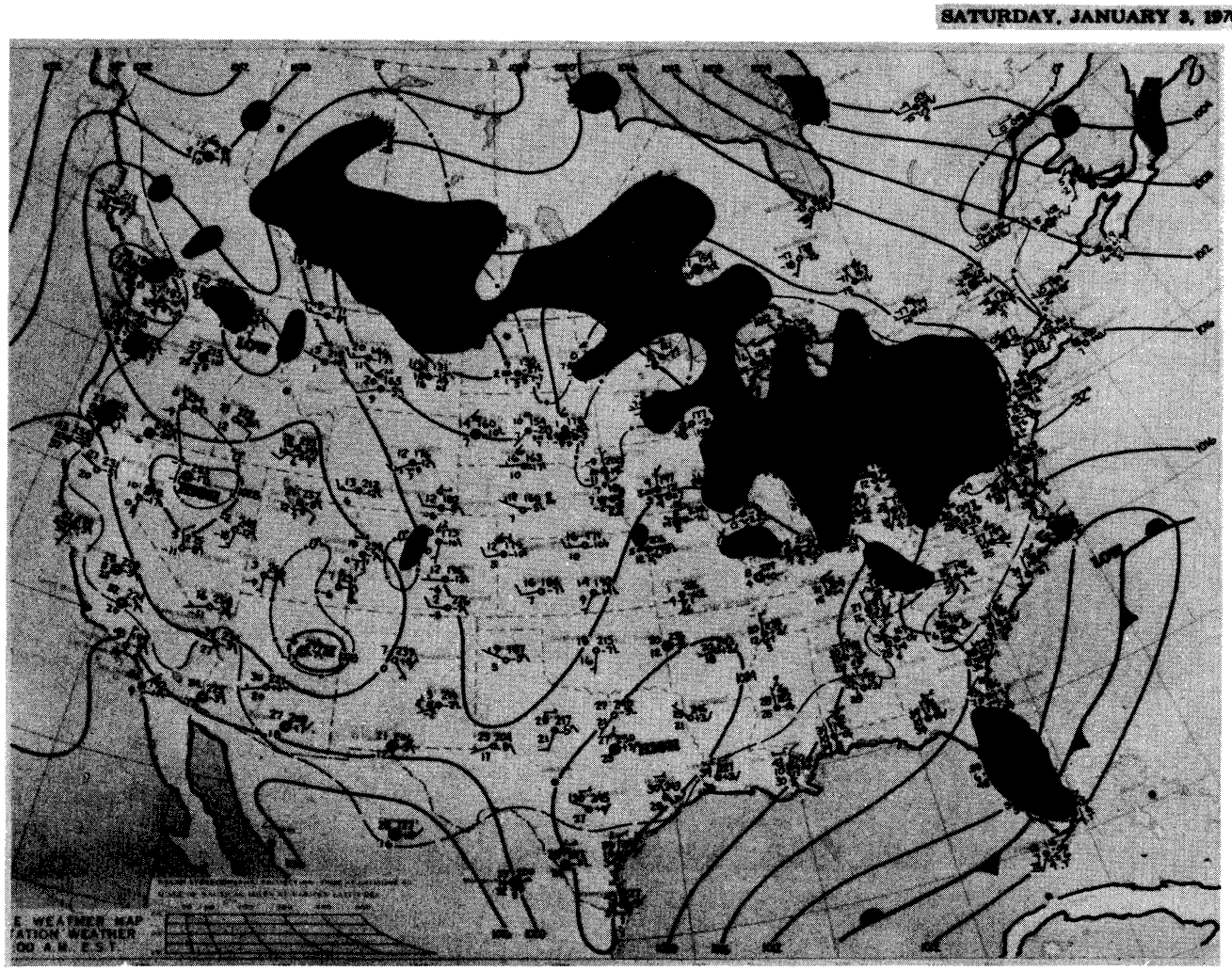

Figure 130. U. S. Weather Service surface map, 7:00 a. m., E. S. T., January 3, 1970.

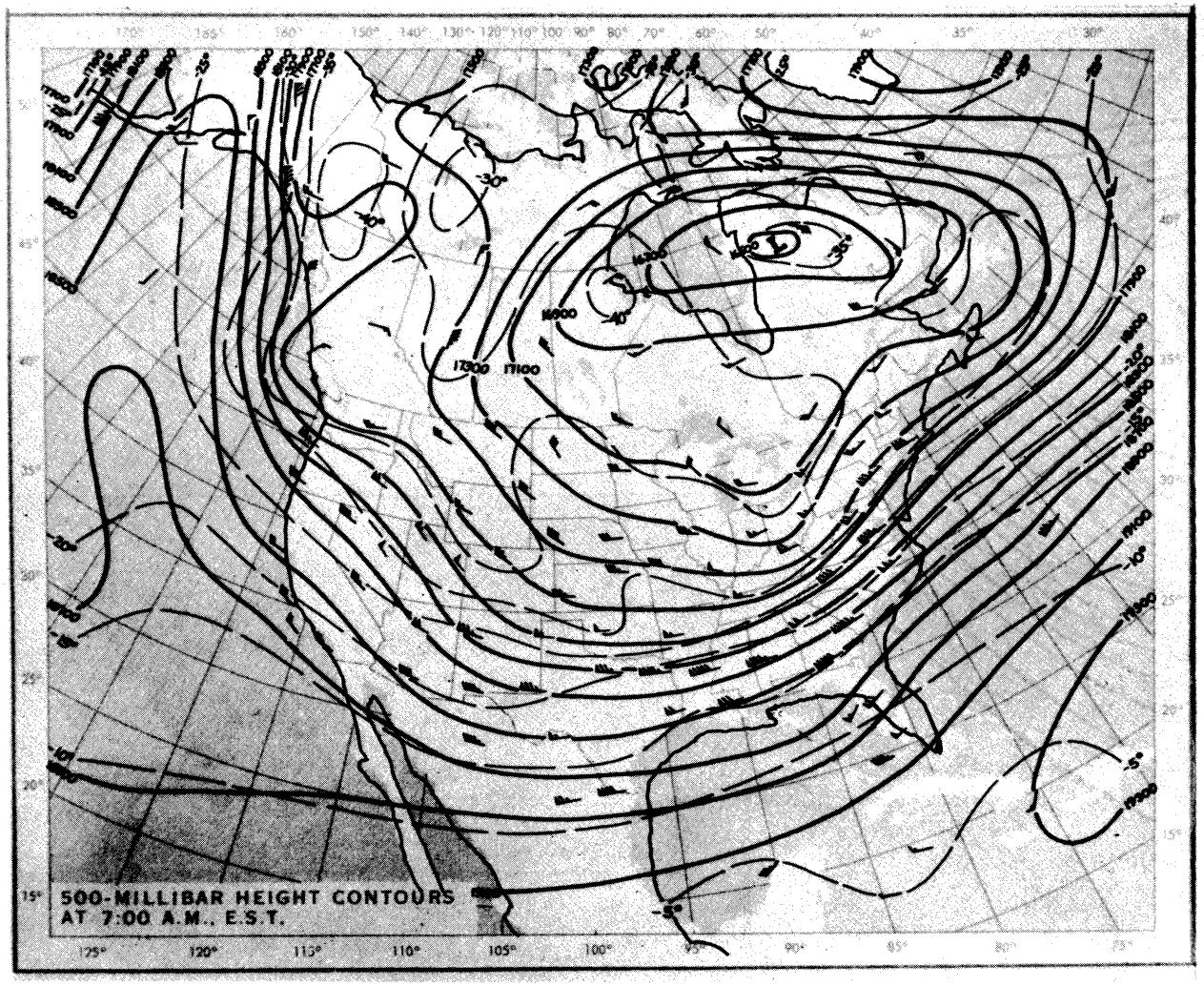

Figure 131. 500 - millibar height contours, 7:00 a.m., E.S.T., January 3, 1970.

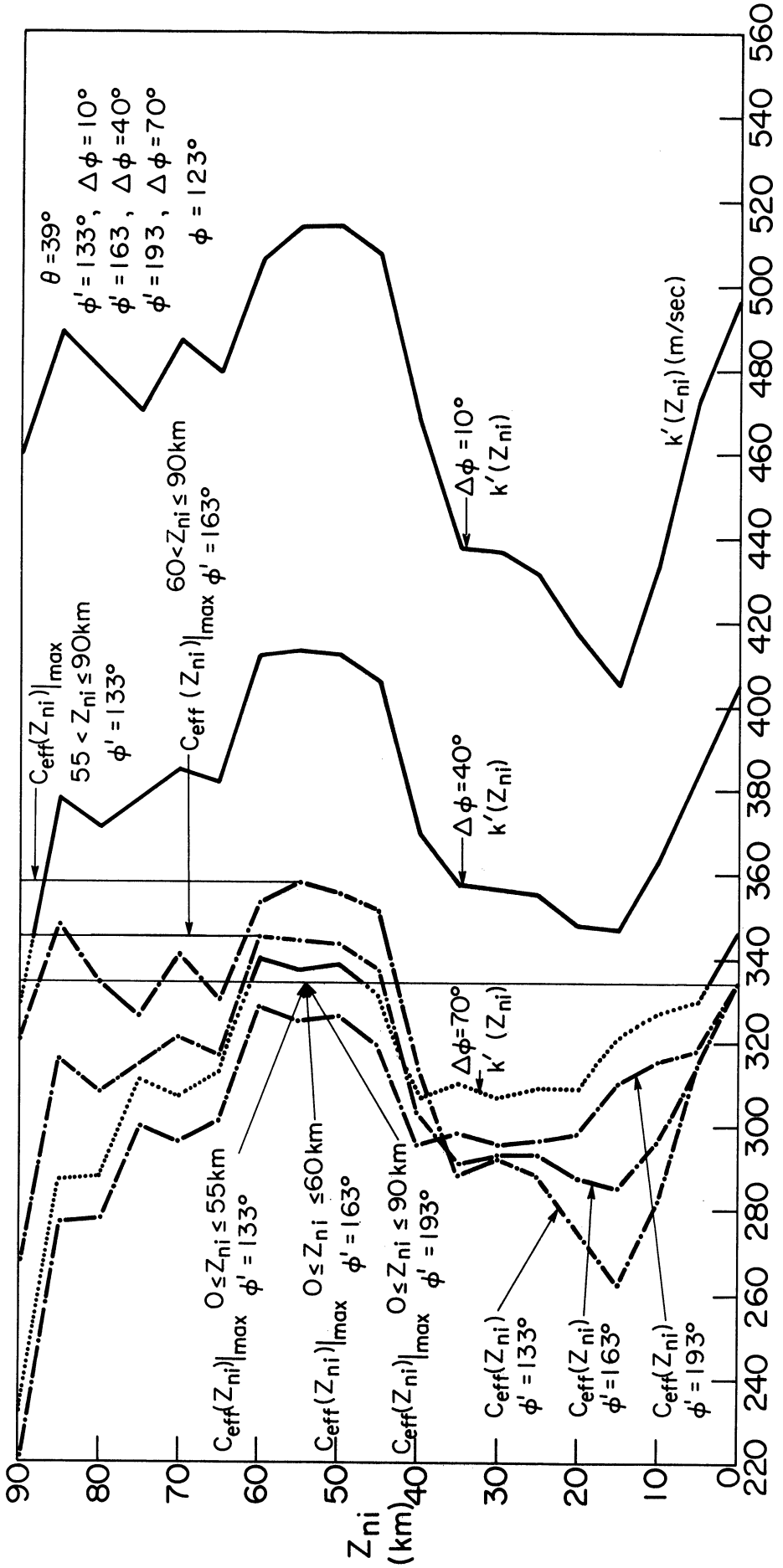

Figure 132. Refraction analysis for azimuth intervals to the East of the trajectory for the Lost City Meteorite entry. Dotted portions of curves represent situations for which ray paths to the ground are not allowed.

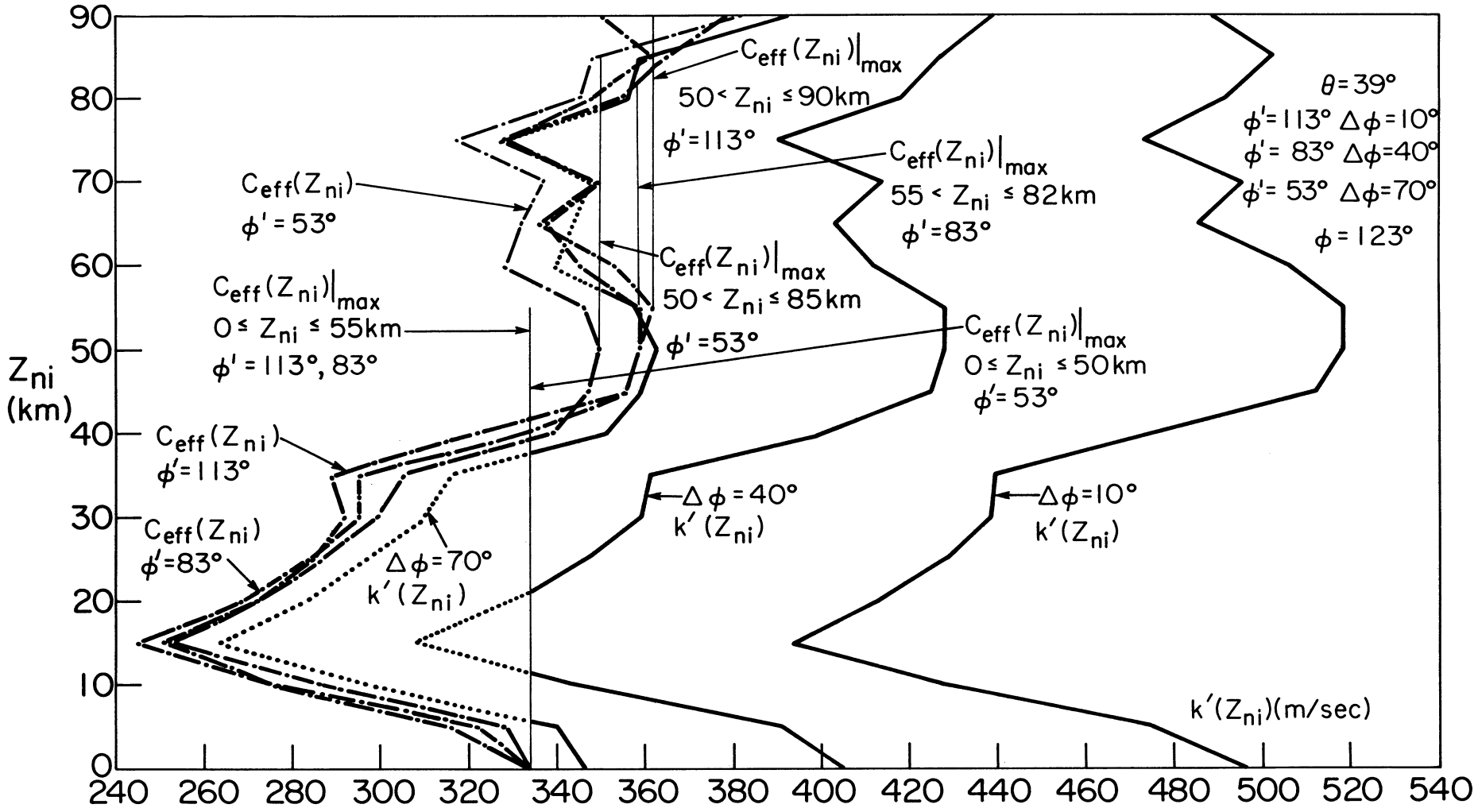

Figure 133. Refraction analysis for azimuth intervals to the West of the trajectory for the Lost City Meteorite entry. Dotted portions of curves represent situations for which ray paths to the ground are not allowed.

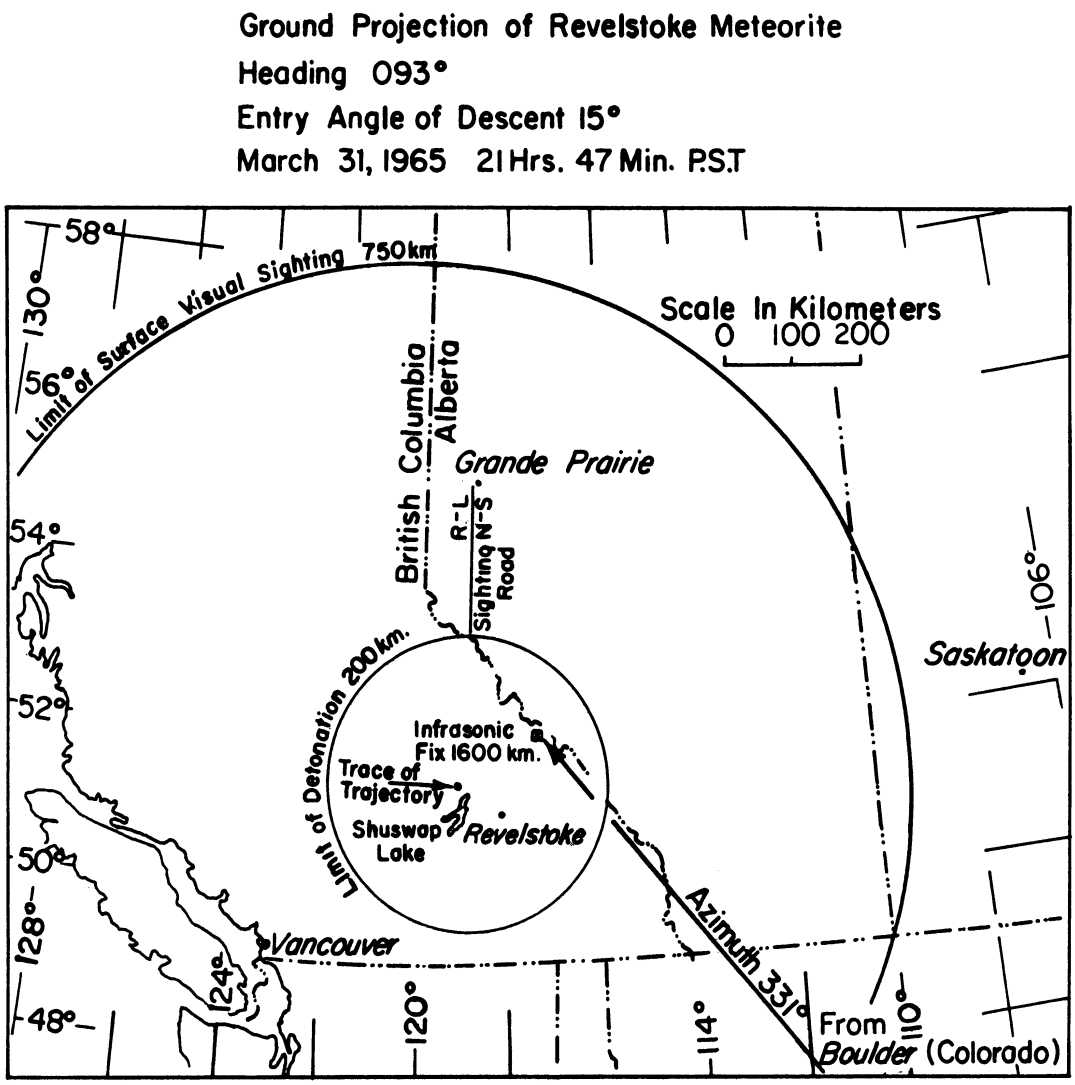

Figure 134. Ground projection of the entry of the Revelstoke Meteorite of March 31, 1965, after Folinsbee et al., 1967.

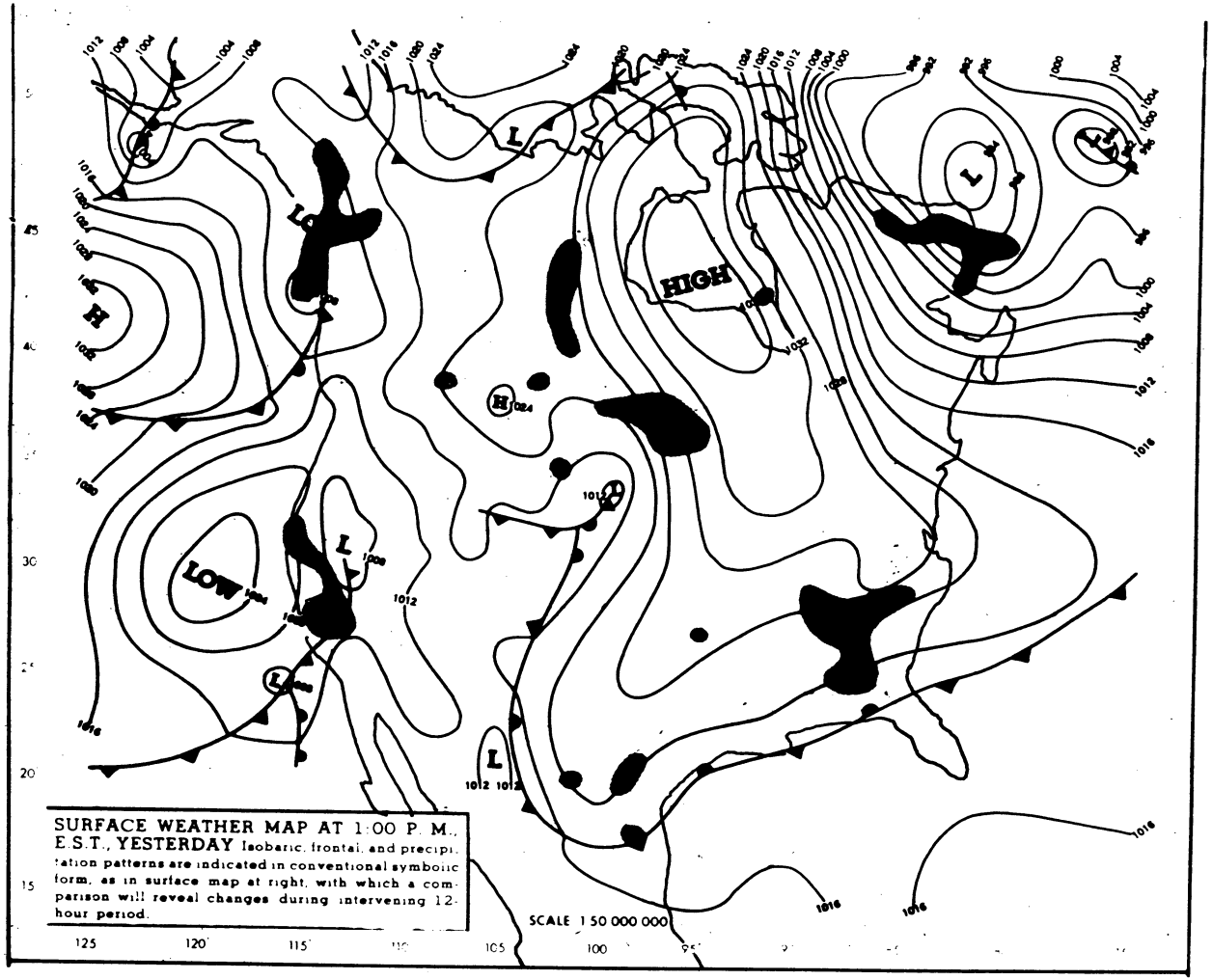

Figure 135. U. S. Weather Service surface map, 1:00 p. m., E. S. T., March 31, 1965.

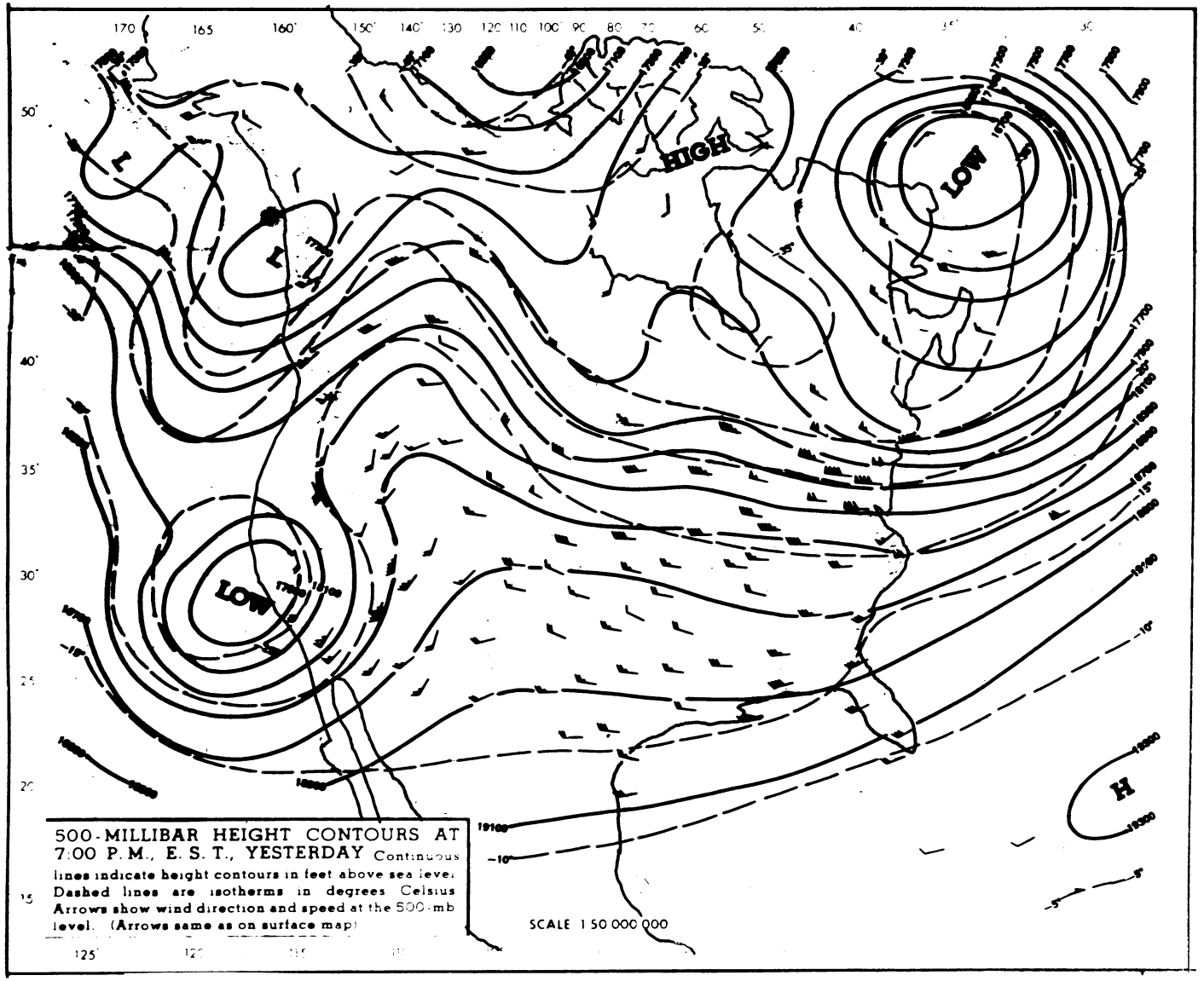

Figure 136. 500 - millibar height contours, 7:00 p.m., E.S.T., March 31, 1965.

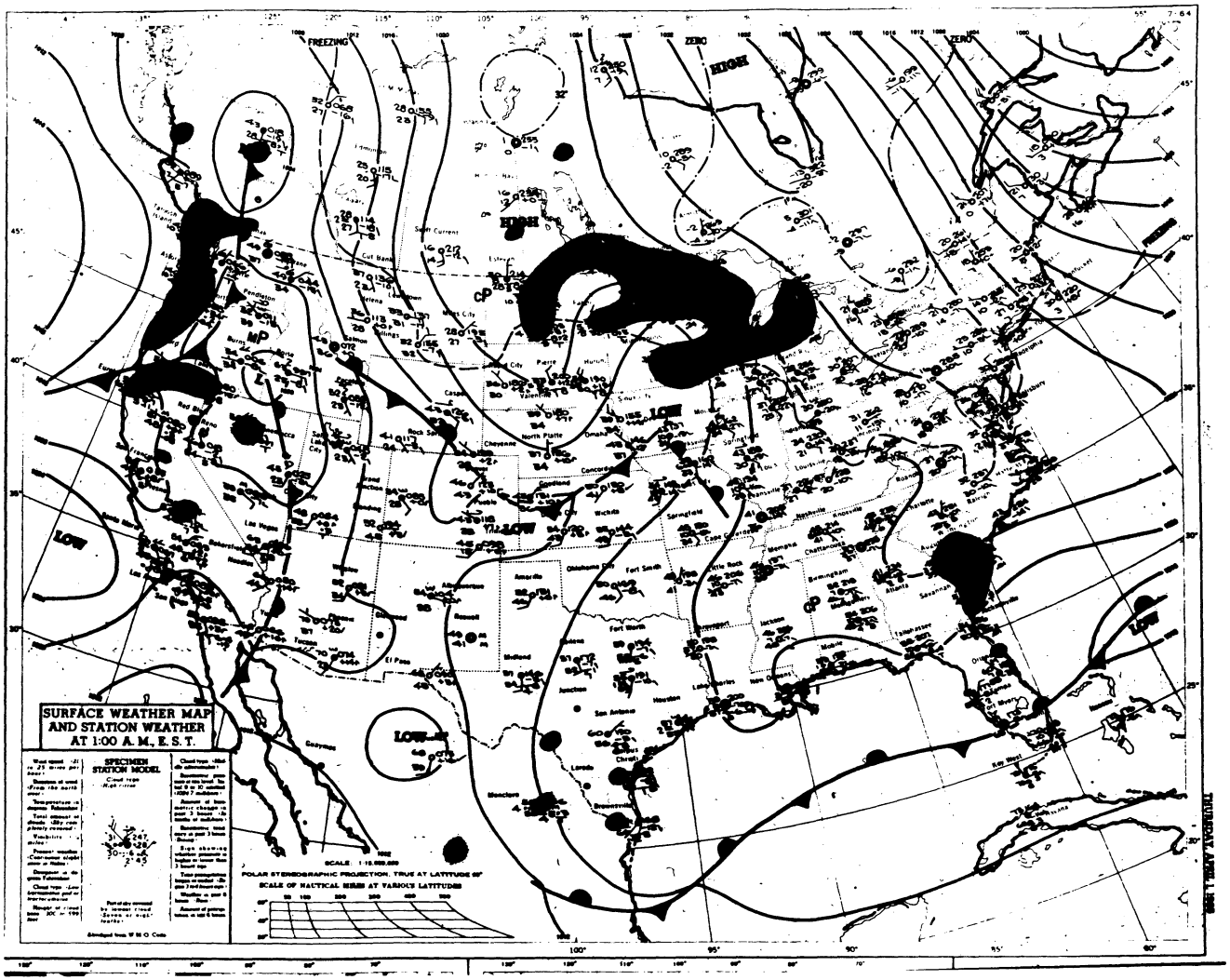

Figure 137. U. S. Weather Service surface map, 1:00 a. m. E. S. T., April 1, 1965.

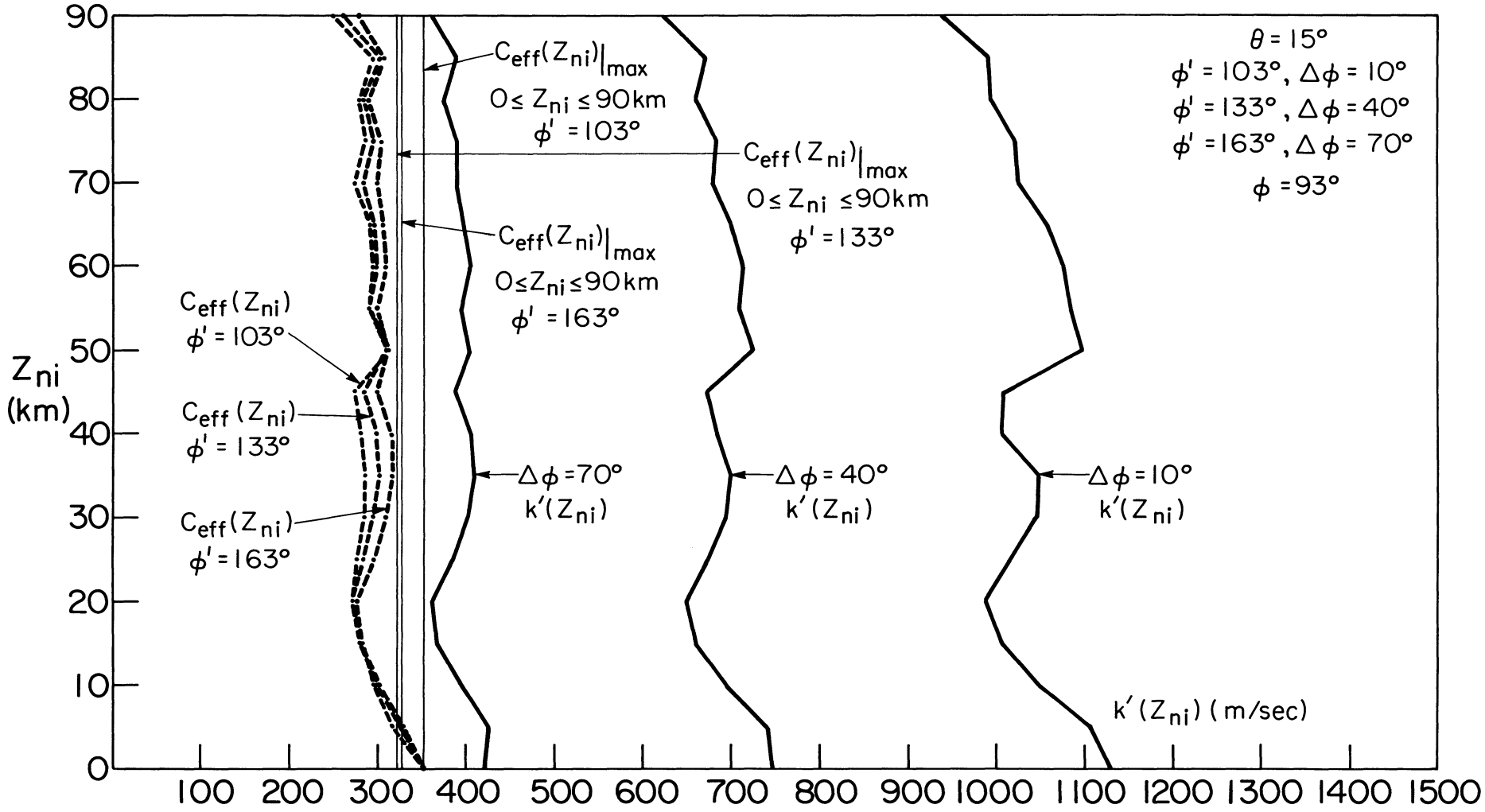

Figure 138. Refraction analysis for azimuth intervals to the North of the trajectory for the Revelstoke Meteorite entry. Dotted portion of curves represent situations for which ray paths to the ground are not allowed.

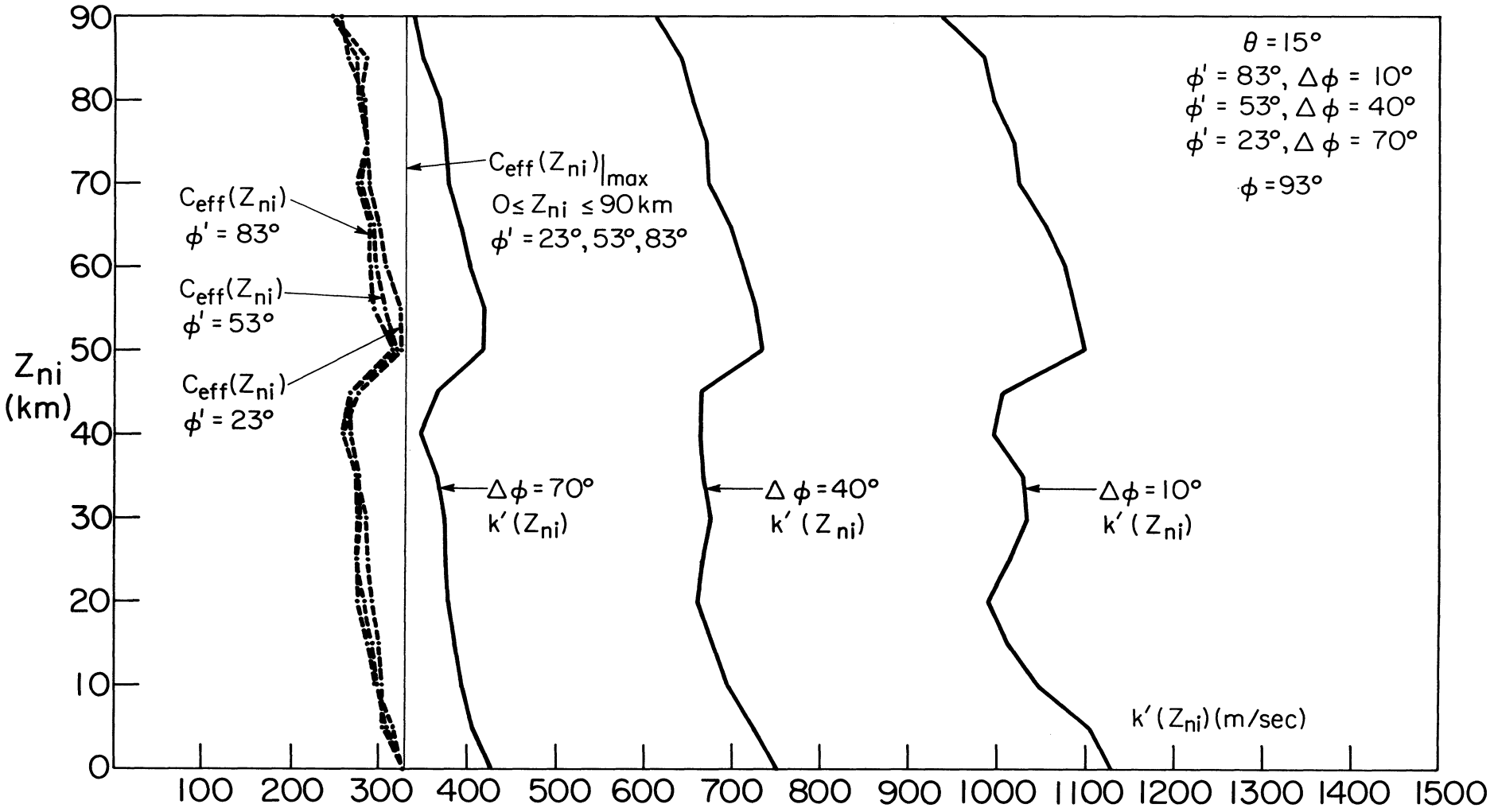

Figure 139. Refraction analysis for azimuth intervals to the South of the trajectory for the Revelstoke Meteorite entry. Dotted portion of curves represent situations for which ray paths to the ground are not allowed.

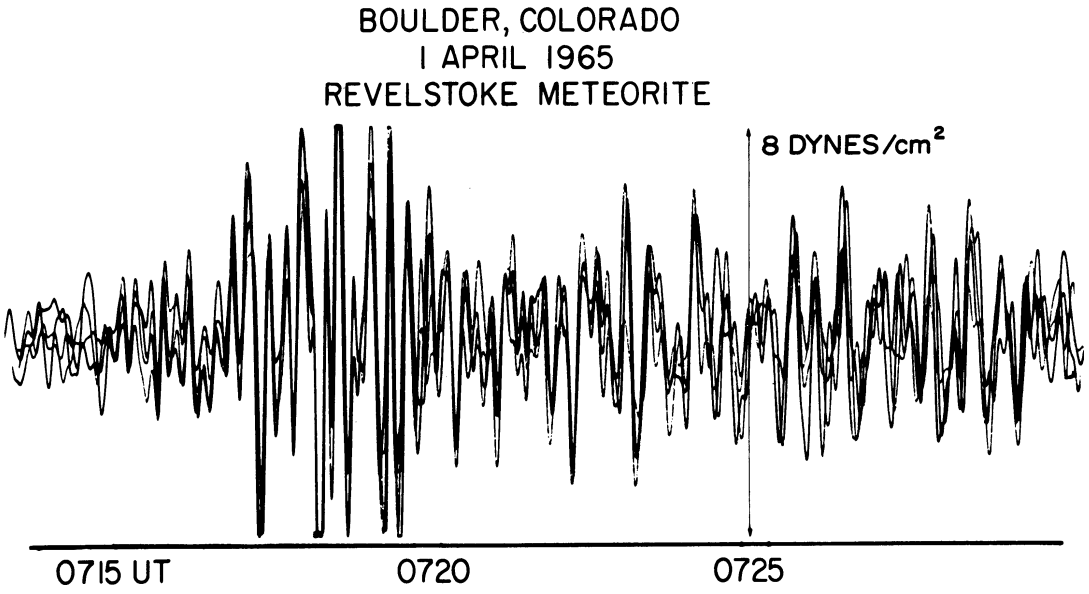

Figure 140. Airwaves from the Revelstoke Meteorite as recorded in Boulder, Colorado on the NOAA microbarograph system, after Goerke, 1972.

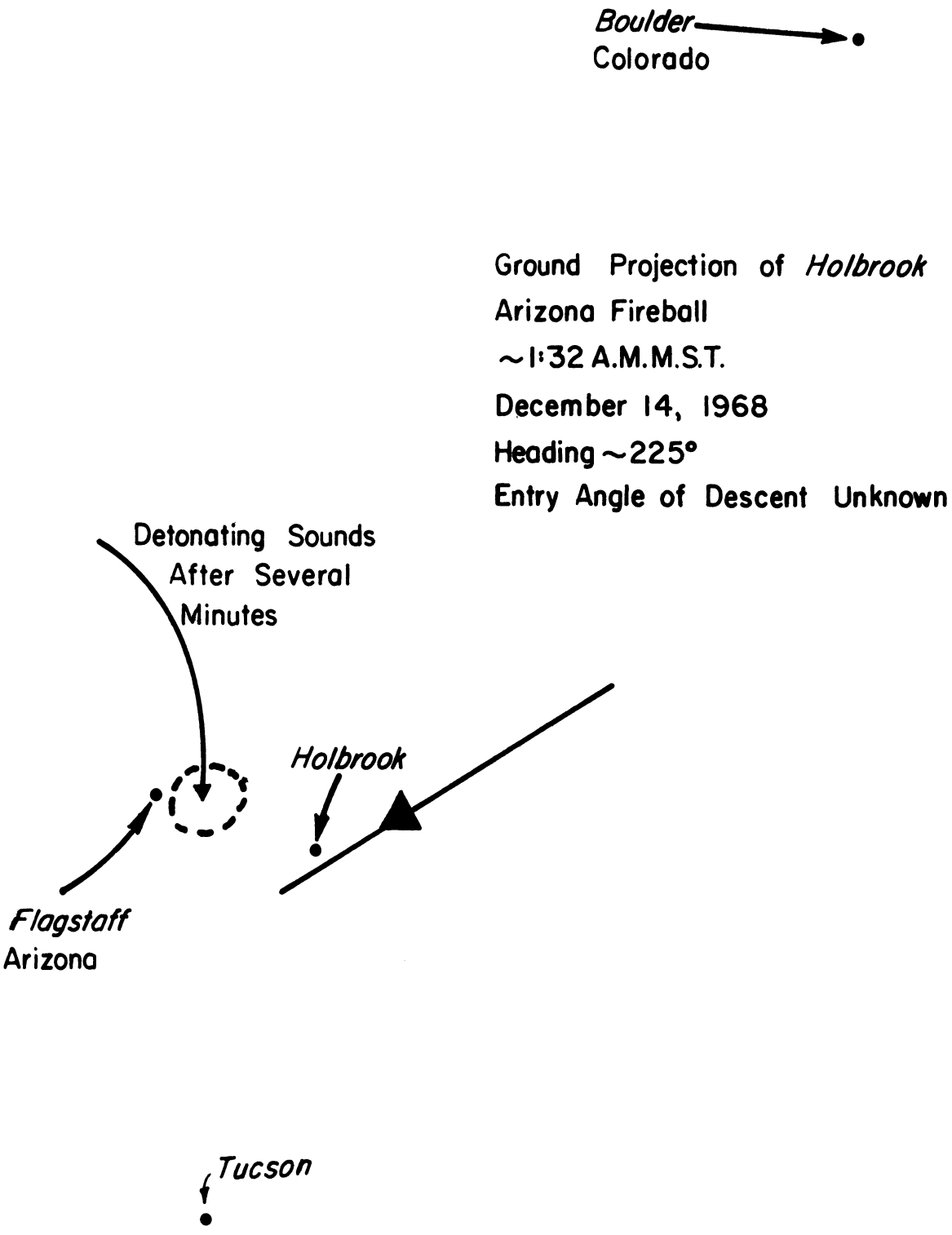

Figure 141. Ground projection of the entry of the Holbrook Arizona Fireball of December 14, 1968, after Goerke, 1972 and Shoemaker, 1972.

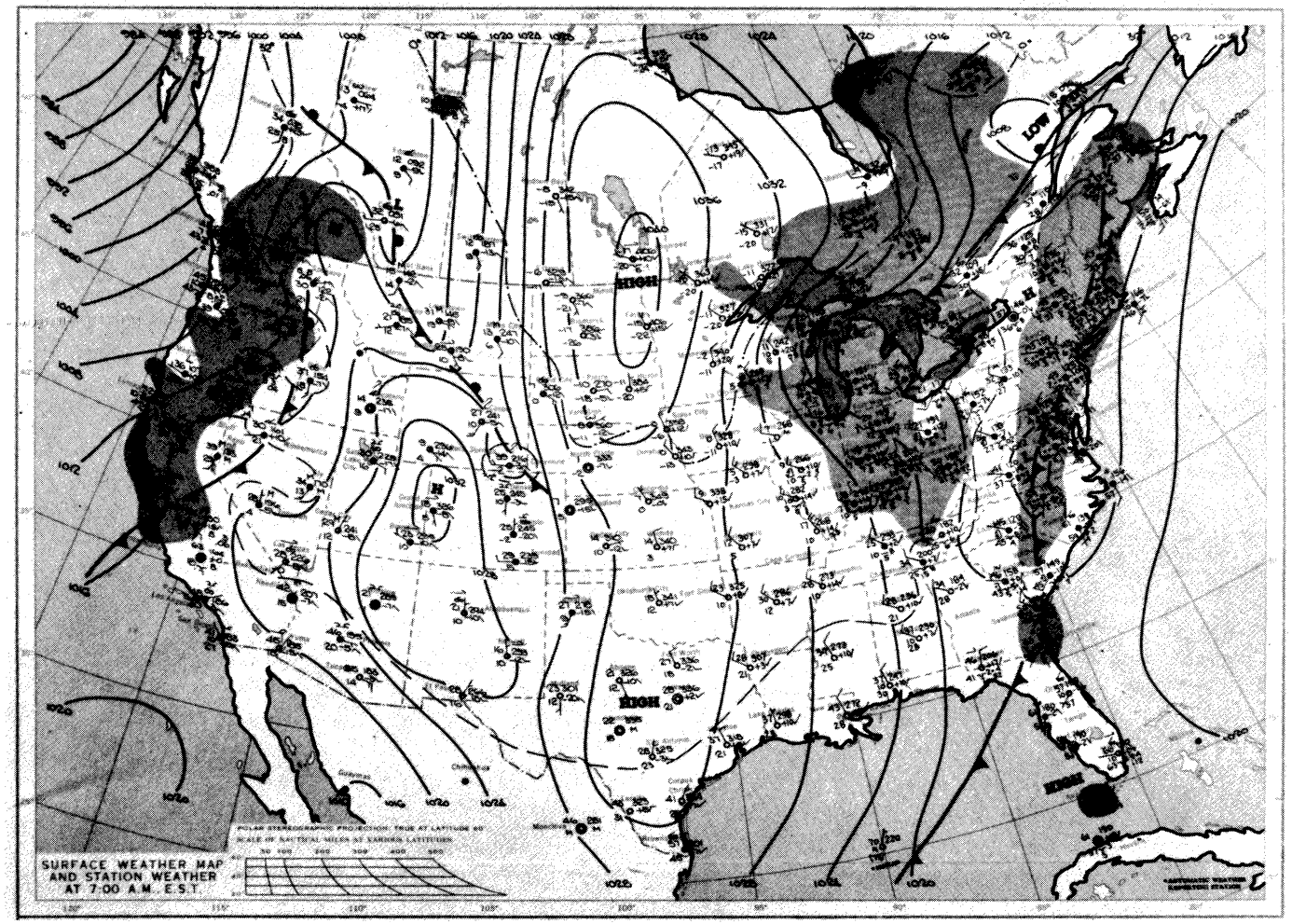

Figure 142. U. S. Weather Service surface map, 7:00 a. m., E. S. T., December 14, 1968.

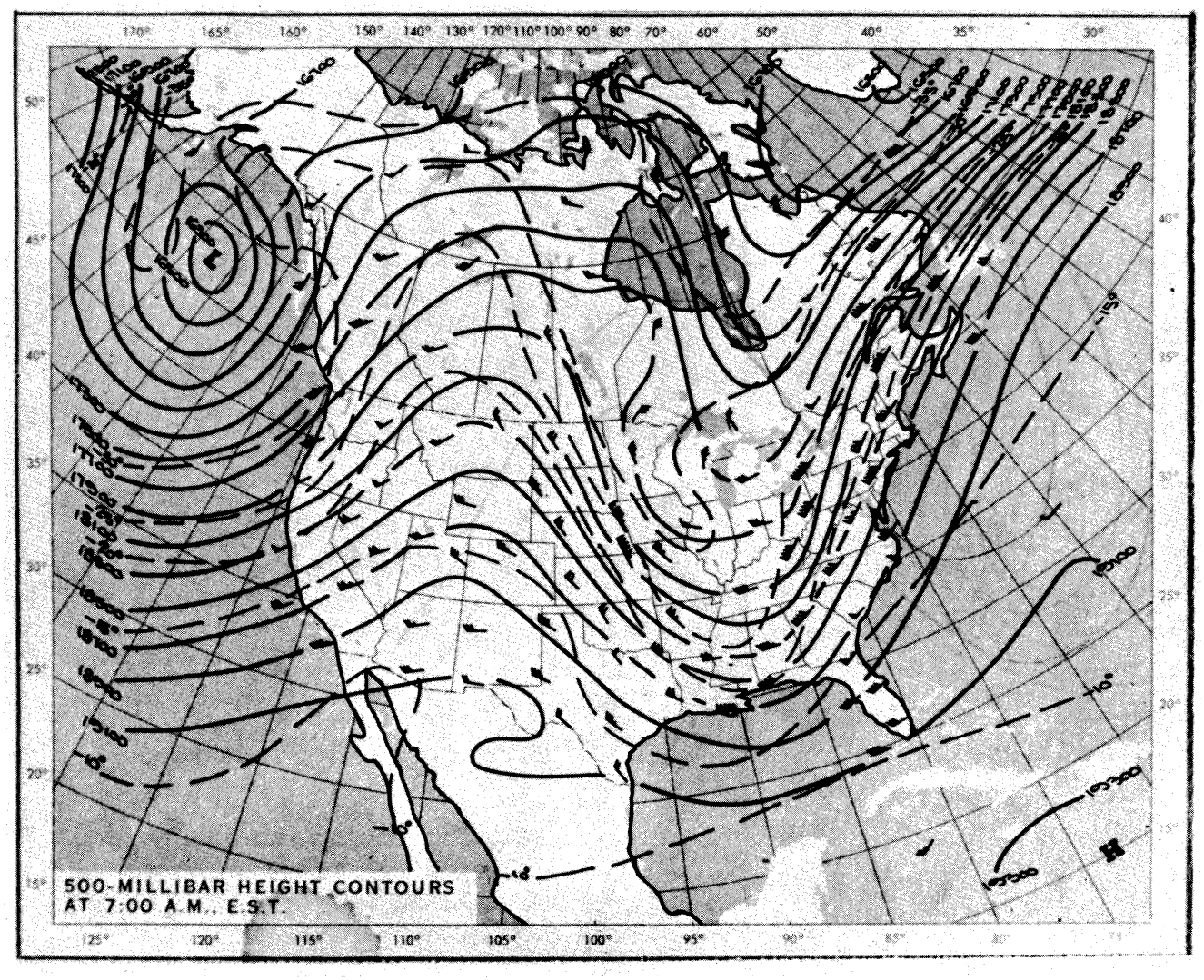

Figure 143. 500 - millibar height contours, 7:00 a.m., E.S.T., December 14, 1968.

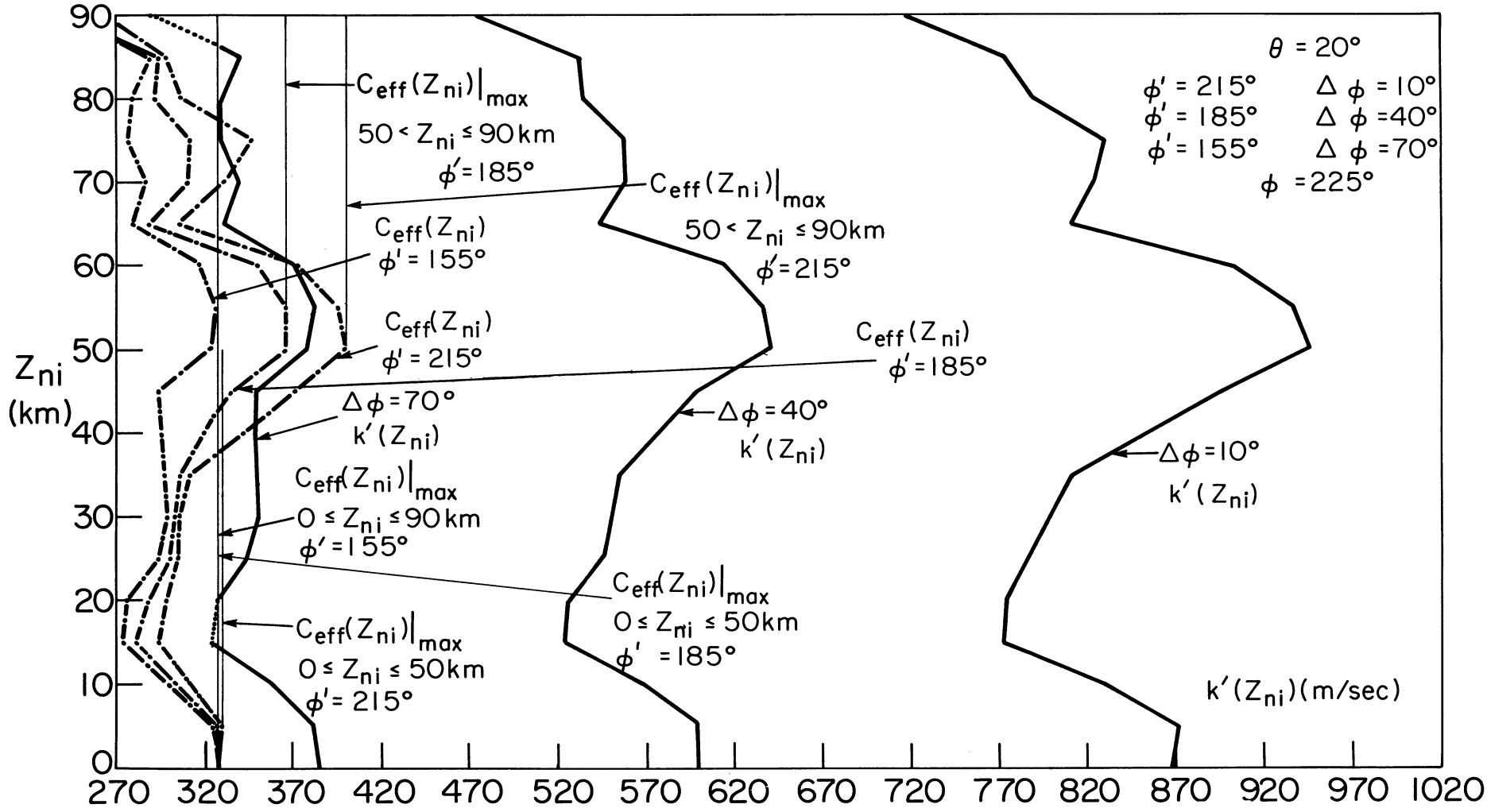

Figure 144. Refraction analysis for azimuth intervals to the North of the trajectory for the Holbrook Arizona Fireball entry. Dotted portions of curves represent situations for which ray paths to the ground are not allowed; $\theta = 20^{\circ}$.

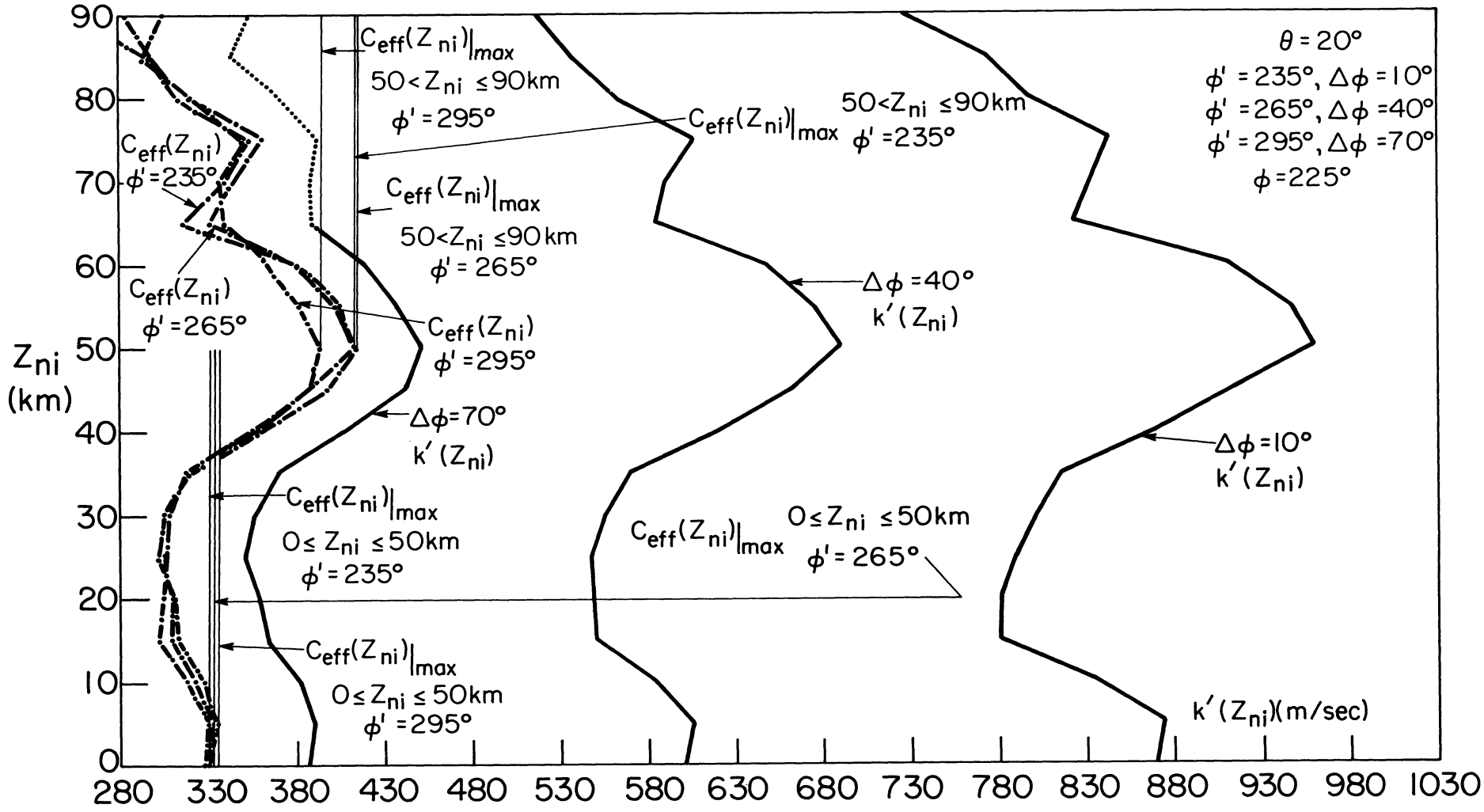

Figure 145. Refraction analysis for azimuth intervals to the South of the trajectory for the Holbrook Arizona Fireball entry. Dotted portions of curves represent situations for which ray paths to the ground are not allowed; $\theta = 20^{o}$.

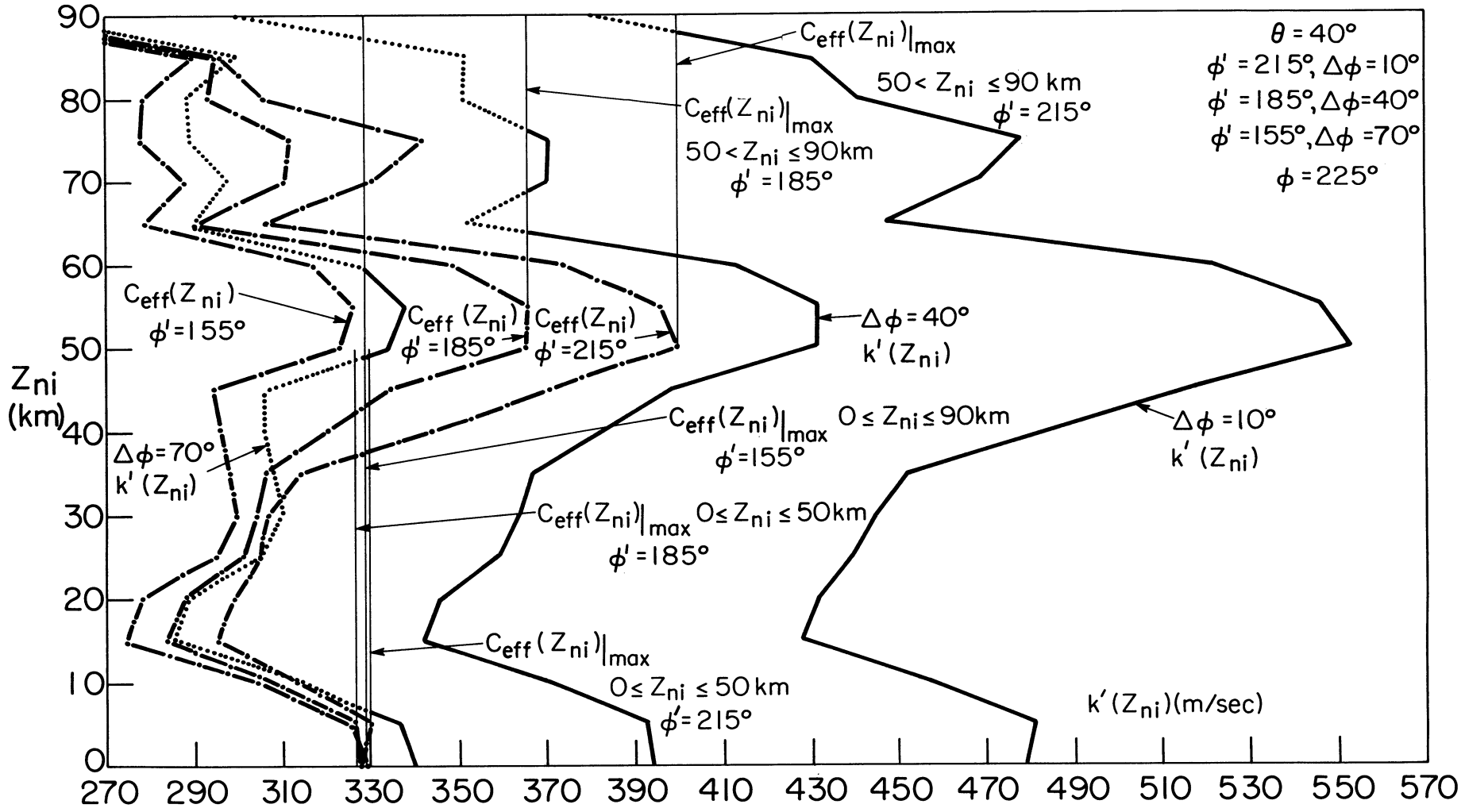

Figure 146. Refraction analysis for azimuth intervals to the North of the trajectory for the Holbrook Arizona Fireball entry. Dotted portions of curves represent situations for which ray paths to the ground are not allowed; $\theta = 40^{\circ}$.

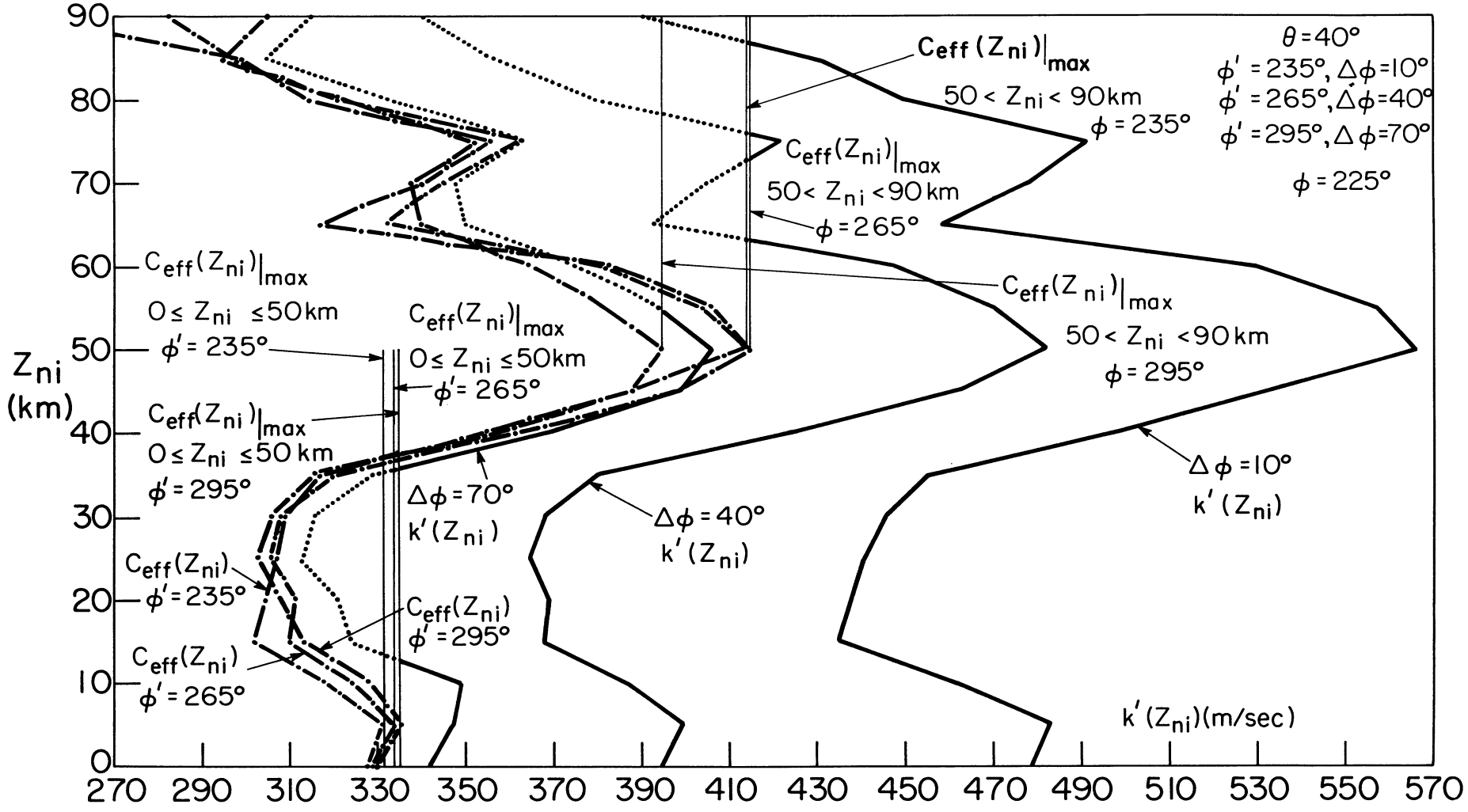

Figure 147. Refraction analysis for azimuth intervals to the South of the trajectory for the Holbrook Arizona Fireball entry. Dotted portions of curves represent situations for which ray paths to the ground are not allowed; $\theta = 40^{\circ}$.

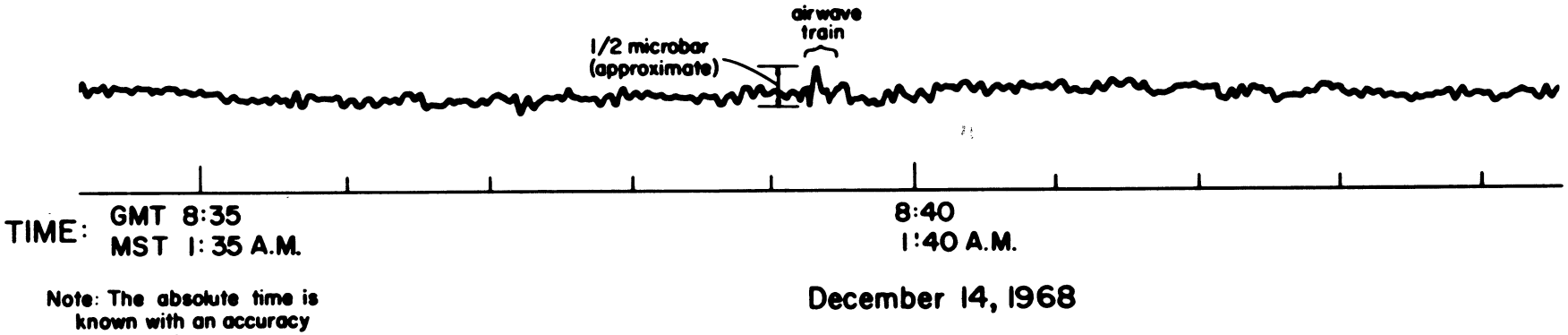

Figure 148. Ariwaves from the Holbrook Arizona Fireball as recorded in Flagstaff, Arizona on the U. S. Geological Survey microbarograph system, after Shoemaker, 1972.

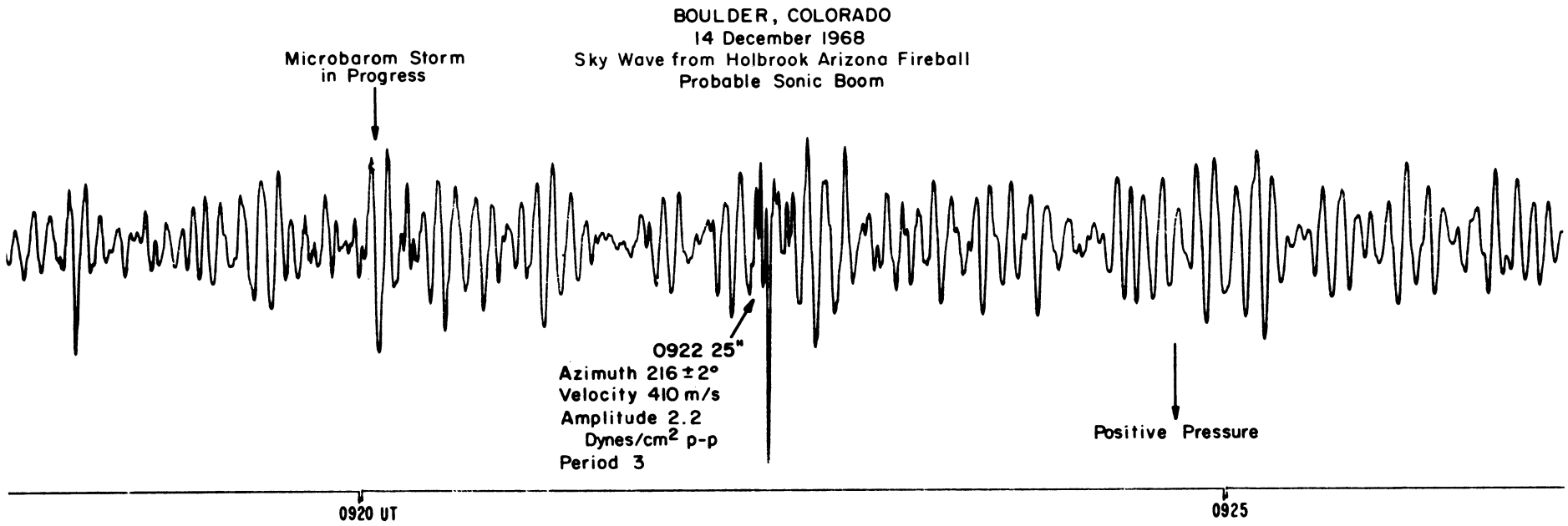

Figure 149. Airwaves from the Holbrook Arizona Fireball as recorded in Boulder, Colorado on the NOAA microbarograph system, after Goerke, 1972.

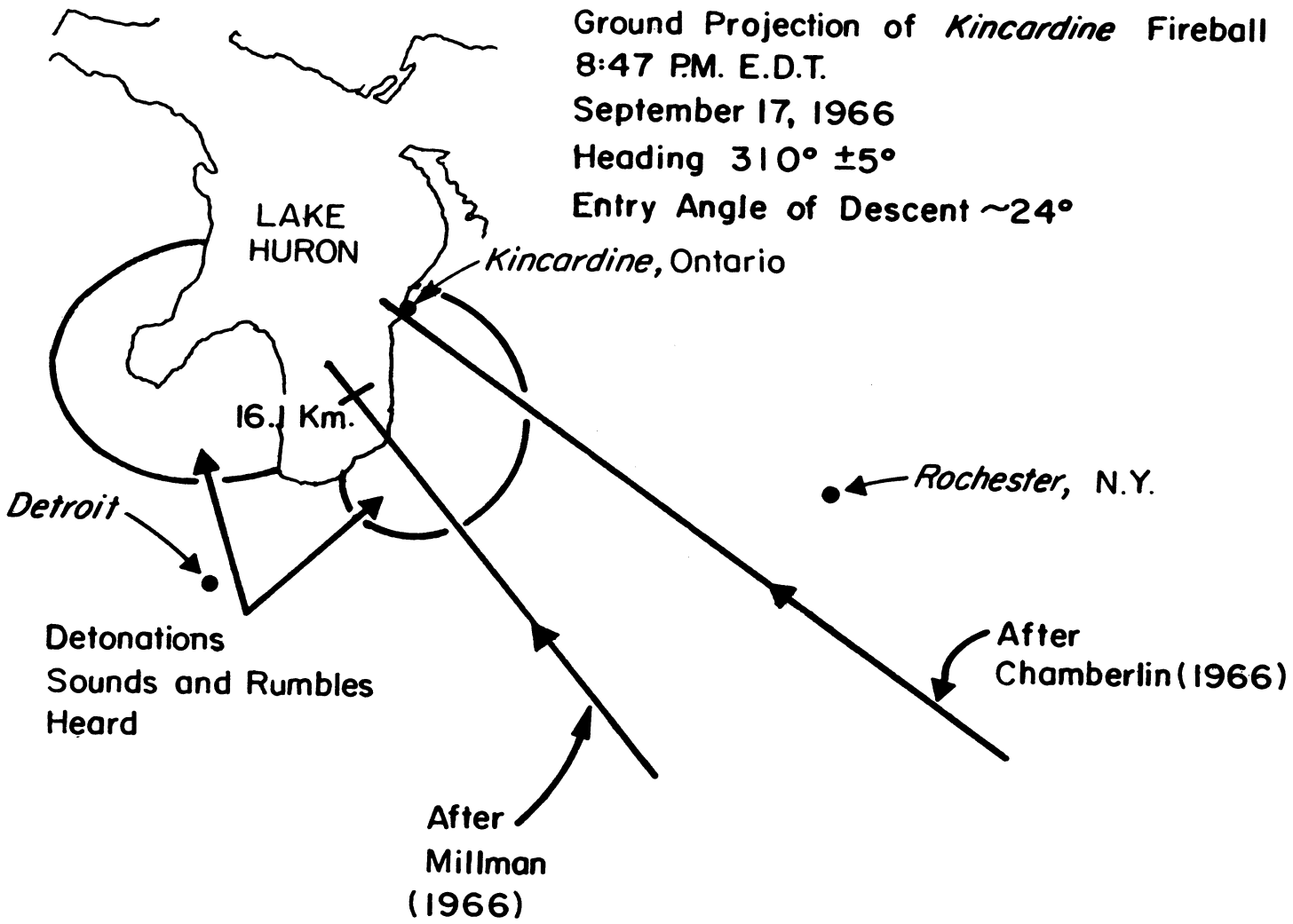

Figure 150. Ground projection of the entry of the Kincardine Fireball of September 17, 1966, after Goerke, 1966 and Chamberlinn, 1968.

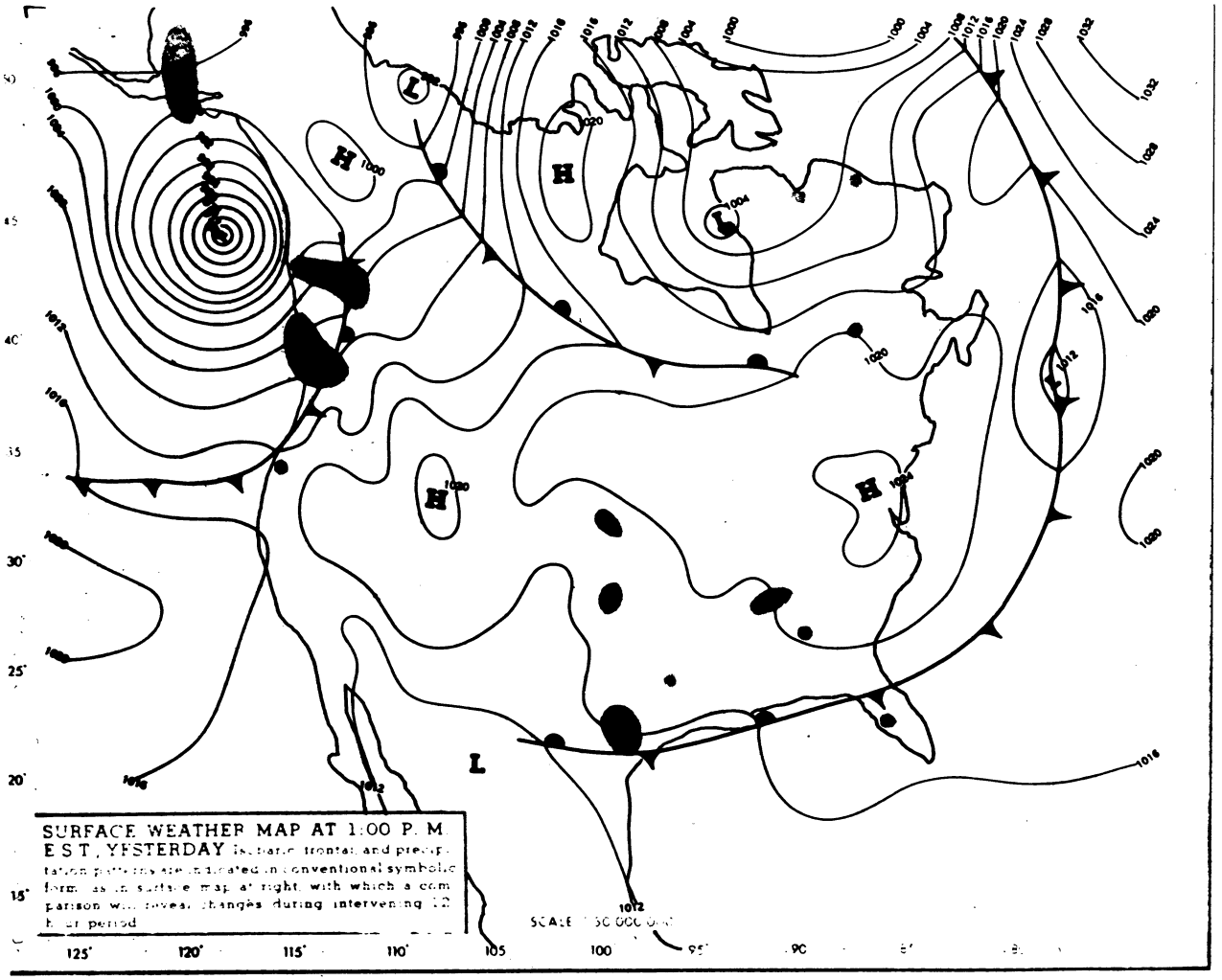

Figure 151. U. S. Weather Service surface map, 1:00 p. m. E. S. T., September 17, 1966.

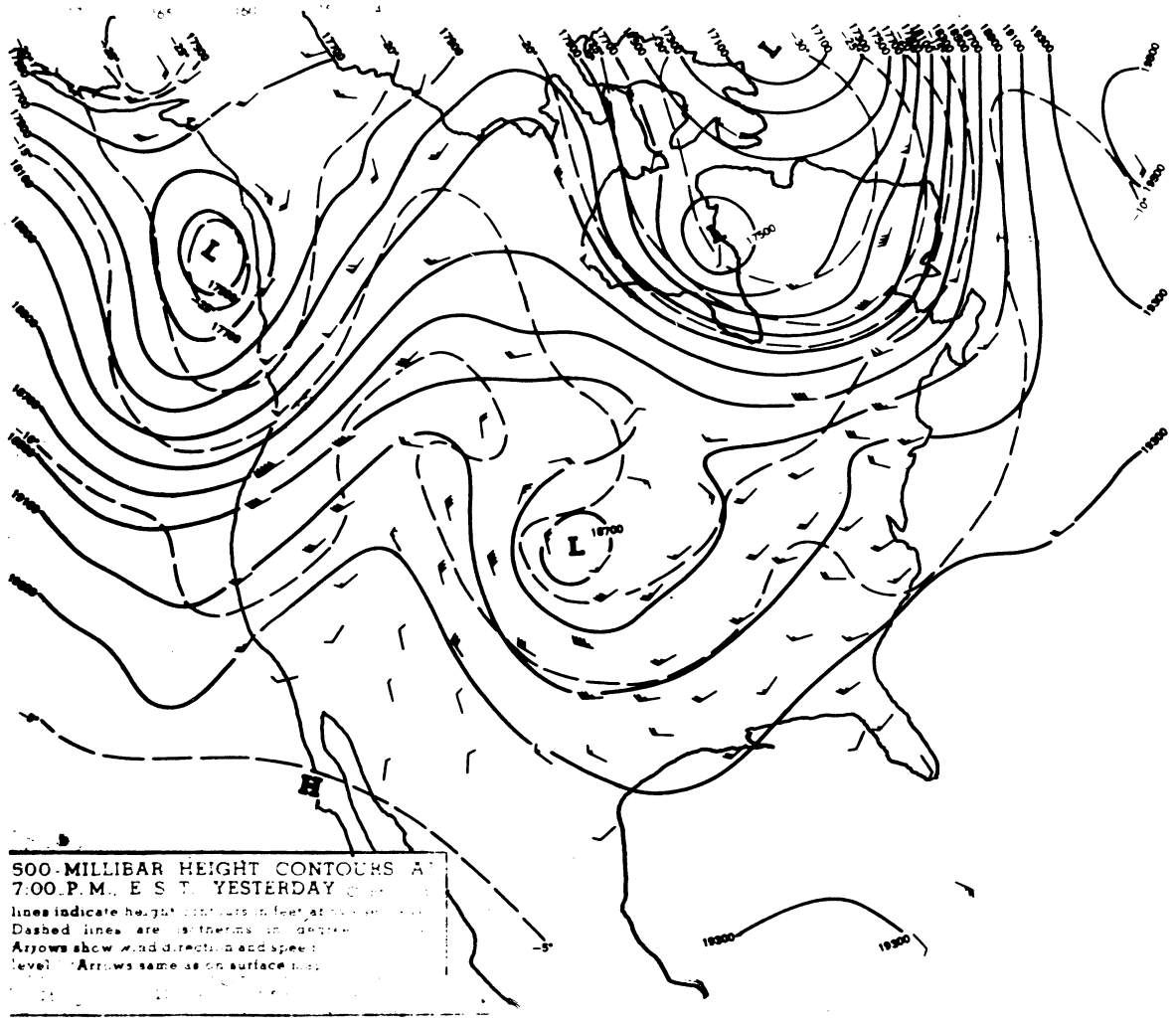

Figure 152. 500 - millibar height contours, 7:00 p.m. E.S.T., September 17, 1966.

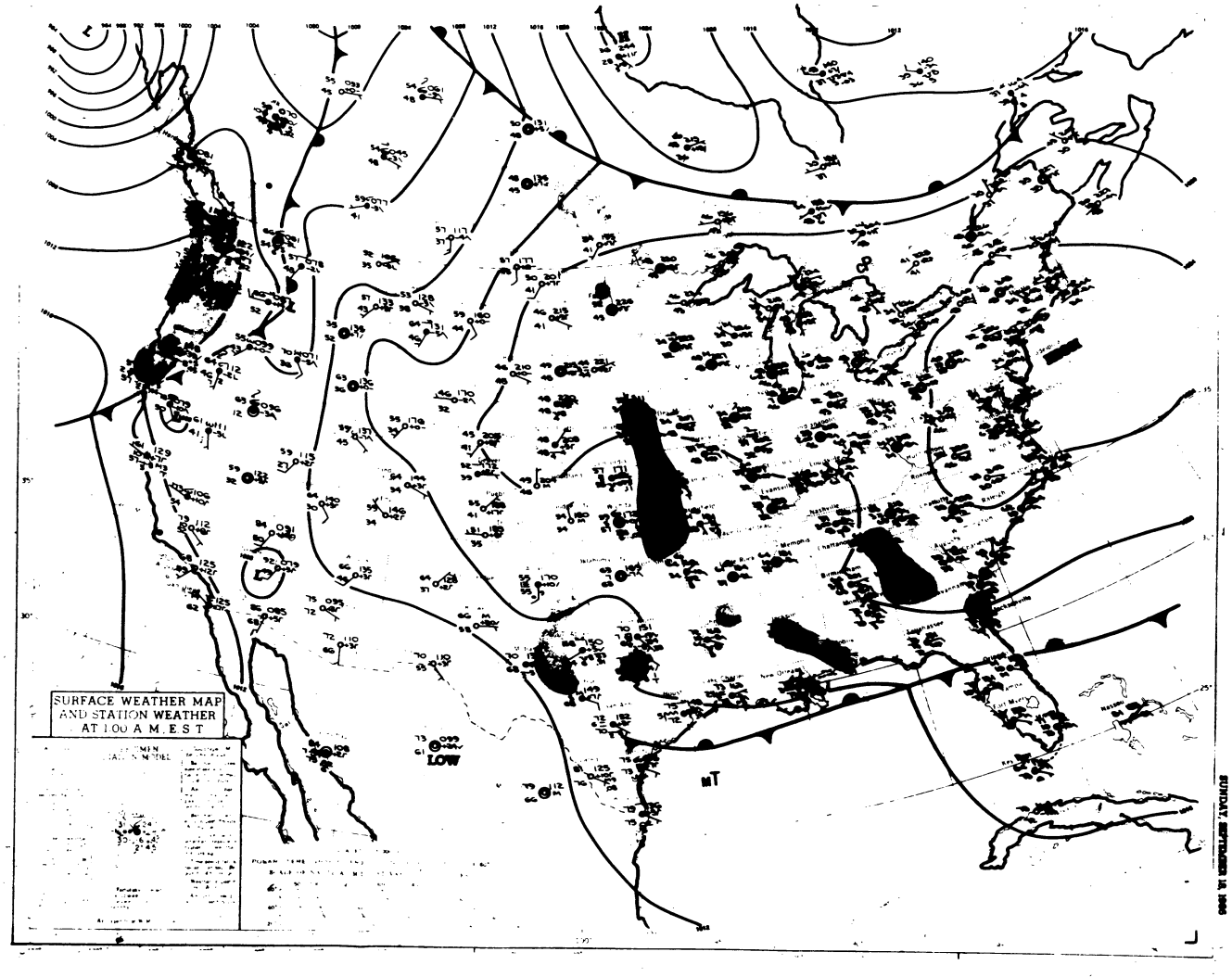

Figure 153. U.S. Weather Service surface map, 1:00 a.m. E.S.T., September 18, 1966.

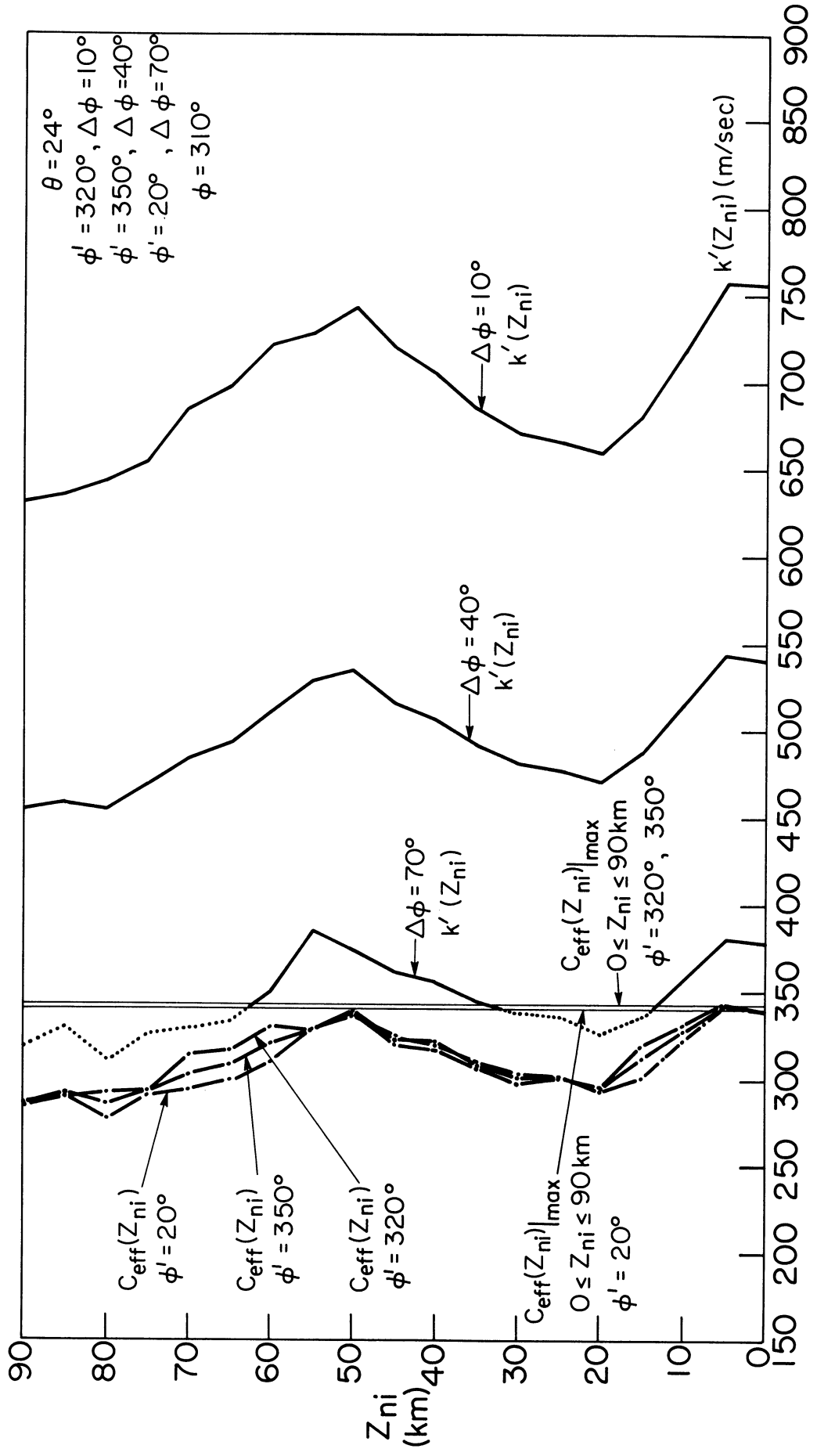

Figure 154. Refraction analysis for azimuth intervals to the South of the trajectory for the Kincardine Fireball entry. Dotted portions of curves represent situations for which ray paths to the ground are not allowed.

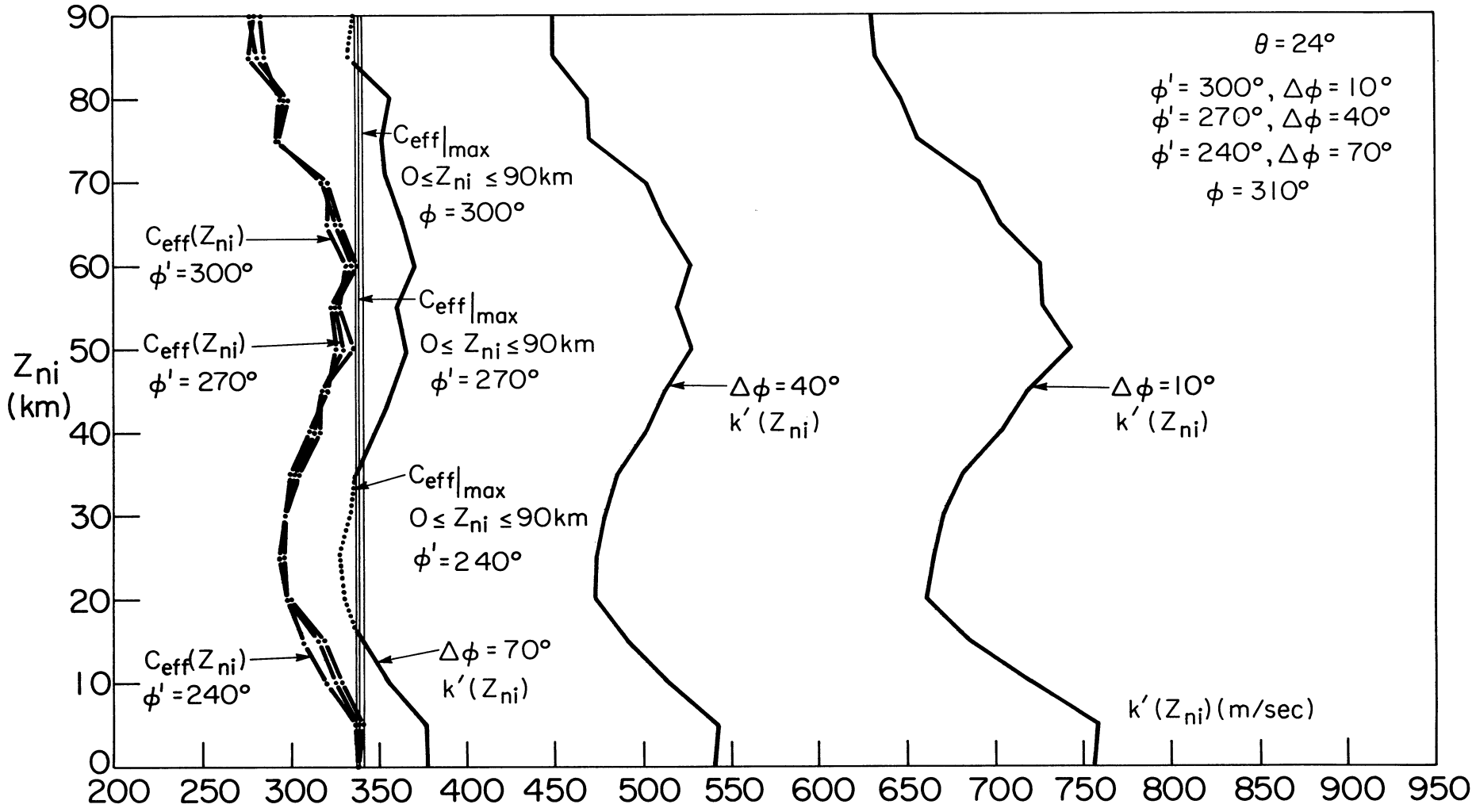

Figure 155. Refraction analysis for azimuth intervals to the North of the trajectory for the Kincardine Fireball entry. Dotted portions of curves represent situations for which ray paths to the ground are not allowed.

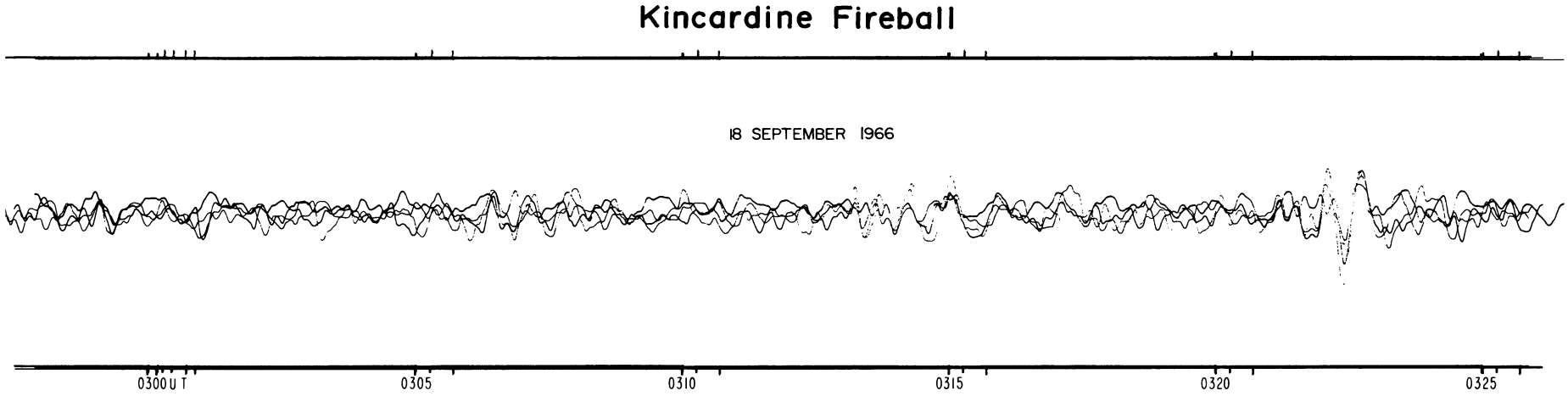

Figure 156. Airwaves from the Kincardine Fireball as recorded in Boulder, Colorado on the NOAA microbarograph system, after Goerke, 1966.

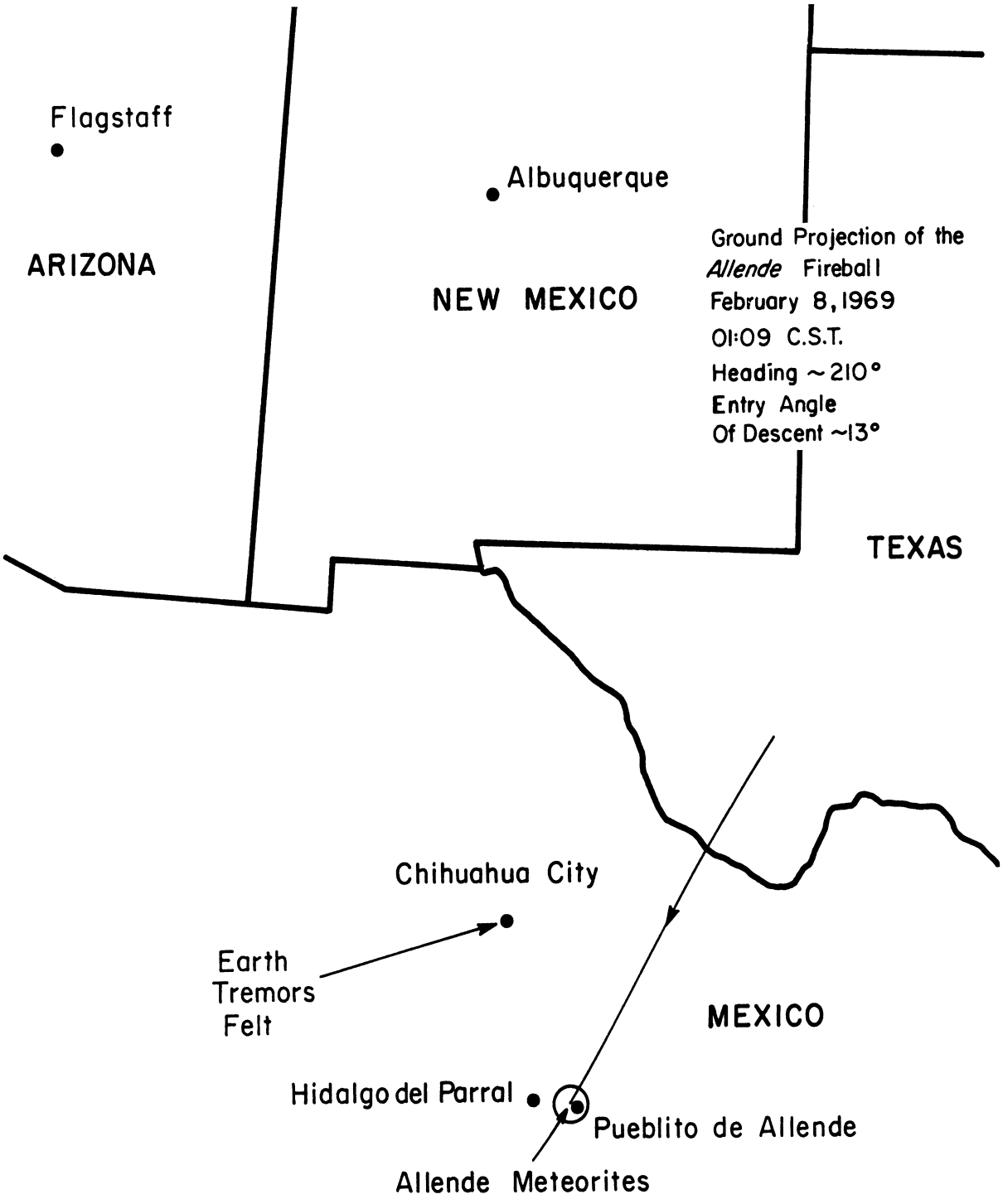

Figure 157. Ground projection of the entry of the Allende Fireball of February 8, 1969, after Fireman, 1969 and Carr, 1970.

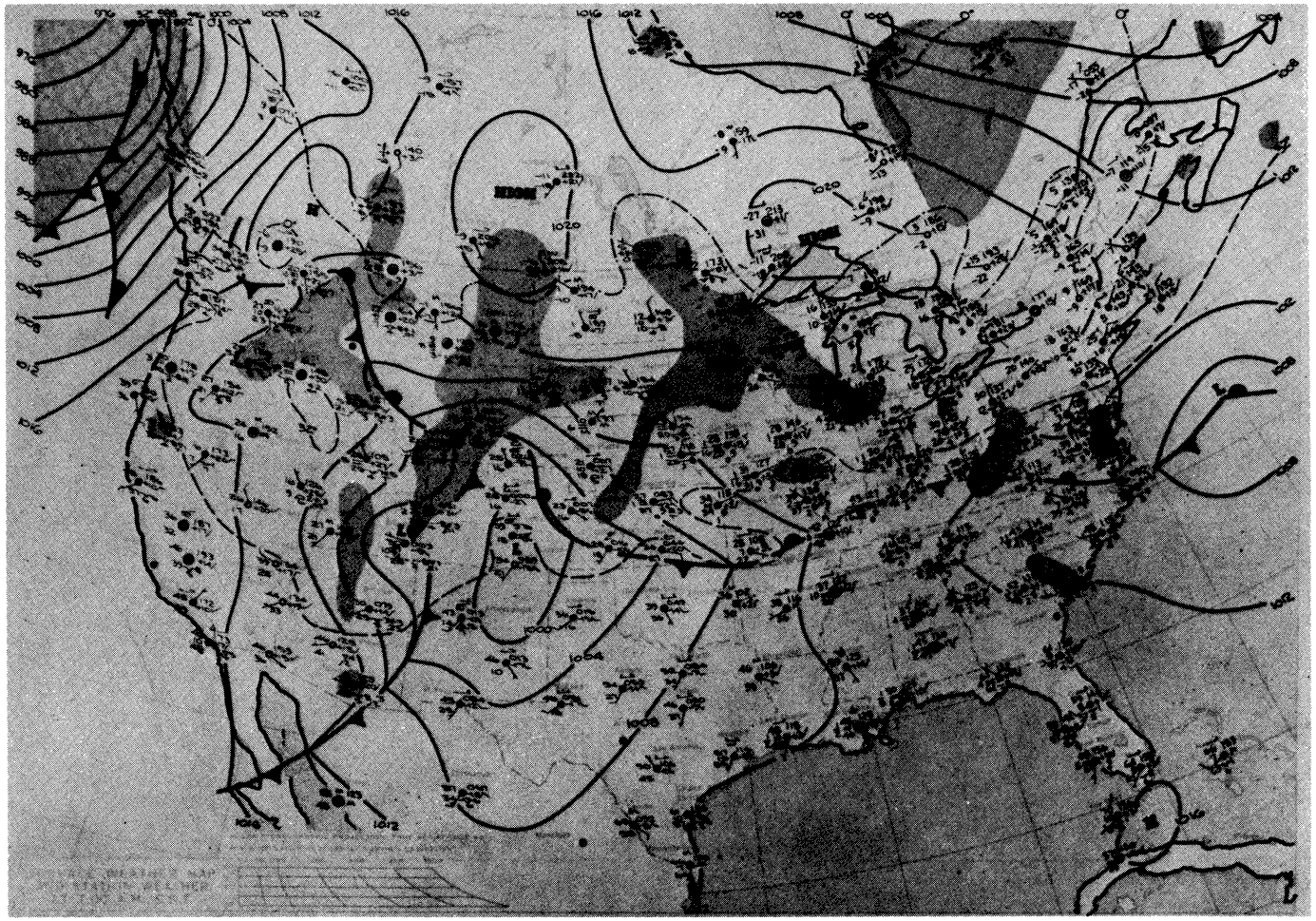

Figure 158. U.S. Weather Service surface map, 7:00 a.m. E.S.T., February 7, 1969.

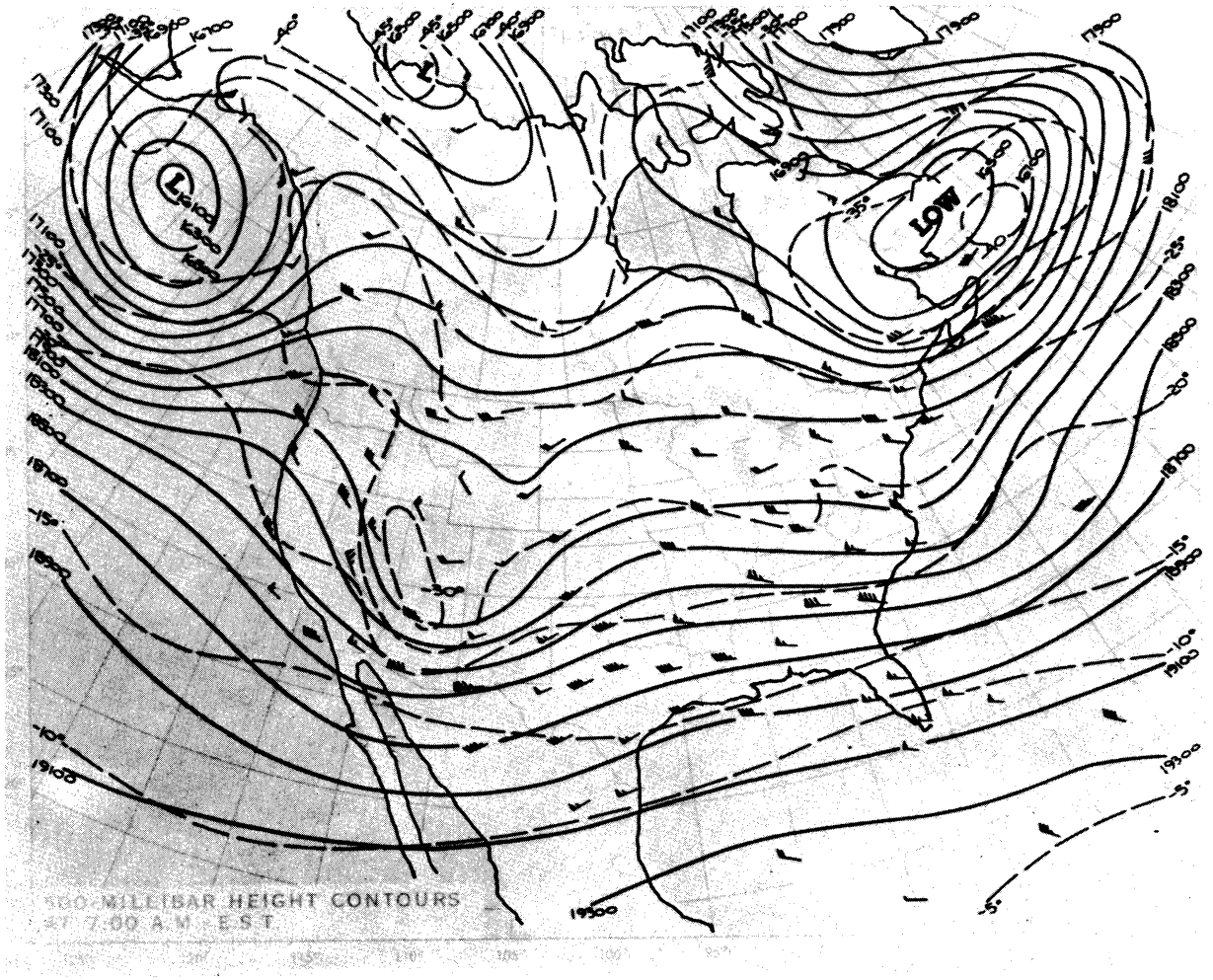

Figure 159. 500-millibar height contours, 7:00 a.m. E.S.T., February 7, 1969.

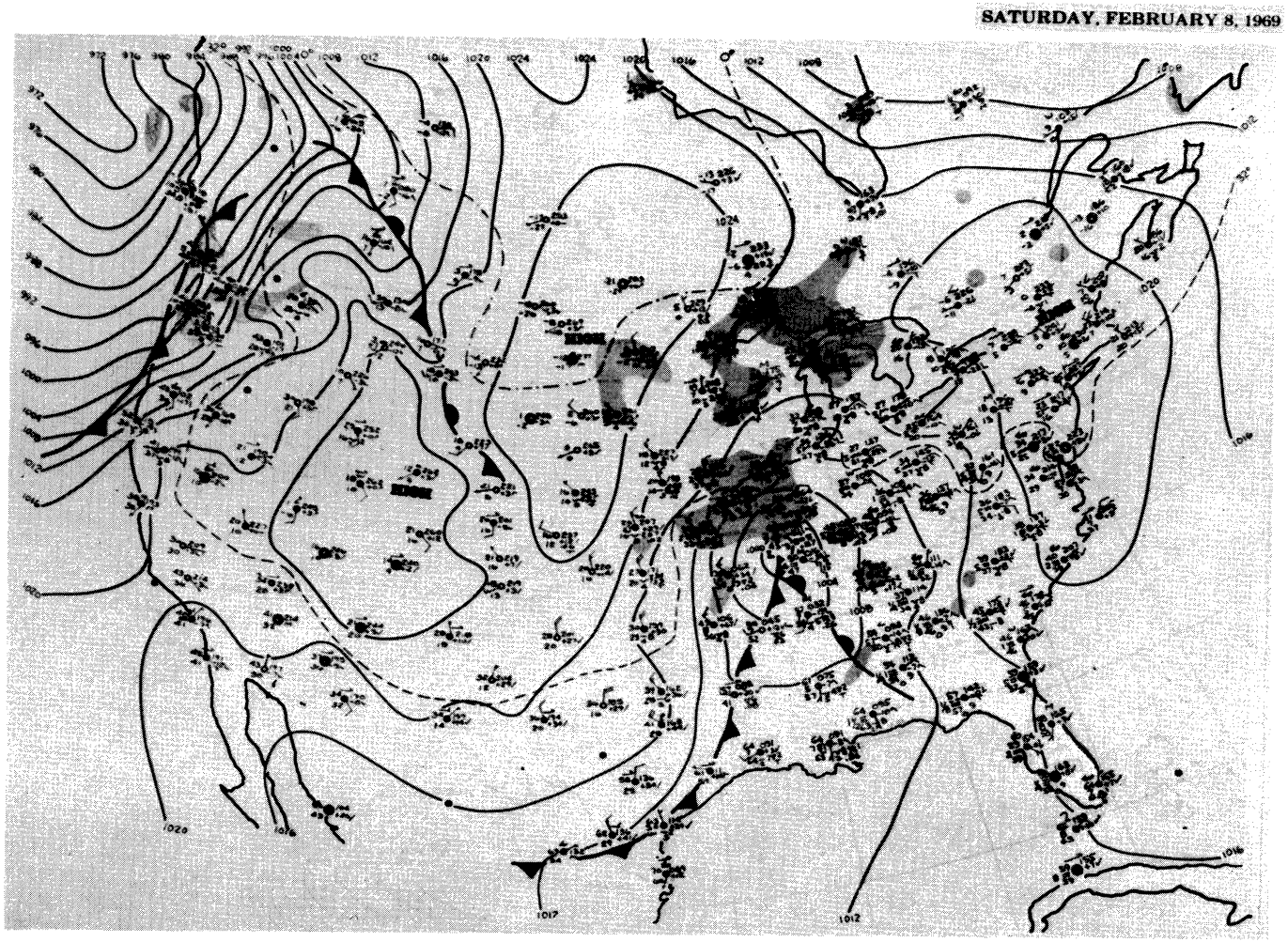

Figure 160. U. S. Weather Service surface map, 7:00 a. m. E. S. T., February 8, 1969.

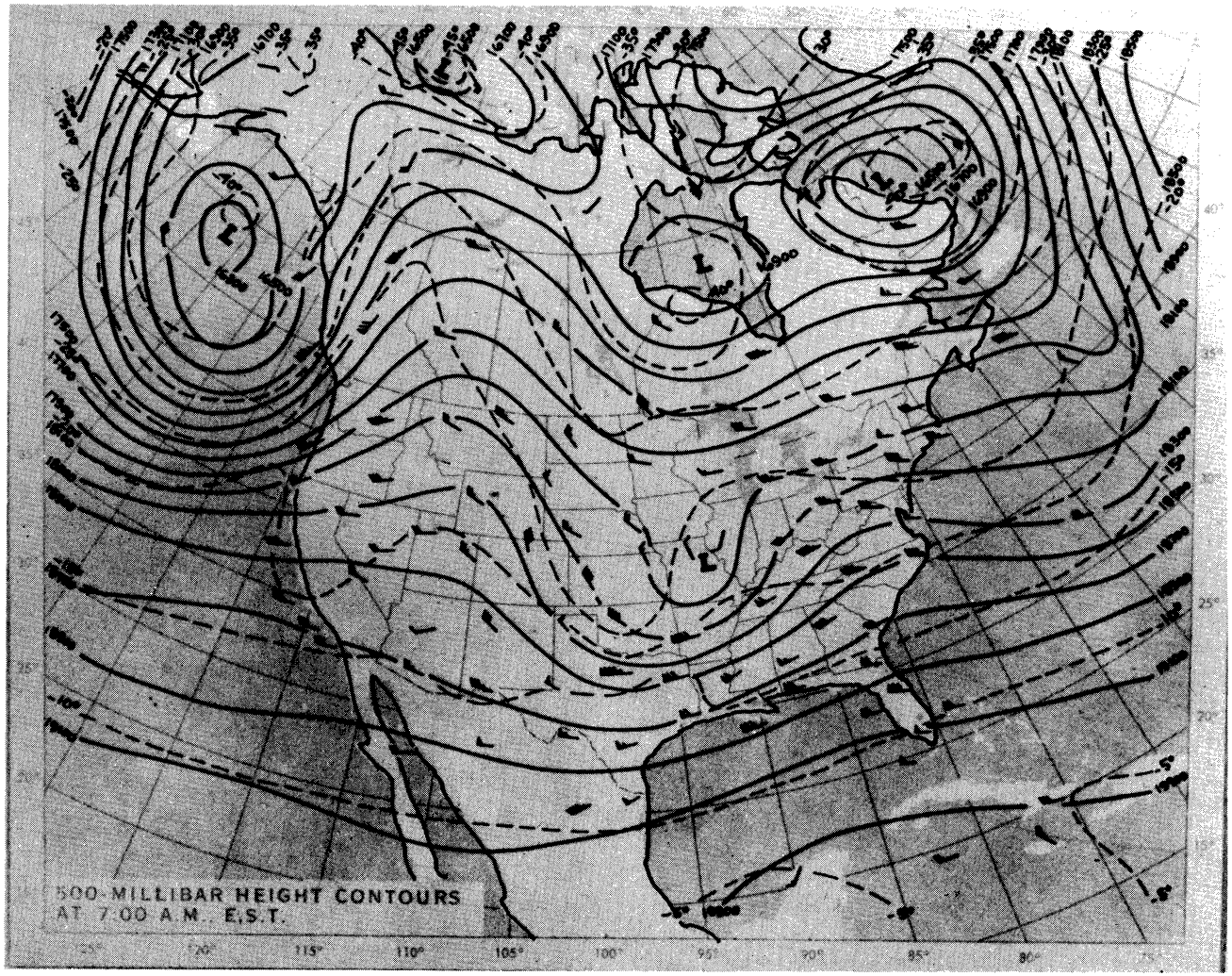

Figure 161. 500 - millibar height contours, 7:00 a.m. E.S.T., February 8, 1969.

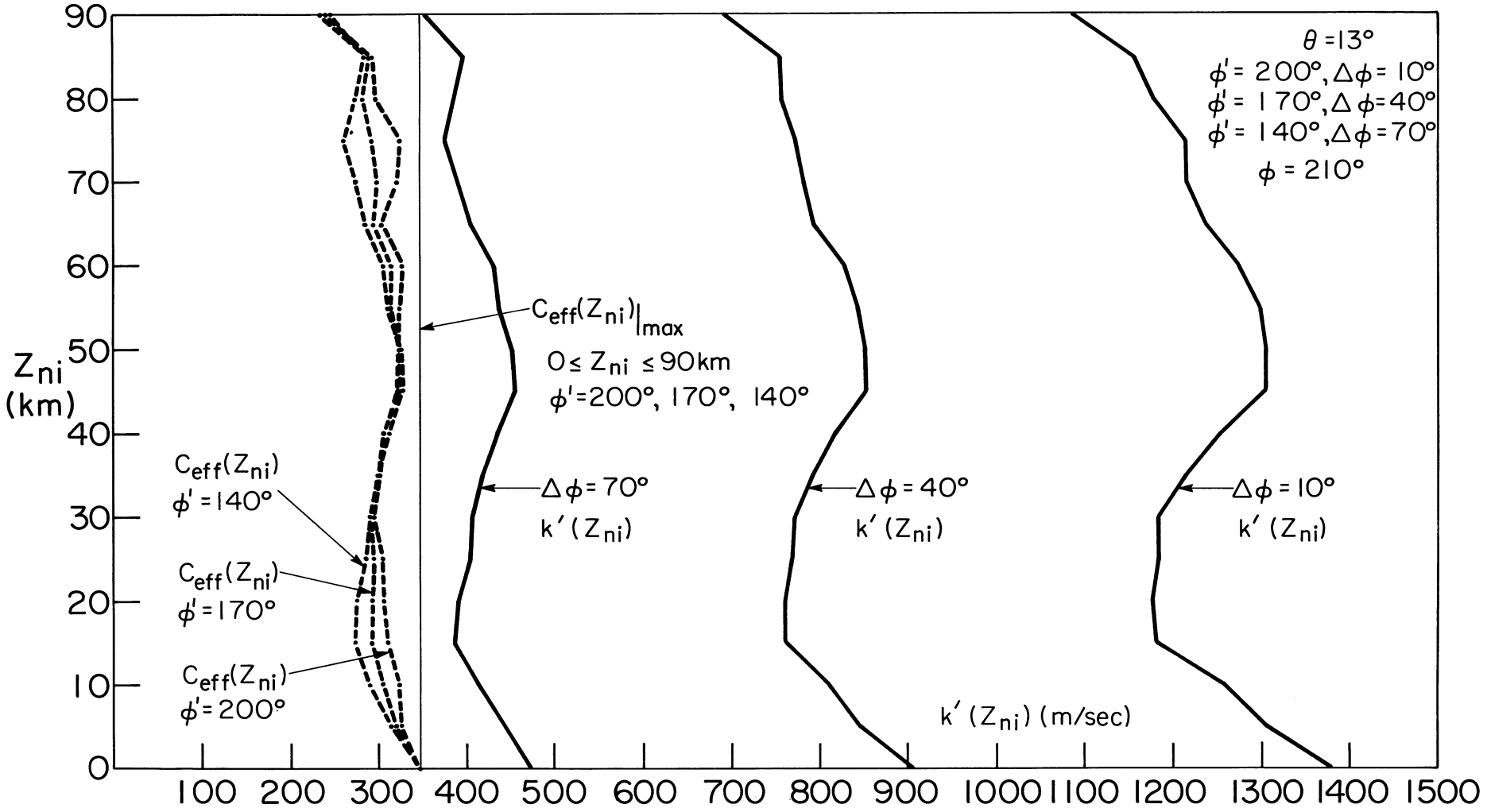

Figure 162. Refraction analysis for azimuth intervals to the West of the trajectory for the Allende Fireball entry. Dotted portions of curves represent situations for which ray paths to the ground are not allowed.

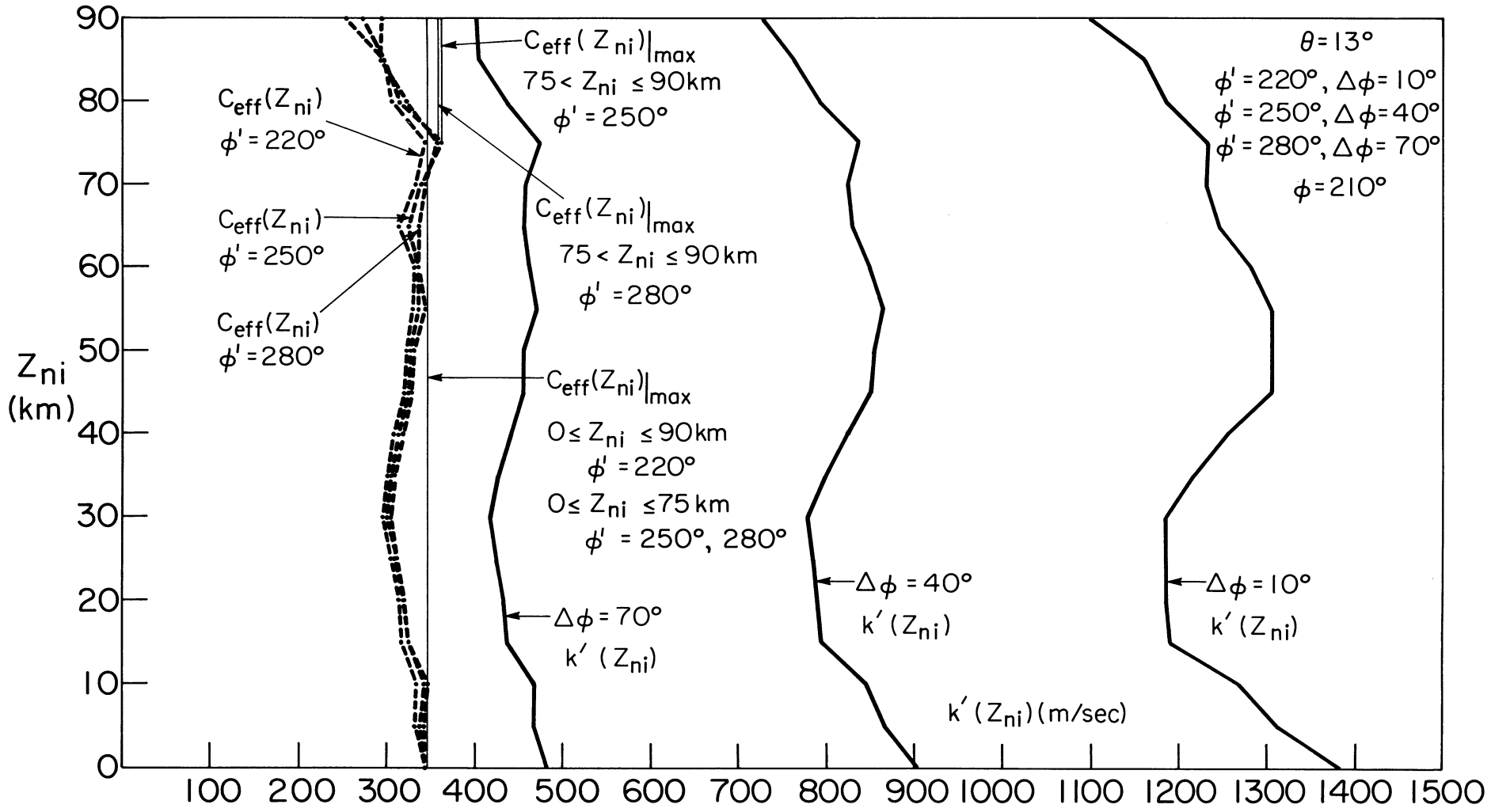

Figure 163. Refraction analysis for azimuth intervals to the East of the trajectory for the Allende Fireball entry. Dotted portions of curves represent situations for which ray paths to the ground are not allowed.

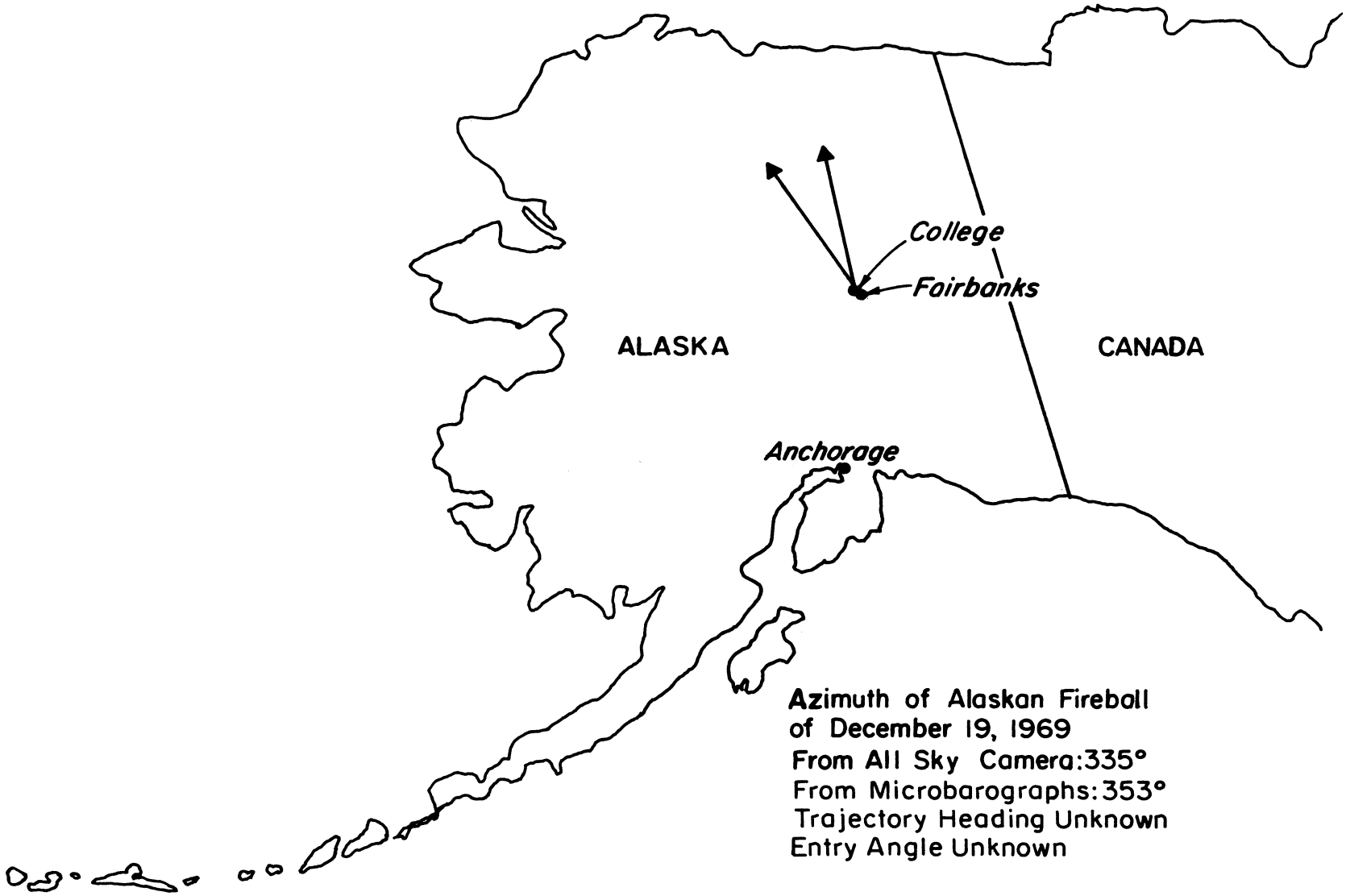

Figure 164. Entry map for the Alaskan Fireball of December 19, 1969, after Wilson and Johnson, 1972.

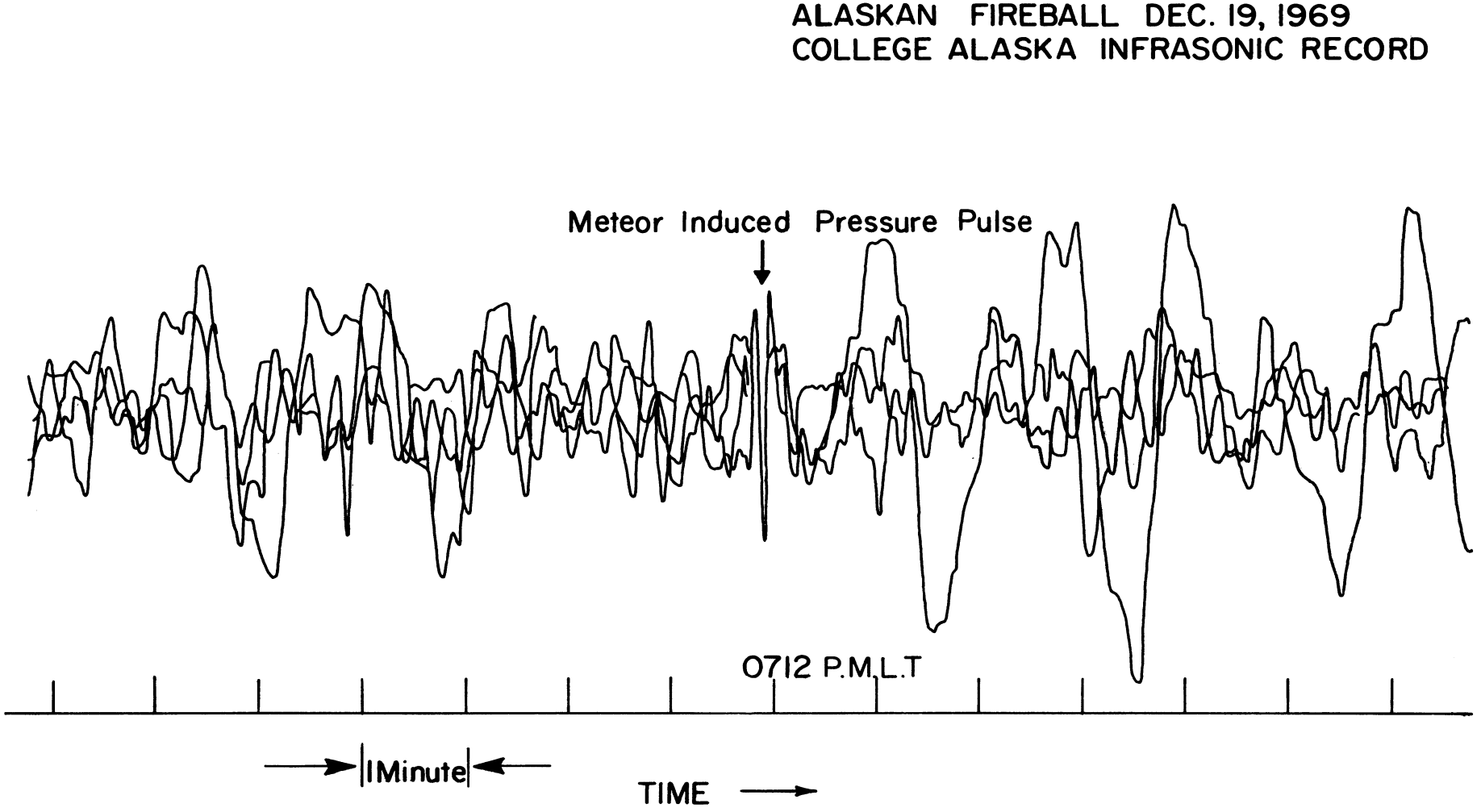

Figure 165. Airwaves from the Alaskan Fireball of December 19, 1969 as recorded in College Alaska on the College microbarograph system, after Wilson and Johnson, 1972.

Table 8

Observed Quantities

Meteor Event	t_e	DATE	t_o	DATE	t_p	$\tau_{g(sec)}$	t_D	$\Delta p_{o \to p}$ (dynes/cm^2)	χ (deg)	β' (deg)	Θ (deg)	ϕ (deg)	V (km/sec)	R_h (km)
Revelstoke	21:47 P. S. T.	3/31/65	00:15 M. S. T.	4/1/65	1 hr 28 min.	16.5	20 minutes	4.0	331	-	15	093	12	1150
Holbrook - B	01:32 M. S. T.	12/14/68	02:22 M. S. T.	12/14/68	43 minutes	2.5	10 seconds	1.1	216±2	43	-	225	-	720
Holbrook - F	01:32 M. S. T.	12/14/68	01:39 M. S. T.	12/14/68	7 minutes	4	12 seconds	0.25	-	-	-	225	-	134
Kincardine	20:47 E. D. T.	9/17/66	02:49 U. T.	9/18/66	2 hr 2 min.	54	34 minutes	1.25	75±2	-	24	310±5	-	2270
Alaskan Fireball	18:54 L. T.	12/19/69	19:12 L. T.	12/19/69	18 minutes	12	-	2.3	353	34	-	-	-	327

TABLE 8 (concluded)

	Calculated Quantities									Assumed Quantities				
Meteor Event	$R_{z\to g}$ (km)	d' at z=0 (km)	R_o (m)	d_m (m)	m (g)	E_z (ergs)	E_o (ergs/cm)	x_g	p_z (dynes/cm^2)	$R_{z\to t}$ / $R_{z\to g}$	$D_{ws}(R)$ z→t	$D_L(R)$ t→g	ρ_m (g/cm^3)	z_z (km)
Revelstoke	1705	$3.85\cdot10^4$	518.6	13.7	$4.0\cdot10^9$	$2.9\cdot10^{21}$	$8.4\cdot10^{13}$	$3.3\cdot10^3$	$9.88\cdot10^3$	0.5	0.1	0.5	3.0	34
Holbrook-B	792	$2.12\cdot10^4$	54.1	* 1.53	$5.6\cdot10^5$ - $5.6\cdot10^6$	$3.5\cdot10^{17}$ - $3.5\cdot10^{18}$	$8.0\cdot10^{11}$	$1.5\cdot10^4$	$2.81\cdot10^4$	0.5	0.05	0.5	0.3-3.0	27
Holbrook-F	147	$1.49\cdot10^5$	177.4	* 5.01	$2.0\cdot10^7$ - $2.0\cdot10^8$	$1.3\cdot10^{19}$ - $1.3\cdot10^{20}$	$4.8\cdot10^{11}$	$8.3\cdot10^2$	$4.88\cdot10^2$	0.5	0.05	**0.1	0.3-3.0	57
**Kincardine	2497	$4.03\cdot10^5$	1761.1	* 49.7	$1.9\cdot10^{10}$ - $1.9\cdot10^{11}$	$1.2\cdot10^{22}$ - $1.2\cdot10^{23}$	$1.9\cdot10^{13}$	$1.4\cdot10^3$	$1.93\cdot10^2$	0.5	0.1	0.5	0.3-3.0	64
Alaskan Fireball	360	$4.87\cdot10^4$	452.1	* 12.8	$3.3\cdot10^8$ - $3.3\cdot10^9$	$2.0\cdot10^{20}$ - $2.0\cdot10^{21}$	$1.8\cdot10^{12}$	$8.0\cdot10^2$	$2.75\cdot10^2$	0.5	0.1	0.5	0.3-3.0	61

* Indicates d_m, m and E at V = 11.2 Km/sec

** See text